TAMPEREEN TEKNILLINEN YLIOPISTO
TAMPERE UNIVERSITY OF TECHNOLOGY

Kalle Lintinen

Photopolymerizable Liquid Fullerene, Phthalocyanine and Porphyrin Derivatives

Synthesis, Analysis and Photocurrent Generation

Julkaisu 942 • Publication 942

Tampere 2010

Tampereen teknillinen yliopisto. Julkaisu 942
Tampere University of Technology. Publication 942

Kalle Lintinen

Photopolymerizable Liquid Fullerene, Phthalocyanine and Porphyrin Derivatives

Synthesis, Analysis and Photocurrent Generation

Thesis for the degree of Doctor of Science in Technology to be presented with due permission for public examination and criticism in Festia Building, Auditorium Pieni Sali 1, at Tampere University of Technology, on the 3rd of December 2010, at 12 noon.

Tampereen teknillinen yliopisto - Tampere University of Technology
Tampere 2010

ISBN 978-952-15-2492-9 (printed)
ISBN 978-952-15-2494-3 (PDF)
ISSN 1459-2045

Abstract

Photopolymerizable liquid monomers of fullerene, phthalocyanine and porphyrin were synthesized, polymerized and used as photoactive materials in organic solar cell structures. The design of the molecules requires the combination of three major parts: the functional core of the original molecules, alkylic side chains for liquid state and polymerizable end groups. The harsh conditions of the chromophore synthesis require a modular design, where the chromophore core and polymerizable tails are synthesized separately, and combined later by mild acylation.

A means of ultra-thin-film polymerization, both photo and thermal, were devised. All of the chromophores could be polymerized as ultrathin films. Because of their high absorbances, it was possible to use UV-Vis spectroscopy to monitor polymerization indirectly; as the films were of only a few monomer units thick, it was possible to dissolve the unreacted monomer residues afterwards and thus determine polymerization degrees as a function of the absorbance of the polymerized film.

The molecules were studied extensively to yield the parameters for thin film preparation, photopolymerization, and photocurrent generation. While the monomers were liquid at room temperature, the hardness of the polymers was that of cross-linked epoxy plastics.

The porphyrin monomer was used to study photopolymerization kinetics due to its unique self-photoinitiating properties. Polarization modulation IR spectroscopy was used to study real-time photopolymerization of the porphyrin monomer at varying temperatures, yielding rate constants and the activation energy of the reaction. It was the first published study of ultra-thin-film polymerization kinetics.

The monomers were polymerized *in situ* to form bilayers, bulk heterojunctions or hybrids of both, to create a photoactive structure for photocurrent generation. An extensive set of samples was prepared and studied. The monomers employed in this work were optimized for easy photopolymerizability and as such produced un-

optimal power conversion efficiency. Nevertheless the basic structure of the polymer lends itself well to modification for improved organic photovoltaic performance.

Preface

I would like to thank my supervisor Prof. Helge Lemmetyinen for providing me the opportunity to conduct my research in a field new to our group and patiently waiting for so long until results started coming. I especially thank my co-supervisor Dr. Alexander Efimov, who has helped me to become the synthetic chemist that I am now and withstood the copious amount of broken glass during my first year. I thank Alexander for allowing me to plot through the uncharted territory of polymer chemistry, in which none of us were experts when starting this study.

I also thank Prof. Nikolai Tkachenko for helping me whenever I had questions about physics or spectroscopy. Dr. Vladimir Chukharev owes my gratitude for teaching me to use various instruments in the lab.

The work wouldn't have been possible without the help of all the co-authors in our department and elsewhere. The work that took only days for you would have lasted forever to learn and to execute by myself.

All of my co-workers have made my work enjoyable and the coffee table conversations provided much-needed breaks for the sometimes very long days. I thank my 'roommate' Dr. Kimmo Kaunisto for the conversations on science and for his advice when I wanted a second opinion on anything.

Most of all I want to thank my family for being there, during good and the less good times. I appreciate how my father, Sakari, for always being interested in what I was doing, my mother, Merja, for pampering me on my visits home, my brother, Risto, to help me get distracted from work and my sister, Eveliina, for all the trips during which I could recharge my batteries. I also thank God for making me who I am.

This work was carried out at the Department of Chemistry and Bioengineering, Tampere University of Technology between August 2005 and December 2010. I gratefully acknowledge the department for financing this study.

Tampere, December 2010

Kalle Lintinen

Contents

Abbreviations and symbols

AFM	atomic force microscopy
Alq3	tris(8-hydroxyquinolinato)aluminum
ATR-IR	attenuated total reflectance IR spectroscopy
B9ox	2,4,6-tris-(9-oxiranyl-nonyloxy)-benzaldehyde
Br9ox	2-(9-bromo-nonyl)oxirane
C_{60}	buckminsterfullerene
CLF	chloroform
CuPc9ox	copper tetrakis[α(2-methoxyphenyl)(9-oxirane)nonanoate]phthalocyanine
DBU	1,8-diazabicycloundec-7-ene
DCC	dicyclohexylcarbodiimide
DCM	dichloromethane
DMAP	N,N-dimethylaminopyridine
DMF	dimethylformamide
DMSO	dimethylsulfoxide
DSC	differential scanning calorimetry
E_a	activation energy
FB9ox	1-methyl-2-[2,4,6-tris(9-oxiranyl-nonyloxy)-phenyl]-fulleropyrrolidine
FF	fill factor
FLM	fluorescence lifetime microscopy
FT-IR	Fourier transformation IR spectroscopy
GPC	gel permeation chromatography
H_2Pc9ox	tetrakis[α(2-methoxyphenyl)(9-oxirane)nonanoate]phthalocyanine
HETPP	tetrakis-[3-(2-hydroxyethoxy)phenyl]porphyrin
IPCE	incident-photon-to-electron conversion efficiency
IR	infrared
I_{SC}	short circuit current
IQE	internal quantum efficiency
ITO	indium tin oxide
k	rate constant
MCPBA	*meta*-chloroperbenzoic acid
MPPN	3-(3-hydroxymethylphenoxy)phthalonitrile
NMR	nuclear magnetic resonance

OLED	organic light emitting diode
OMAN071	p-(octyloxyphenyl)phenyliodonium hexafluoroantimonate
ONA	9-oxiranyl-nonanoic acid
OPV	organic photovoltaics
P3HT	poly(3-hexylthiophene)
Pa	Pascal
PCE	power conversion efficiency
PM-IRRAS	polarization modulation infrared spectroscopy
P- FB9ox	poly(FB9ox)
P- H_2Pc9ox	poly(H_2Pc9ox)
P-TAEP	poly(TAEP)
rt	room temperature
s	second
SC	spin-coating
T	temperature
TAEP	tetrakis-[3(2-hydroxyethoxy-2-(9-oxirane)nonanoate)phenyl]porphyrin
TFA	trifluoroacetic acid,
THBA	trihydroxybenzaldehyde
TMPPc	tetrakis[α(2-hydroxymethylphenyl)phthalocyanine
U_{OC}	open circuit voltage
UV	ultraviolet
UV-Vis	ultraviolet-visible spectroscopy
α	conversion
η	viscosity
λ	wavelength
ν	frequency

List of Publications

The thesis is based on the work contained in the following publications, which are hereafter referred to by their Roman numerals:

I **Cationic Photopolymerization of Liquid Fullerene Derivative under Visible Light**
Kalle Lintinen, Alexander Efimov, Sami Hietala, Shijo Nagao, Pasi Jalkanen, Nikolai Tkachenko, Helge Lemmetyinen
J.Pol. Sci. A **2008**, *46*, 5194–5201.

II **Monitoring Ultrathin Film Photopolymerization of Tetra-Alkylepoxyporphyrin by UV-Vis Spectroscopy**
Kalle Lintinen, Linda Storbacka, Alexander Efimov, Sami Hietala, Risto Ahorinta, Nikolai Tkachenko, Helge Lemmetyinen
J.Pol. Sci. A **2009**, *47*, 6095–6103.

III **Real-Time IR Study of Ultra-thin Film Photopolymerization of Liquid Porphyrin Monomer**
Kalle Lintinen, Niko Granqvist, Alexander Efimov, Helge Lemmetyinen
Macromol. Rapid Commun. **2010**, 31, 1977–1980.

IV **Photocurrent Generation by Cationically Polymerized Fullerene-Phthalocyanine Composite**
Kalle Lintinen, Linda Storbacka, Alexander Efimov, Antti Tolkki, Nikolai Tkachenko, Helge Lemmetyinen
Sol. Energy Mater. Sol. Cells, accepted with revision.

Author's contribution

Kalle Lintinen has both planned and carried out almost all of the experimental work and data analysis and written all the publications listed above.

1 Introduction

For some time it has been apparent that the energy and resource consumption of the world surpasses the current capacity of the world to renew itself.[1] Of the existing renewable sources of power the most prominent by far is the sun – it generates, directly or indirectly (in the form of fossil fuels), nearly all of the renewable and non-renewable energy that we consume. For the sun to become a major direct source of our energy, we need an efficient way to convert the energy of sunlight into electricity or fuel. Since the early fifties solar cells have been an option; however for a long time their price was so punishingly high that they were only applicable only for the most extreme applications, such as satellites or relay stations without access to power lines.[2] Even today solar cells constitute a very minor proportion of the world's energy production.

An exciting new approach is organic photovoltaics, which offers the prospect of extremely cheap manufacture and easy installation due to the possibility of making solar panels light and flexible. For the past couple of decades the performance and reliability of such structures has been increasing greatly and the current record efficiency of organic solar cells is over 7 %.[3] However, even though the commercialization of organic photovoltaics has begun with a few dedicated companies, no product is available yet for purchase. At the moment the situation is similar to the early days of inorganic solar cells; only relatively expensive, custom-made products are promised for the first commercial wave, such as mobile phone charging bags, or laptop powering sun shades in the case of organic solar cells.[4,5] When the expense of production has been decreased and reliability has increased sufficiently, organic solar cells should be able to replace many conventional means of power generation, starting from powering individual homes and offices to someday providing enough electricity for plug-in automobiles.

A sister technology to organic solar cells is organic light emitting diodes (OLEDs), which take in electricity and emit light, and has already begun to change the market by enabling the production of extremely thin, bright, and power-efficient mobile phone displays and TV sets.[6] A recent approach for the production of OLEDs has been to photopolymerize the active layer that produced photons out of electrons, producing improved performance over an unpolymerized structure.[7-9] Photopolymerization in specific and *in situ* polymerization in general are an attractive way to reduce the cost of organic nanophotonic production, as the structures formerly achieved only by ultrahigh vacuum evaporation can be attained by much less demanding production methods. Thus far photopolymerization and other means of *in situ* polymerization have not been used in organic solar cells, largely due to the limitations, which photoactive materials pose on the polymerization.

The conventional UV light source of photopolymerization causes the monomers to bleach and the common photoactive materials are crystalline and as such do not polymerize.

Visible light photopolymerization is a solution to problems associated with bleaching of monomers due to ultraviolet illumination and is a prospective way to reduce costs by using blue LEDs instead of conventional UV light sources. Several groups have been studying both naturally occurring molecules, such as curcumin[10,11] and synthetic ones, such as thioxanthone[12,13] for light absorbing co-initiators for visible light photopolymerization. The synthesis of liquid photoactive molecules, which can be used for photopolymerization, requires meticulous design to incorporate both of the desired function of the original material and photopolymerizability.

Means of analyzing thin film polymerization have been few, mostly being restricted to real time attenuated total reflectance infrared (ATR-IR) spectroscopy, used for films of micrometer scale.[14,15] Polarization modulation-IR spectrometry is a known technique, which enables the study of ultra-thin films (even monomolecular), but due to the inconvenience of the traditional optical bench set-up, the method was limited for a long time for the analysis of less demanding samples.[16,17]

In the present study three types of photopolymerizable chromophores were synthesized, namely fullerene, phthalocyanine and porphyrin derivatives. Several iterations of the fullerene monomer were attempted, until a suitable monomer with all of the required characteristics for photopolymerization was obtained. The phthalocyanine monomer required the design of a modular synthesis where the harsh conditions of the phthalocyanine macrocycle formation and the epoxidation of the polymerizable oxirane group were separated. The modular approach was applied to porphyrin synthesis as well. All of the monomers were decorated with long alkyl chains to lower the melting point and were provided with a polymerizable group, oxirane. The three monomers were fully characterized, polymerized by various methods, and used in the fabrication of organic photovoltaics.

Two methods were devised for analyzing ultrathin film polymerization: an indirect method using ultraviolet-visible (UV-Vis) spectroscopy and a direct real-time polarization modulation-IR spectrometry method, applied in detail to the porphyrin monomer. The UV-Vis method uses the simple fact that the residual unreacted monomer can be rinsed off after polymerization, which enables the determination of the polymerization yield of any monomer film detectable by UV-Vis spectrometry. The PM-IRRAS method combines the ease of use of a novel instrument requiring no optical bench and the self-photoinitiating nature of the porphyrin monomer. The real-time analysis of ultrathin film polymerization kinetics was, as far as we know, the first of its kind used.

The devised PM-IRRAS method enables the preparation of several identical samples, whose polymerization at various temperatures can be monitored. The obtained polymerization graphs can be fitted to the exponential equation of polymerization and rate constants, *k*, can be calculated. The rate constants, along with temperature data, yield the activation energy of oxirane photopolymerization. The results with the porphyrin monomer indicate that the method can be used for ultra-thin-film polymerization analysis in general, as even monomolecular layers produce a detectable IR spectrum.

Photovoltaic samples were prepared of the synthesized monomers and polymerization parameters were modified to optimize the structure for photocurrent generation. It could be seen that the high alkylic content of the polymer increased the resistance of the active layers, yielding a lower efficiency than with conventional non-polymeric pthalocyanine-fullerene based photovoltaics. However it was shown that with the polymeric approach it is possible to prepare hybrid structures combining both the efficient charge transfer of a structure with separate layers of electron acceptors and donors (bilayer), and the high surface area of a mixture of donors and acceptors (bulk heterojunction), and to produce a much higher power conversion efficiency than with either bilayer or bulk heterojunction individually. Several steps are still required for the devised *in situ* method to yield solar cells with the efficiencies of the current *state-of-the-art* organic photovoltaics. Despite these being only the first steps in obtaining these new types of organic photovoltaics in mild and inexpensive conditions, the initial results show potential in improving the system considerably, but only with careful modification of the monomers.

2 Background

Photopolymerization provides a fast and an easy way to manufacture thin polymeric films. It has already been successfully used in the preparation in nanophotonics, especially OLEDs,[9,18,19] but before this study no photopolymerizable chromophores usable in photovoltaic applications had been prepared. A major hindrance to the application of photopolymerization into organic photovoltaic manufacture has been the crystallinity of the common chromophores, which makes their polymerization nearly impossible. Another obstacle is the bleaching of the chromophores under ultraviolet light, the most common wavelength region used in photopolymerization. For photovoltaic applications the polymer layers are required to be fully polymerized to prevent holes and the reduction of efficiency. The ability to determine the properties of polymerization and the polymer surfaces is key to their use in photovoltaics. In the next paragraphs a brief study of the literature of the fields relevant to the current study is discussed.

2.1 Photopolymerization

The field of photopolymerization has become increasingly important, especially in coatings, inks and photoresists, but also in entirely new fields, such as adhesives, laser imaging and 3D-photostereolithography.[20] Recently it has been applied to nanophotonic applications, especially to organic light emitting diodes (OLEDs), as well.[7-9] The definition of photopolymerization is polymerization, which is initiated by incident radiation. Photopolymerization causes a liquid monomer to form a non-tacky solid.[20] Common photopolymerization is very fast and occurs in less than 1 s.

Regularly photopolymerization requires at least two components: a monomer and an initiator. However there are some cases where the monomer is purely initiated by light irradiation, without the assistance of an initiator. The most important monomers are polyols, anhydrides, diacids, epoxides, (meth)acrylic acids and their esters, styrene and diisocyanates. Besides monomers, most commercial applications also use oligomers, which increase both the polymerization speed and the original viscosity of the photopolymerizable formulation, which makes the end-use easier. The most common region of the electromagnetic spectrum that is used in photopolymerization is the ultraviolet (UV) region. The most commonly used light source, Hg/Xe lamp, has major emission peaks ranging from 254 nm to 365 nm, corresponding with the energies of 4.9 eV to 3.4 eV. The energy of the photons is enough to cleave the initiator molecules, producing either a radical species

or an ionic species (cation or anion) that initiates the polymerization. Visible light photopolymerization is a two-step process, where the highest occupied molecular orbital (HOMO) of a photosensitizer (PS) is excited to its lowest unoccupied molecular orbital (LUMO), after which the excited sensitizer creates a complex with the initiator, and electron transfer occurs between the two.[10] This results in the cleavage of the initiator molecule. By using visible light for photopolymerization, one can avoid the negative effects of the high energy UV radiation, such as tissue damage and bleaching.

Bleaching is a phenomenon where the UV light used for illumination degrades the polymerizable film. The region, which is often affected, is not the polymer backbone, but rather a separate functional region, which can react with oxygen, where either the functional region or the oxygen is excited.[21,22]

The types of monomers are numerous and their use depends as much or more on the requirements of the final polymer as on their speed of polymerization. At the moment radically photopolymerizable acrylic and methacrylic monomers and oligomers predominate in the commercial field. The monomers polymerize rapidly and the mechanical properties of the polymer are very good, which is very important for practical applications. The major drawback of radical photopolymerization is that it is very oxygen sensitive and requires inhibitors for storage because of self-initiation. For thin film applications this is a significant disadvantage, as the polymerization requires an inert atmosphere. Cationically polymerizable monomers are as abundant as radically polymerizable ones and do not suffer from oxygen inhibition or self-polymerization and have become popular in the fabrication of thin films, especially functional ones. The polymerizable group of such molecules is often a cyclic ether, such as oxirane (more commonly known as epoxy) and oxetane (1,3-propylene oxide). The ring is readily opened by a photoacid generated by a photoinitiator, creating a carbocation, which can open a second ring and create a new carbocation, sustaining polymerization as long as there is monomer available.

Cationic photopolymerization has many positive features over radical photopolymerization of thin films, as it is not oxygen sensitive and is not prone to self-polymerization. Currently the most popular types of cationic photoinitiators are onium salts, especially iodonium and sulfonium (Figure 2.1). Direct photolysis of an iodonium initiator occurs according to Scheme 2.1, where the formation of the photoacid, $HMtX_n$, requires a side step of hydrogen abstraction from a hydrogen donor (Scheme 2.1).[23] Visible light photopolymerization requires an efficient electron, energy, or hydrogen transfer between the sensitizer and the initiator. (Technically the commonly used name sensitizer is misleading, as the name implies that the molecule only sensitizes the reaction, but in fact the sensitization reaction is nearly always irreversible. For this reason the term co-initiator is

preferred.) In cationic photopolymerization it is the cation that determines the energy of the photon required to initiate the reaction, as it is the absorbing moiety of the salt, but after the photoacid is formed, the speed of the polymerization is purely determined by the strength of the anion. A key feature of cationic photopolymerization is the use of acids possessing anions of very low nucleophilicity. Therefore, most cationic photoinitiators are based on salts of nonnucleophilic anions, such as BF_4^-, PF_6^-, AsF_6^-, and SbF_6^-. Among these anions, the hexafluoroantimonate anion (SbF_6^-) forms the strongest superacid,[24] and therefore is used for most monomer films that are hard to polymerize. Pure phenylonium salts are practically never used, as their solubility in common solvents is very poor. Instead all of the commercial and bespoke onium initiators have at least one alkylic group to enhance solubility. As the solubilizing group has practically no effect on the photoinitiation efficiency, there are quite a few different options of sulfonium and iodonium initiators available that are used nearly interchangeably.

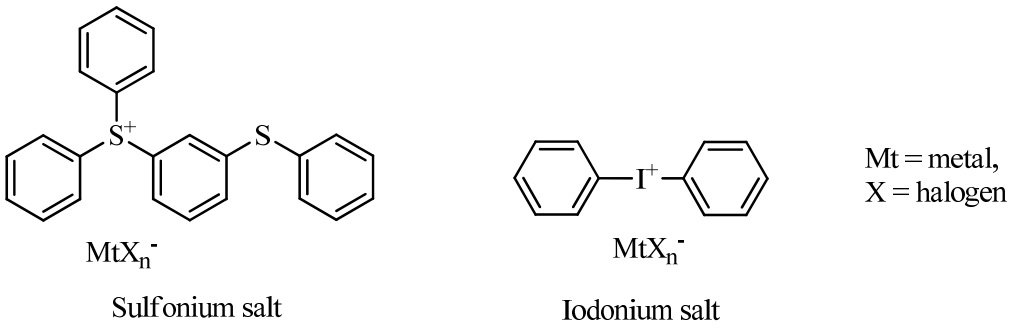

Figure 2.1. Chemical structure of the sulfonium and iodonium salts.

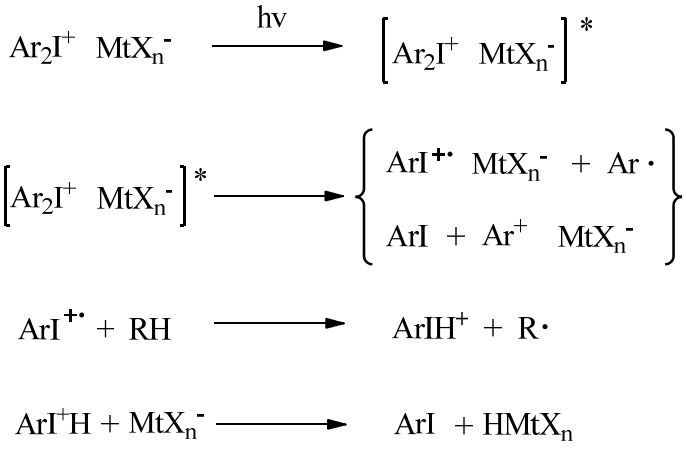

Scheme 2.1. Direct photolysis mechanism of diaryliodonium salt.

2.1.1 Porphyrin as an Initiator for Photopolymerization

Porphyrin has been used as an initiator in epoxy polymerization since the 1980's, but as aluminum chloride, with no photoreaction.[25,26] Ohkuma e*t al*. introduced two-photon sensitized polymerization of vinyl ethers by a zinc complex of porphyrin.[27] They irradiated an absorption band at 630 nm (Q-band –the first excited singlet state) of porphyrin and, after the intersystem crossing to the first excited triplet state, they irradiated this excited state with 470 nm light to excite the first triplet T_1 state to a higher triplet T_n state. Electron transfer from the T_n excited porphyrin to photoacid generator triphenyl sulfonium trifluoromethanesulfate initiated the cationic polymerization of isobutyl vinyl ether.

The exact mechanism of porphyrin functioning in visible light photopolymerization has not been addressed before, but the general mechanism of visible light polymerization has been published in various papers (Scheme 2.2).[10,11,28-32] The co-initiator, or photosensitizer (PS), is excited to a higher energy state, after which the photosensitizer yields an electron to the diaryliodonium initiator. The photosensitizer yields a proton to the counter anion of the initiator. The diaryliodonium initiator cleaves, leaving an iodoaryl molecule and an aryl radical. The aryl radical combines with the photosensitizer radical, forming a species whose absorption is red shifted in comparison to the photosensitizer absorption spectrum.

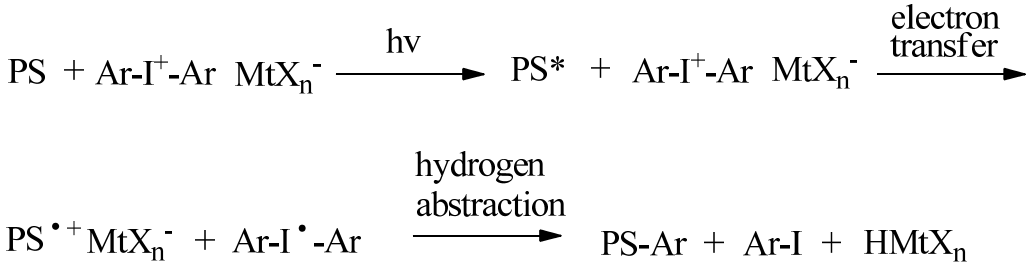

Scheme 2.2. The general mechanism of photolysis in visible light photoinitiation.

2.1.2 Photopolymerization of Functional Molecules

Photopolymerization has been adopted to the manufacture of functional materials, especially for the production of organic light emitting diodes (OLEDs).[7-9,19,33] Photopolymerization enables the solution processing of multilayer active structures that would be mutually soluble in their monomeric form. However the requirements for such structures are much more demanding than for

regular photopolymerization, as the main function of the monomer is to efficiently reproduce the nanophotonic function of the original molecule (electroluminescence in the case of OLEDs). The functional monomers are much bulkier and thus much more viscous than the conventional monomers. The prepared film thicknesses are always much thinner than conventional coatings (in the order of some hundreds of nanometers for OLEDs), as they depend on the nanometer scale for the desired function of the structure. Also the photoactivity of the molecules cause them to be susceptible to bleaching due to UV illumination.[34]

Müller *et al*. showed that by incorporating cationically photopolymerizable oxetane units into monomers they were able to fabricate a pixelated matrix display.[7-9,19] For their application there was no need for multilayer structures, but for the application of photopolymerization to the fabrication of organic solar cells, multiple layers would need to be photopolymerized consecutively.

Although thin film polymerization and photopolymerization have been known for a long time, the problems associated with polymerizing large, functional, monomers, such as the ones in this work, have not been addressed in great detail. The aforementioned work on OLEDs, which are photopolymerizable or photo-cross-linkable, has been very thin on the study of polymerization conditions.[33,35-38]

In practice many polymerizable groups can be used for functional thin film photopolymerization, but some references state that only oxetane can be used for these types of polymerizations.[35] In literature the choice of substrate is mostly determined by the application. In general all of the OLEDs produced by photopolymerization were prepare on indium tin oxide (ITO) covered glass substrates. The influence of temperature was never explicitly addressed – most studies were either conducted at room temperature if possible, or at a certain elevated temperature, without good reason stated for choosing the temperature.[39,40]

2.2 Fullerenes, Porphyrins and Phthalocyanines

Fullerene (Figure 2.2 A) is the third allotrope of carbon, besides graphite and diamond, and was discovered only in the middle 80's.[41] Fullerenes are formed of both 6-membered rings, which fused to themselves would form a planar graphene layer, and of 5-membered rings, which cause the structure to curve into a ball. The most common fullerene is Buckminsterfullerene, C_{60}, which is a molecular replica of a common football, which took its inspiration from the architect Buckminster Fuller, who first came up with the geodesic dome structure that describes both. All of the carbon atoms in fullerenes are sp^2 hybridized, leaving an additional electron of each atom to be delocalized

in the structure. This allows C_{60} to accept six additional electrons, making it an ideal molecule for the use of organic photovoltaics as an electron acceptor.

Buckminsterfullerene in itself is not very commonly used in any real applications, chiefly due to its poor solubility. For photovoltaic applications, the [6,6]-phenyl-C_{x+1}-butyric acid methyl esters [X]PCBM of fullerenes C_{60} and C_{70} (where X denotes the number of carbon atoms in the fullerene) are the most common, as they enable solution processing with conjugated polymers. Due to the multitude of double bonds fullerene has, it can be relatively easily synthesized into myriads of forms, one category of which has been polymers.[42] Different ways of polymerizing fullerene range from all carbon, side chain, main chain to cross linked structures. Depending on the application to which fullerene is to be used, different demands drive varying approaches. For instance photovoltaics require fullerene to be separated into its own phase, but still have a very small distance to the electron donating group and retain proper band gap and electron mobility. Up to now no fullerene polymer has produced comparable photovoltaic efficiencies to PCBM containing structures, but no reason exists why this situation could not change.

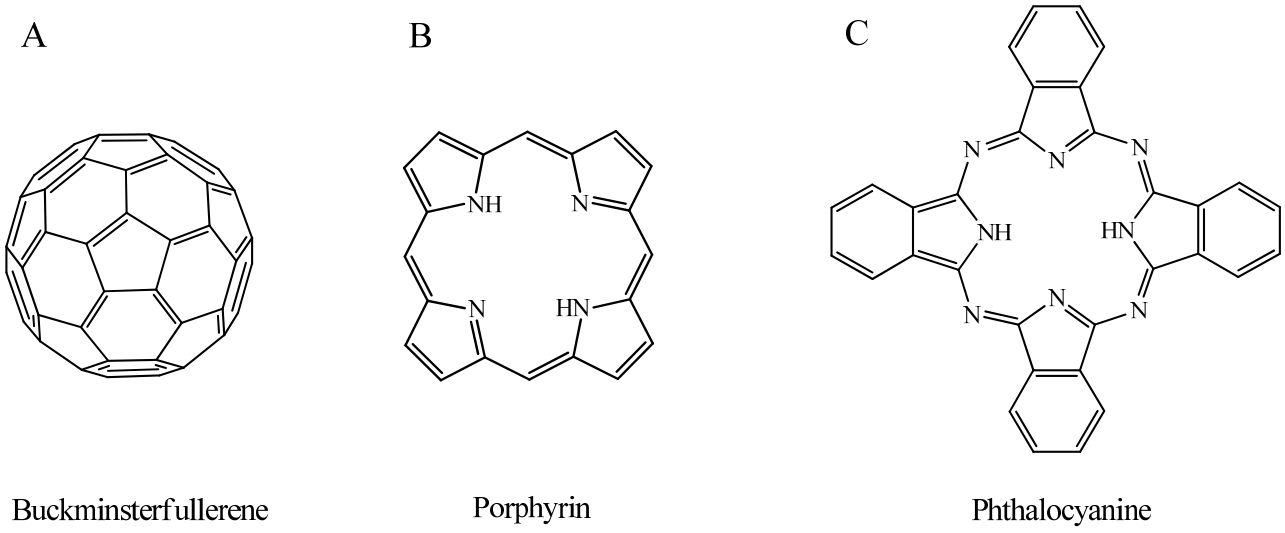

Figure 2.2. Chemical structures of buckminsterfullerene (A, C_{60}), porphyrin (B) and phthalocyanine (C).

Porphyrin (porphine, the simplest of porphyrins is shown in Figure 2.2 B) is a conjugated, organic, macrocycle that is the subunit of both heme (of hemoglobin) and chlorophyll. The porphyrin unit can function both in photochemical reactions and guest-host chemistry, such as the transfer of oxygen in blood. The molar absorption coefficient of porphyrin is extremely high, >200 000 M^{-1} cm^{-1}, enabling its use in extremely small quantities. In addition to its high absorptivity, porphyrin yields the energy of its excited state rapidly and efficiently.[43] Porphyrins have been used in numerous applications examining the basic science of different photochemical phenomena.

Recently porphyrin has also been introduced as a co-initiator in photopolymerization, where porphyrin absorbs visible light.[27]

Phthalocyanine (Figure 2.2 C) is structurally related to porphyrin. It has azo bridges connecting isoindole units, whereas porphyrin has methene bridges between pyrrole rings. Despite their structural similarity, the method of their synthesis and their absorption properties differ quite a bit. Due to the improved absorbance in the visible region of phthalocyanine over porphyrin, it can be successfully used in the preparation of organic photovoltaics. Structures with fullerene and phthalocyanine have yielded some of the best efficiencies of organic photovoltaics to date.[44] However, one of the main problems of efficient photovoltaics produced this far has been that the current method of manufacturing layers of phthalocyanine and/or fullerene requires ultrahigh vacuum evaporation, which defeats the promise of cheap production. If there was a way of reproducing the already achieved 5.7 % power conversion efficiency[44] in a solution processed phthalocyanine-fullerene structure, the efficiency would come close to commercial viability.

2.2.1 Synthesis of Liquid Photoactive Molecules

Various fullerene derivatives have been synthesized since fullerene became commercially available.[41,42,45] Especially the synthesis of polymers containing fullerene has been the focus of hundreds of publications. The synthesis of the polymer is greatly affected where in the polymer the fullerene moiety resides. There are cases where pure C_{60} are fused together at high pressure or in solution, under UV irradiation,[46] but as the formed fullerene polymers are insoluble in any solvent, and sometimes lose their functionality,[47] their practical application are few. On the other hand a fullerene moiety can be attached to a polymerizable group, to form a pendant-chain structure.[48,49] However for most of such polymers the increased fullerene content results in low solubility and difficulty in further processability. Fullerene moieties have also been attached to conductive polymers,[50,51] for the specific purpose of obtaining a polymer usable for organic solar cell preparation. Up to now, the polymers have not been comparable with PCBM in photovoltaic efficiency.

For a fullerene derivative to be photopolymerizable *in situ* in ambient pressure, it is required to be liquid. In 2006 Michinobu *et al.* found that by incorporating three long alkylic chains (min. 12 carbons long) into a fulleropyrrolidine through a phenyl group, the molecules could be made liquid at room temperature, with viscosities ranging from ~10^5 Pa·s for 12 carbon chains to ~10^3 Pa·s for 20 carbon chains.[52] The fullerene derivatives retain their electrical properties. Cyclic voltammetry

showed a similar reduction potential as for pure C_{60} and electron mobility of ~0.03 $cm^2 V^{-1} s^{-1}$ at 20 °C.

As with the fullerene derivative, a phthalocyanine derivative has to be liquid to be photopolymerizable (unless a way of photopolymerizing stacked phthalocyanine crystals is found). Before this work there was one publication on the photopolymerization of a phthalocyanine derivative, used in functionalizing a surface for a field effect transistor.[53] The phthalocyanine derivative was based on a molecule with four methyl-capped and four methacryl-capped trioxyethylene side chains. The photopolymerization itself had to be conducted on a (trimethoxysilyl)propyl methacrylate treated glass surface.

Other approaches of obtaining liquid, liquid crystal or amphiphilic phthalocyanines have been developed.[53-59] The general characteristic of the molecules was that the phthalocyanine was decorated with two long groups (mostly polyoxyethylene, but also alkylic and polysiloxane) at each benzo ring of the phthalocyanine, or with one long branched alkylic chains at each benzo ring.[60,61]

Liquid porphyrin had not been synthesized before this work, but a porphyrin derivative with a similar approach as presented in paper II and III was published a year after paper II.[62]

The incorporation of polymerizable moieties into materials with charge transporting properties has been under some study of late. Bacher *et al*. has published acrylic capped triphenylenes, which can be photopatterned and used in OLEDs,[33] Domerq *et al*. reported on methacrylic capped bis(diarylamino)biphenyl for use as hole transporting layer for OLEDs.[37] Kastler et al. published a hexabenzocoronene monomer with six acryl capped alkylic spacers for charge carrier applications.[63] The uniting factor for all of these monomers is their medium size and radically polymerizable functional group (acrylic or methacrylic). The problem with radical polymerization is oxygen inhibiting the polymerization, as the ambient oxygen reacts more readily with the radical initiator species than with the monomer, thus requiring all radical polymerizations to be conducted in an inert atmosphere, at least for full polymerization up to the sample surface.[64]

Cationically photopolymerizable monomers have produced the best results for charge transporting applications. Bacher et al. reported on incorporating two alkylic capped oxetane moieties into a diphenylbenzidine core.[7] UV illumination of the monomer with diphenyliodonium hexafluoroantimonate initiator yielded a patterned structure with micrometer resolution. They extended the approach to several different monomers and were able to produce functional OLEDs with the monomers.[8,9,19]

2.3 Tools of Polymer and Polymerization Analysis

An essential part of polymer studies is the analysis of polymerization and the polymer. There is a wide variety of methods of analysis, some more common than others. Certain methods that are a mainstay of linear polymer analysis, such as gel permeation chromatography (GPC), used in molecular weight determination, are totally incompatible with the analysis of cross-linked polymers.

Polymer films can be analyzed by spectroscopic and thermal methods, hardness measurements, and by methods of molecular scale interaction. Of the spectroscopic methods by far the most common is Fourier transformation infrared spectroscopy (FT-IR), but other methods are also in use, such as UV-Vis absorption analysis and fluorescence analysis. Of the thermal analytical methods the most common is differential scanning calorimetry (DSC) and its close relative, thermogravimetric analysis (TGA). Optical pyrometry is a spectroscopic tool for thermal analysis, especially designed for photopolymerization.[65]

Many of the aforementioned methods cannot be applied directly for the analysis of thin films (10-100 nm scale) typically used in organic photovoltaics, or other nanoscale applications. This is due to the very low signal intensities corresponding to small thicknesses. If the molar absorption coefficient (ε) of the monomers is high enough and polymerization causes changes in the UV-Vis absorption spectrum, UV-Vis spectroscopy can be used. The infrared absorption peak intensities corresponding to functional groups in molecules are highly related to sample thicknesses, so for IR analysis of ultrathin films, advanced methods, such as polarization modulation infrared reflection adsorption spectroscopy (PM-IRRAS), have to be used.

Knowing the structure of surfaces is crucial to any application that endeavors to take advantage of the nanoscale phenomena on them. Methods such as atomic force microscopy (AFM) take advantage of the forces acting upon probes that are at a close proximity to the sample surface. In hardness measurements a load is placed upon a sample and the area of indentation can be used to calculate how hard or soft the material is. For samples that are only some tens or hundreds of nanometers thick, indentation devices using highly specialized tips are required, but the hardness of even such thin samples can still be measured.[66,67]

2.4 Organic Photovoltaics

The conversion of the energy of photons into electricity, *i.e.* the photovoltaic effect, has been known since 1839, but it took until 1954 before the first crystalline silicon photovoltaic device was developed at Bell laboratories.[68] In a conventional solar cell a semiconductor material, typically crystalline Si, is doped to form a *p*-*n* junction. The *p*-side contains an excess of positive charges (holes), and the *n*-side contains an excess of negative charges (electrons). An electric field forms in between these two layers and the electrons and holes, created through the absorption of Si, diffuse through the layer, where they are accelerated by the field and are collected by their respective electrodes. The theoretical efficiency of this kind of a structure is ~32 %, which is determined by the Shockley-Queisser limit, which states that all of the excessive energy beyond the band is lost. The current record efficiency for a silicon solar cell is 25 %.

Organic photovoltaics (OPVs) are significantly different from conventional inorganic photovoltaics in their mechanism. Whereas in a conventional cell electron-hole pairs are generated throughout the bulk semiconductor and need to be separated by the built-in electric field, organic photovoltaics are governed by an excitonic process. Photons create an exciton (a bound electron-hole pair), which remains bound until the excitons reach an interface between *p*-type and *n*-type organic semiconductor, at which the electron are immediately separated when generated.

While the difference between the two types of solar cells might seem small, it causes drastically different photovoltaic behavior.[69] In practice this means both that the distance between the generated exciton and the *p*-*n* interface needs to be shorter than the exciton diffusion length and that both the *p*-phase and the *n*-phase have to be continuous until their respective electrodes (or buffer layers).

Of course besides the different mechanism of charge generation and separation, the difference of materials between organic photovoltaics and inorganic photovoltaics is much more pronounced. While the wavelength of the absorbed light in inorganic photovoltaics is governed by the difference between valence and conduction band of the semiconductor, i.e. band gap, the organic semiconductors are governed by the difference between the highest occupied molecular orbital (HOMO) and the lowest unoccupied molecular orbital (LUMO) of the organic molecules used. In practice most of the absorption is in the *p*-type semiconductor phase. The typical *p*-type molecule is a highly conjugated molecule (polymer or macrocycle) with electron donating groups (usually containing nitrogen or sulfur atoms) within the conjugated part.

Previously the best polymeric organic photovoltaic performance was obtained with a polymer - fullerene bulk heterojunction (BHJ), where poly(3-hexylthiophene) (P3HT) was blended with phenyl-C_{61}-butyric acid methyl ester (PCBM). P3HT is a *p*-type polymer, and a donor (D) of electrons, with thiophene units providing the majority of absorption of light and hole conduction, and the hexylic groups (in regioregular polymer) providing solubility for spin-coating and good crystallization when annealed.[70] PCBM is an *n*-type molecule, and an acceptor (A) of electron, with a fullerene moiety for electron conduction and a phenylbutyric acid methyl ester moiety for similar purposes as the hexyl group in P3HT. With P3HT:PCBM blend it is possible to convert over 90 % of the photons of the P3HT absorption maximum of 520 nm into electrons that are collected by the electrode (the concept of incident photon to electron conversion efficiency, IPCE).[71,72] Better overall efficiencies are obtained, when the whole solar spectrum can be collected, which has led to the use of other polymeric donors that have a broader absorption spectrum than P3HT, while still retaining IPCE values as high as that of P3HT.[3] Bulk heterojunction, where the *n*-type and *p*-type molecules are mixed to provide an increased surface area between the two, overcomes the short exciton diffusion length of the materials.[73]

Extending the traditional BHJ structure, there is high interest in tandem cells, where two active structures are connected with an ultrathin intermediate layer to effectively combine two solar cell structures into one.[74] This approach in principle could yield a power conversion efficiency (PCE) of 15 % against the theoretical limit of 11 % for a single layer structure.[74] This is because the difference between the LUMO level of the acceptor and the HOMO level of the donor determines the open circuit voltage (U_{OC}) of the device and if the absorption of the active structure is extended to cover the red part (and the IR part) of the spectrum, it will reduce the maximum extractable voltage. However if the HOMO-LUMO difference is higher, corresponding with a higher voltage, it will automatically result in the cutting of the absorption spectrum of the active layer in the middle of the solar spectrum. With a tandem cell structure it is possible to combine two materials with different HOMO-LUMO gaps, corresponding with different U_{OC} and as long as the short circuit currents (I_{SC}) and the fill factors (FF) of the layers match, the U_{OC} of the tandem cell is the sum of the respective U_{OC} of the layers and the theoretical PCE is the sum of PCEs of the individual layers. In practice this has only been achieved with unoptimal layer structures, yielding a PCE of 6.7 %,[75] the record at its time of publication, which lies below the current record of 7.4 %, obtained by a single active structure cell.[3]

A major challenge in producing effective tandem cells is stacking two active structures while retaining the performance of both structures. There are three main categories of the cells:[74]

(I) Tandem organic solar cells where both the bottom (in front of the light illumination) and the top (back) cells are based on low-molecular-weight evaporated molecules.

(II) Hybrid tandem organic solar cells in which one of the cells, either bottom or top cell, is processed from solution while the other cell is based on vacuum-deposited low-molecular-weight materials.

(III) Fully solution-processed tandem organic solar cells where both the bottom and top cells are processed from solution.

The most successful tandem cells of type I are phthalocyanine-fullerene structures, where both of the layers had a core of hybrid planar-mixed molecular heterojunction (PM-HJ) of phthalocyanine: phthalocyanine/fullerene mixture: fullerene with the front cell absorbing the higher wavelength photons (centered at 650 nm) and the back cell (with 4, 4', 4''-tris(3-methyl-phenyl-phenyl-amino)triphenylamine [mMTDATA] for shorter wavelength absorption, centered at 450 nm), increasing the efficiency of Pc:C_{60} solar cell from 5.0 % to 5.7 %.[44]

The second category enables the use of materials with different HOMO-LUMO gaps and reduces the number of vacuum processing steps. However the highest recorded efficiency thus far remained a relatively low 4.6 %,[76] at least in comparison to category I.

The third category will almost inevitably become the standard if tandem cells will ever be mass produced. Kim et al.[75] obtained the aforementioned 6.7 % PCE by combining PCPDTBT (poly[2,6-(4,4-bis-(2-ethylhexyl)-4H-cyclopenta[2,1-b;3,4-b']dithiophene)-alt-4,7-(2,1,3-benzothiadiazole)]): $PC_{60}BM$ and P3HT:$PC_{70}BM$ composites with a TiO_x electron transport and collecting layer. The sol-gel process used in the fabrication of the TiO_x middle layer and the different solvents used in spin-coating of active layers enabled multiple layer deposition. Solution processing multiple active layers without dissolving previous layers has to be addressed when designing type III tandem cells.

Generally organic semiconductors used in organic photovoltaics have high absorption coefficients (usually $>10^5$ cm^{-1}) and a low carrier (hole/electron) mobilities (typically from 10^{-6} cm^{-2} V^{-1} to 10^{-3} cm^{-2} V^{-1}). While the carrier mobility would be too small for inorganic solar cells, the very small thickness of the OPVs ensures that the resistance of the active layers does rise above 10 Ω cm^2 for the current *state-of-the-art* structures,[77] which allows for an efficient charge extraction.

3 Materials and Methods

The experimental aspects regarding the synthesized molecules, other used compounds, the used instruments, and the devised methods are discussed in this chapter. Especially relevant are the analytical tools used to analyze polymerization and the final polymer. The instrumentation regarding photocurrent sample preparation and analysis are also discussed.

3.1 Compounds

Three main target molecules (all cationically polymerizable liquids) were synthesized for this work: fullerene, phthalocyanine and porphyrin derivatives. The design and synthesis of the molecules is presented in chapter 4.1.

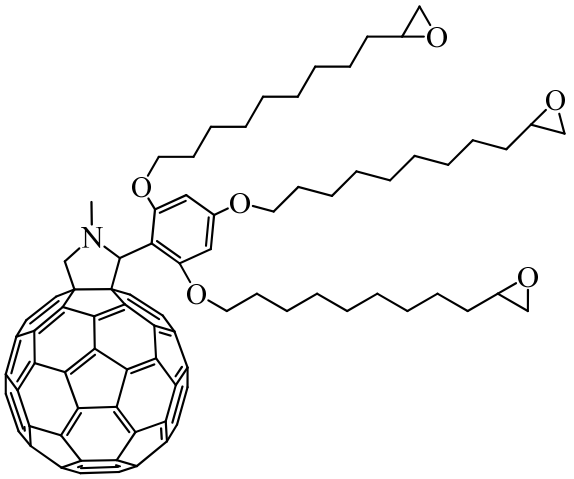

FB9ox

Figure 3.1. Molecular structure of the fullerene monomer FB9ox.

3.1.1 Fullerene Derivative

The initial goal was to synthesize a photopolymerizable fullerene molecule. After preparing several fullerene derivatives, a suitable monomer structure was found (FB9ox, Figure 3.1). The molecule can be easily synthesized, photopolymerized (paper I) and used in organic photovoltaics (paper IV). The molecule consists of a fullerene moiety, which is required in electron/energy transfer and

electron transport in organic photovoltaics, a pyrrolidine linker, which enables a phenyl moiety to be attached, and three nonyloxyoxirane moieties, lowering the melting point of fullerene and enabling photopolymerization.

3.1.2 Phthalocyanine Derivative

After the fullerene monomer had been synthesized and shown to photopolymerize, a phthalocyanine derivative was designed (XPc9ox, Figure 3.2). Phthalocyanine is a commonly used donor in organic solar cell production and almost always used in conjunction with fullerene. As with the fullerene derivative, the design and synthesis of the phthalocyanine derivative required multiple iterations, until a suitable molecule was prepared. The molecule consists of a phthalocyanine core, to act as an electron donor and a hole conductor, four oxymethylphenoxy linkers to enable functionalization of the core by acylation, with an oxiranyl-nonanoyl moiety for low melting point and photopolymerizability. The molecule was used in photovoltaic sample preparation (paper IV).

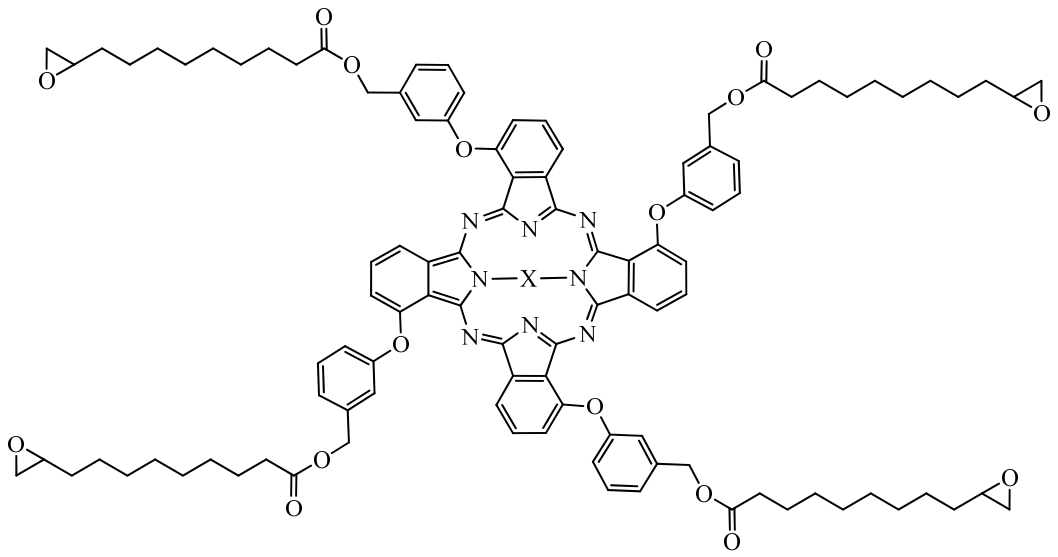

Figure 3.2. Molecular structure of the phthalocyanine monomer XPc9ox.

3.1.3 Porphyrin Derivative

After the modular approach to synthesizing a polymerizable liquid chromophore (*i.e.* phthalocyanine) was designed, it was very easy to apply the method to another chromophore,

porphyrin (TAEP Figure 3.3). Our group had previously synthesized a porphyrin with hydroxyethoxyphenyl groups for the creation of double linked porphyrin-fullerene dyads.[78] The alkyloxiranylcarboxylic acid used in the liquid phthalocyanine synthesis could be linked to the tetrahydroxyporphyrin as well. The molecule consists of a porphyrin core, hydroxyethoxyphenyl linkers to enable esterification, and oxiranyl-nonanoyl moieties for low melting point and photopolymerizability.

The same properties that make porphyrin an interesting molecule in photochemical research enabled the porphyrin monomer to be used in photopolymerization analysis. The porphyrin core can absorb visible light and pass the energy to a photoinitiator, which cleaves and forms a photoacid that starts a ring opening polymerization reaction by opening the oxirane moieties. This makes it possible to analyze photopolymerization kinetics of an ultrathin layer of the highly viscous TAEP monomer. The monomer was studied in papers II and III.

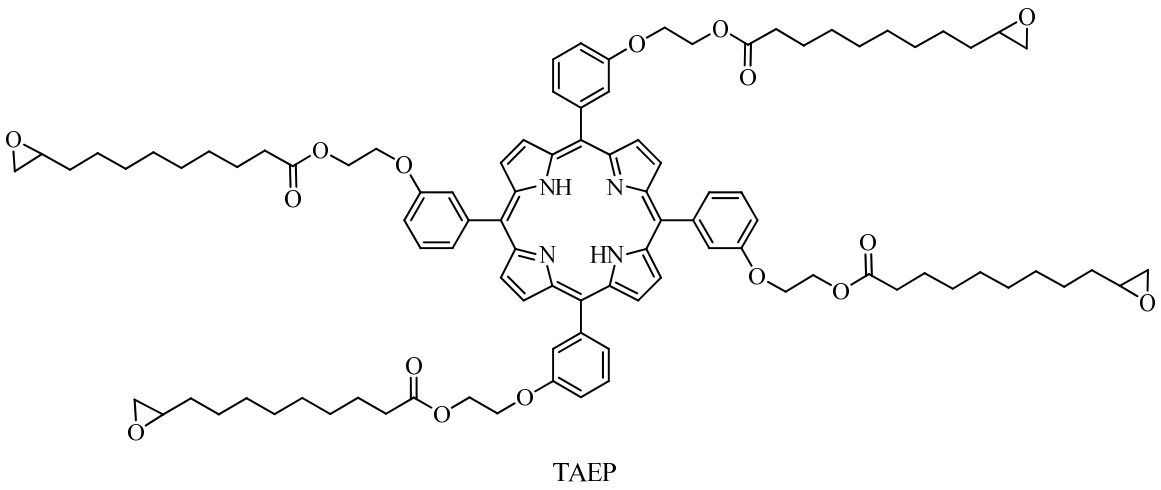

Figure 3.3. Molecular structure of the porphyrin monomer TAEP.

3.2 Thin Film Polymerization

Thin film polymerization of the three main monomers, as well as some of the precursors, was studied in the present work. The initiator and co-initiator were chosen for their proven efficacy. Different substrates were tested until suitable ones were found. A method used for photopolymerizable OLED production was adapted for sample preparation and various photoreactors were used.

3.2.1 Initiators

The polymerization of highly viscous large monomers requires much more efficient initiators than regular small molecular weight monomers of low viscosity, as increased viscosity is linked with reduced reactivity.[79] The final strength of a cationic photoinitiator is not in the cationic photoactive part, but rather in the anion. The photocleavage of the cation results in the monomer/solvent, or an intermediary, to yield a proton to the anion, creating a photoacid. For the photoacid to be strong enough to initiate polymerization, the counteranion has to be very non-nucleophilic. The anions most commonly used (in the order of reducing nucleophilicity) are BF_4^-, PF_6^-, AsF_6^-, and SbF_6^-.[24] For commercial applications PF_6^- is the most common, as it contains no heavy metals. However it does not produce a strong enough photoacid to initiate the photopolymerization of highly viscous monomers. Hexafluoroantimonate anion (SbF_6^-) forms the strongest acid of these and was used as the counteranion in all polymerizations in this work.

The cationic part of the photoinitiator consists of a photocleavable bond between a positively charged atom and a phenyl group. Two of the most commonly used types of cationic initiators are diaryliodonium and triarylsulfonium salts.[80] There are two major requirements of the initiators: 1) it is soluble and miscible with the monomer, 2) it produces a photoacid when illuminated with light. Because of the need of solubility the initiators are never in their pure form when used in actual applications, but have solubilizing groups attached to them. As the efficiency of photocleavage is not much related to the type of solubilizing group, nor is the strength of the formed photoacid, the number of different variations of photoacids is mostly due to different companies providing different photoinitiators. Triarylsulfonium salts absorb in the near UV and are therefore favored by the industry. They, however, cannot be adapted to visible light photopolymerization. Diaryliodonium initiators absorb farther in the UV spectrum, but are able to be used in visible light photopolymerization, as they can partake in energy transfer between a visible light co-initiator (literature calls them sensitizer, but as a sensitizer should only sensitize a reaction, not be consumed by it, the term is avoided in this thesis). The initiator used for the published papers was *p*-(octyloxyphenyl)phenyliodonium hexafluoroantimonate (OMAN071, Figure 3.4).

The co-initiator curcumin (Figure 3.4), derived from the yellow coloring, turmeric, was used as co-initiator in the visible light photopolymerization of the fullerene and phthalocyanine derivatives.[81] Curcumin was also tested on the porphyrin derivative, but it was found that the monomer TAEP acted as a more efficient co-initiator of its own photopolymerization.

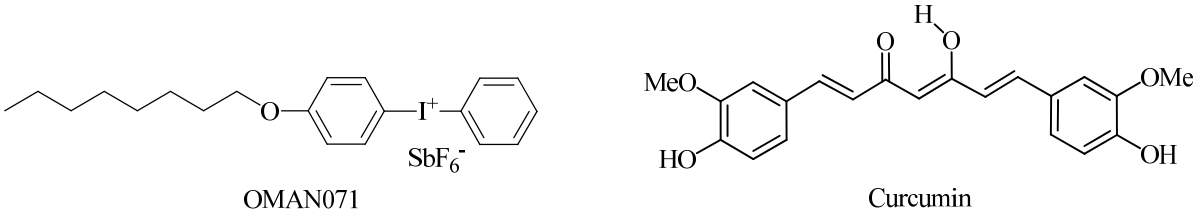

OMAN071 Curcumin

Figure 3.4. Molecular structure of the initiator OMAN071 and co-initiator curcumin.

3.2.2 Substrates

Initially the substrate was not considered to play a major role in photopolymerization, so even flexible plastic films, such as Mylar™ were used. On such films it was possible to study the photopolymerization of the less viscous precursors (see paper I), but the actual chromophore monomers would not polymerize, especially when studying sub-micrometer films. However it was found that for thin films the substrate would need to be solid and flat. Glass substrates were used at first. Polymerization was possible, but only at a high temperature and often producing very uneven films. Quartz and indium tin oxide (ITO) coated glass both enabled the preparation of films that were suitable for further use. The smoothness of substrates is a prerequisite for proper wetting of the surface, which can be aided by surface treatment for increased hydrophilicity.

The proper method of substrate preparation was found to be to clean the substrate surface with abrasion with a chloroform-soaked cotton cue-tip, then washing the substrates in acetone and chloroform in ultrasonic bath. After the solvent was discarded the substrates were washed with aqueous sodium dodecyl sulfate (SDS) solution, rinsed with milliQ water, washed with isopropanol and dried for 60 minutes at 150 °C in vacuum and N_2 plasma treated before use.

3.2.3 Film Preparation

When the goal is to obtain as uniform thin films as possible, the method of film preparation is crucial. For this work nearly all films were prepared by spin-coating (SC). In SC the desired compound is dissolved in a solvent and spread over the substrate, which is spun until a thin film of the compound is deposited and all of the solvent has evaporated. Solvent properties influence the crystallization of the compounds and their phase separation, when using several compounds. Due to the wide scope of this work, only chloroform was used, as it produced films that were very even

(roughness less than 1 nm), which could be fully polymerized. Other solvent might have affected solar cell efficiency, but probably not photopolymerization.

3.2.4 Photoreactor

Photopolymerization and especially its analysis require a controlled environment. The following setup was developed for use in this work. The basic photoreactor (Figure 3.5) consists of a heating plate covered with a Petri dish with a filter to cut off the UV region of the Hg/Xe medium pressure UV-Vis light source that is directed at the sample at a set distance. Temperature is measured by optical pyrometer (OP) from the heating plate surface. There might be a temperature difference between the heating plate and the sample surfaces, but as the difference is the same within all samples of one temperature, it can be ignored to some extent. The reactor is also masked from ambient light to prevent its influence.

The basic reactor was expanded for real-time IR measurements (Figure 3.6). The heating plate / OP couple was switched to thermo-controlled heater, which enabled accuracy and stability for comparing different temperatures during kinetic measurements. The UV-Vis light source was replaced by a blue LED centered at 450 nm wavelength. The setting also included an IR source and a detector located on either side, mounted on a goniometer.

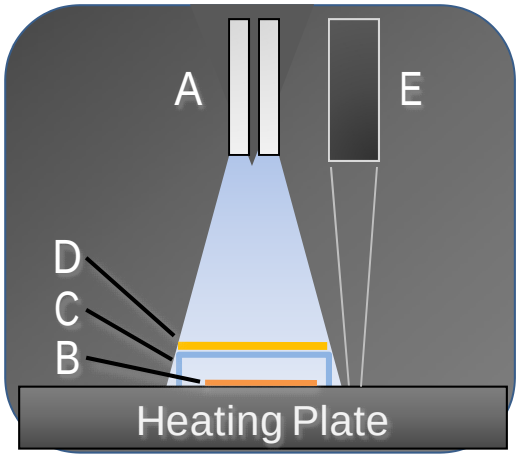

Figure 3.5. Schematic representation of the photoreactor. A sample is placed on a heating plate above which are set optical cables (**A**) that direct the light illuminated from an Hg/Xe light source. The sample (**B**) is covered by a Petri dish (**C**) and a UV cutoff filter (**D**). Temperature is measured by an optical pyrometer (**E**) and the whole device is kept in the dark.

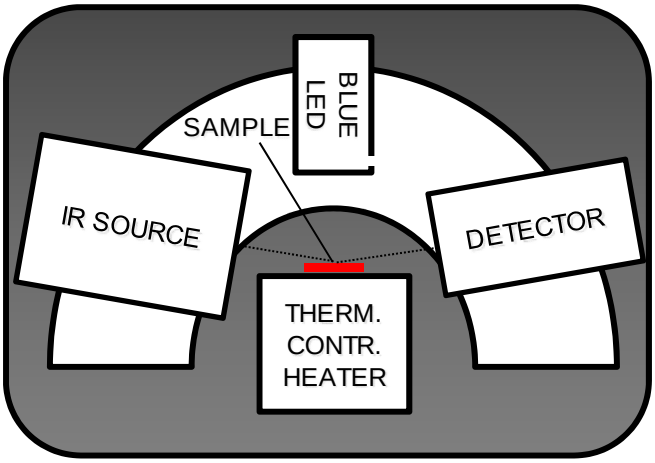

Figure 3.6. Schematic representation of the PM-IRRAS photoreactor.

3.3 Analytical Methods

The monomers were analyzed to obtain the correct parameters for photopolymerization. Photopolymerization was analyzed, first with methods used in literature and later with methods devised specifically for this work. Finally the polymers were characterized to determine their suitability for further applications

3.3.1 Rheology

Rheology is the study of the flow of matter.[82] An integral part of rheology is the study of viscosity, or its 'thickness'. Viscosity of the monomer plays a crucial part in determining the speed of polymerization. It is closely related to the mobility of the molecules in a liquid. There are other significant factors affecting the speed of polymerization, but generally a viscosity below 1 Pa s is required for fast (seconds to minutes) polymerization.[79,83] The monomers were studied with a parallel plate rheometer, in which a relatively thin film of the studied compound is placed on a temperature-controlled plate and a second plate is contacted with the fluid, creating a liquid interface between the plates. Rheometer measures shear force in the fluid when the top plate is rotated (Figure 3.7). In a Newtonian liquid the viscosity of the fluid is independent of the shear stress. In such a case an Arrhenius plot of viscosity against temperature is linear.

All of the samples in this work were tarry liquids at room temperature, whose viscosity caused a shear stress at the upper limit of the rheometer. When the samples were heated, the viscosity lowered as expected and reliable viscosity graphs were obtained.

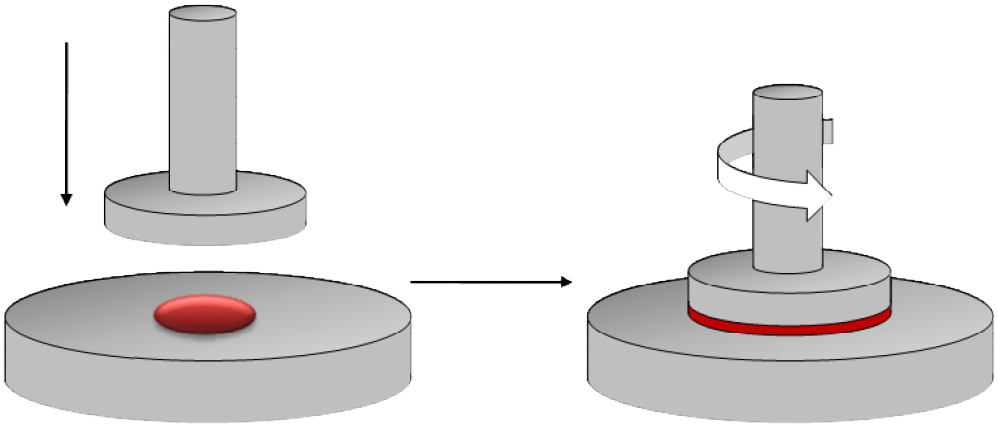

Figure 3.7. Schematic representation of parallel plate rheometry.

3.3.1 FT-IR Spectroscopy: ATR-IR & PM-IRRAS

Fourier transformation infrared spectroscopy (FT-IR) in its all forms is one of the most versatile methods to analyze the chemical nature of polymer structures, as molecules absorb specific frequencies in the IR region that are characteristic to their structure. The frequencies correspond with the vibrations of the functional groups in (usually organic) molecules. This way it is possible to compare the vibrations of the polymerizable moiety of the monomer with the vibrations of the same region after polymerization. Most commonly the reduction of the intensity of the monomer band can be inversely correlated with the increased conversion, α, of the polymer.

Attenuated total reflectance infrared spectroscopy (ATR-IR) was used in the present study to characterize all of the synthesized compounds and the polymerized films. ATR-IR functions through a phenomenon of total internal reflection. A beam of IR light is passed through an ATR crystal and it is reflected from the measured sample. The light passes through ca. 0.5 – 2 μm of the sample. Regular ATR-IR cannot be used in real-time measurement of thin film photopolymerization of the monomers, as the device cannot be heated above a certain level, the sample thickness of the monomer film is very small (~10 nm) for the detection limit, the ATR crystal surface is not smooth enough and the cross-linked polymerization of the monomer would ruin the ATR crystal.

Polarization modulation infrared reflection adsorption spectroscopy (PM-IRRAS) is in certain respects similar to ATR-IR, but overcomes several of the problems associated with ultra-thin-film photopolymerization measurements. In PM-IRRAS a sample is prepared on a reflective surface, illuminated by modulated IR light, which is detected in a regular manner. When the samples are prepared on a conductive (often metal) surface, the relative intensity of *p*-polarized light is enhanced and *s*-polarized light is cancelled (Figure 3.8). Only vibrational modes that have a

transition dipole (or component of the transition dipole) perpendicular to the surface can be observed. The further away the dipole is removed from the surface (beyond a few molecular layers), the more attenuated the effect is.[84,85] An additional advantage of the modulation of light is that isotropic absorptions from the atmosphere are cancelled.

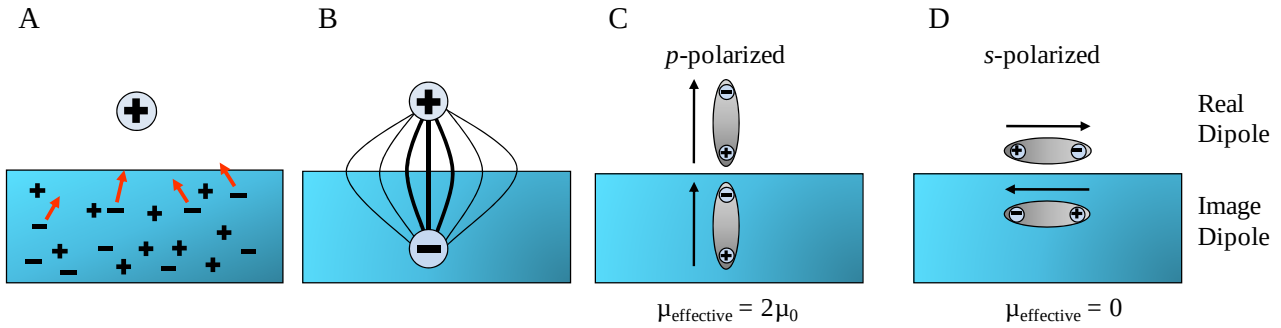

Figure 3.8. Enhancement of perpendicular dipoles and cancelling of parallel dipoles on conductive surfaces. Any charge or dipole near the conductive surface causes a mirroring charge effect on the conductive surface (A-B), thus perpendicular dipoles cause a doubling of the signal (*p*-polarized light in C) and parallel dipoles cause a cancelling of the signal (*s*-polarized light in D).[86]

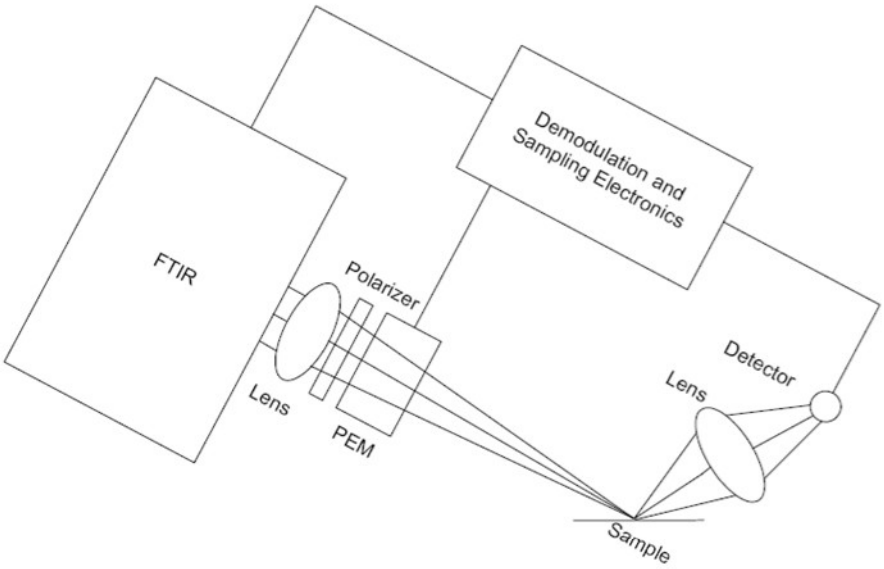

Figure 3.9. Schematic representation of PM-IRRAS.[86]

In conventional PM-IRRAS devices the whole setup is built on an optical bench, which limits the use of accessories. The PM-IRRAS study presented in paper III was conducted in co-operation with KSV NIMA, who have built a PM-IRRAS device specifically adaptable for easy modification (Figure 3.9). In the setup a sample can be placed on a space into which a modulated IR beam is directed. The sample reflects the beam and the IR absorption is subtracted from the beam. The

devise allows for the use of a thermo-controller and optical cables for sample illumination (Figure 3.6).

3.3.2. UV-Vis Spectroscopy

Generally non-conjugated organic molecules absorb only in the UV region of the spectrum, but conjugation and the increased delocalization of electrons causes the energy levels to come closer, in which case the molecules absorb visible light. All of the chromophore monomers studied in this work have large conjugated aromatic systems with delocalized electrons, causing high extinction coefficients, especially in the case of porphyrin and phthalocyanine.

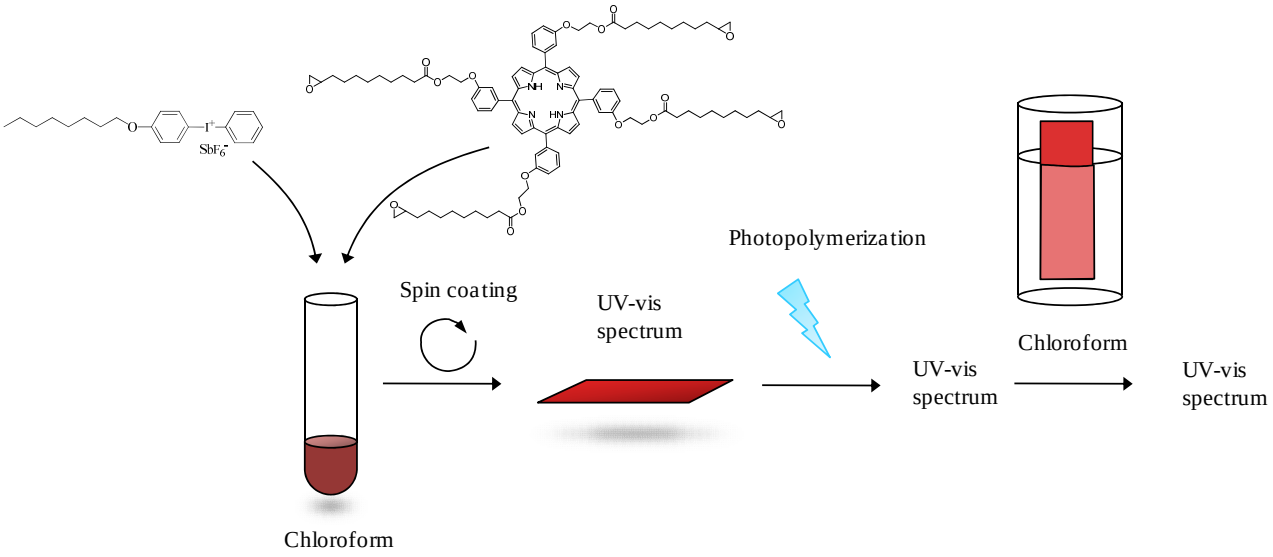

Figure 3.10. Schematic representation of the UV-Vis analysis of photopolymerization.

As polymerization only opens the oxirane rings, which do not contribute significantly to the UV-Vis spectrum, the polymerization itself is not readily visible by UV-Vis spectroscopy. However the high extinction coefficients of the molecules cause even the nanometer scale films of the molecules to have well-resolved absorption spectra. The polymerization fixes the layer of a few monomers in thickness on the substrate; the unreacted monomers can still be dissolved in a suitable solvent and rinsed off the layer, thus causing a difference in absorbance, which is proportional to the yield of polymerization (Figure 3.10).

Ideally if the polymerized sample is rinsed with solvent and the spectrum shows the proportion of the fixed polymer, which has been confirmed to be closely linked to conversion in this work. However as the chromophores have three or four polymerizable groups, it was considered

appropriate to call the value of fixed polymer ‘polymerization yield’ instead of conversion. In the optimal case the two values are equal.

3.3.3 Regular and Photo-DSC

Differential scanning calorimetry (DSC) measures the heat required to increase the temperature of a sample and compares it to a reference. It can be used to detect energy changes related to phase transitions and chemical reactions. DSC is a crucial tool for the analysis of glass transition temperature (T_g) of liquid monomers. The liquid molecules form a glass, when cooled beyond a point at which the viscosity reaches a certain level, formally 10^{12} Pa·s.[87,88] In practice the T_g point is determined by the center point of a dip in heat capacity caused by the glass transition in the DSC cooling curve at 10 K/min. DSC graphs were measured for all of the used monomer to yield their T_g values.

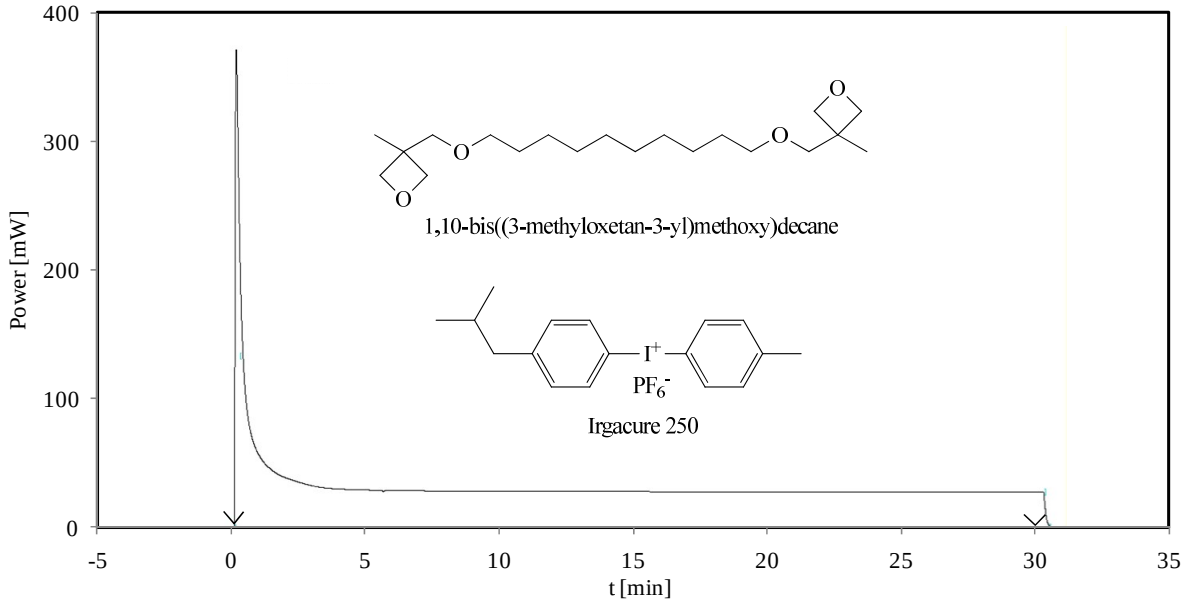

Figure 3.11. Photo DSC graph of bisoxetane photopolymerization.

Another use of DSC is photo differential scanning calorimetry (photo DSC), where the generated heat of photoinduced reactions is measured. The crucial difference between regular DSC and photo DSC, besides the use of light, is that the measurements are conducted isothermally. In photopolymerization the analyzed sample is illuminated, while the photo DSC device cools the sample at the rate by which the polymerization increases the sample temperature, keeping

temperature constant. Photopolymerization of small molecules of low viscosity can be conducted within seconds at low temperature. Figure 3.11 shows the photopolymerization graph of 1,10-bis((3-methyloxetan-3-yl)methoxy)decane, a side product (of compound 15 in Scheme 4.5) of the synthesis of liquid oxetane derivative of fullerene. In such a case the conversion of the monomer can be calculated by dividing the integral of the photopolymerization graph by the known enthalpy of polymerization.

However photo DSC was not convenient for the study of the highly viscous chromophore monomers. There are several issues that hinder the use of photo DSC for such molecules:

(1) The high extinction coefficient of the samples combined with the high amount required causes most of the absorbance to occur on the sample surface.
(2) The roughness of the measuring pan surface is too high even to consider thin film samples.
(3) Thin film preparation by spin coating is not possible due to the cylindrical geometry of the measuring pan.
(4) And additionally the required mass of the sample (several milligrams) is too large for an extensive set of measurements (tens to hundreds of experiments are required), when the synthesis produces product in maximum of some hundreds of milligrams.

Photo DSC was used to test the photopolymerization of the smaller precursors, aiding in setting up the thin film experiments.

3.3.4 Optical Pyrometry

Optical pyrometry (OP) is a relatively new method for the analysis of (photo)polymerization.[65,89] OP measures the thermal (IR) radiation emitted by a warm sample (the same phenomenon is used in heat cameras). OP has been used to study thin film photopolymerization in cases where photo DSC has not been possible. The major difference between OP and photo DSC is that OP does not enable isothermal experiments and thus the OP graphs cannot be integrated to yield the enthalpy of the reaction (at least without complicated corrections). However OP can show the speed of polymerization from the maximum temperature and it can be used to compare different monomers and their polymerization parameters.

OP was used in the initial analysis of benzaldehyde precursor of the fullerene derivative (Figure 3.12) to yield approximate parameters for the fullerene photopolymerization (see paper I). However

the fullerene monomers required different conditions for its photopolymerization, which could not be reproduced with the OP setting. Nevertheless OP was used for accurate temperature measurement when photopolymerizing samples on a heating plate that did not have a precise thermo controller.

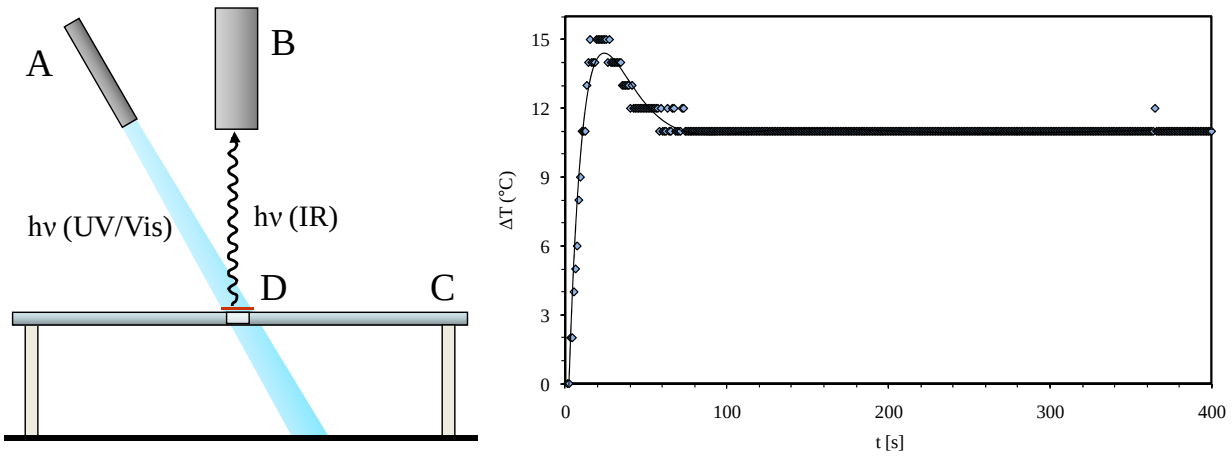

Figure 3.12. Schematic representation of photopolymerization measurement by optical pyrometry (OP): (A) UV-Vis light source, (B) optical pyrometer, (C) sample stand and a (D) sample. The graph shows the photopolymerization of the benzaldehyde derivative of the fullerene monomer FB9ox (compound 18 in Scheme 4.6).

3.3.5 Nanohardness Measurement (Triboindentation)

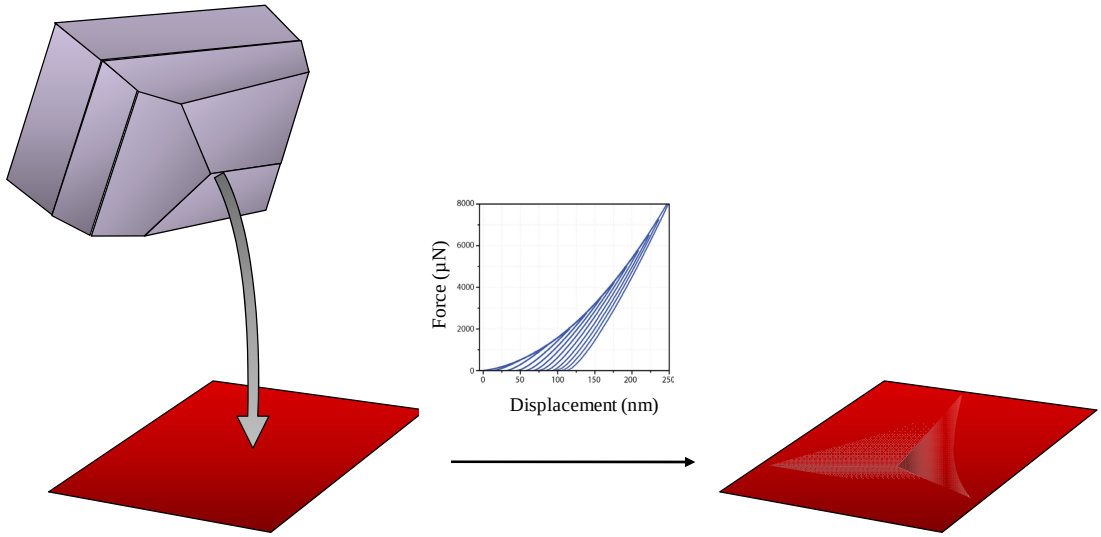

Figure 3.13 Schematic representation of nanoindentation measurement using a Berkovich tip.

The often beneficial property of polymers is their hardness. Cross-linked polymers are quite hard and thus can withstand much more mechanical stress than linear polymers or crystalline organic thin films. The measurement of the hardness of thin films were conducted with dedicated equipment, in which a tip of very specific geometry and high hardness is pressed against a surface and the hardness can be measured by the force required for the indentation of a given depth (Figure 3.13). Several indentations guarantee the accuracy of the measurement.

3.3.6 Fluorescence: Steady State Spectroscopy and Fluorescence Lifetime Microscopy

The fluorescence of the porphyrin and phthalocyanine monomers and polymers are intrinsic photophysical properties of the compounds and can be used for the detection of the photochemical processes in the layers. Fluorescence is caused by the relaxation of a molecule to its ground state (k_f in Figure 3.14) after being excited to the excited state (k_{ex}). The efficiency of fluorescence depends on the efficiency of competing pathways, such as internal conversion (k_d) and intersystem crossing (k_{ISC}). Additionally the chemical environment of the molecule, such as the existence of acceptor molecules affects the fluorescence properties considerably. In fluorescence spectroscopy a fluorescing sample is illuminated at its excitation wavelength (corresponding to its absorption band), after which the emitted photons are counted. The fluorescing properties of porphyrin and/or fullerene layers were analyzed to test the system's applicability to photovoltaics.

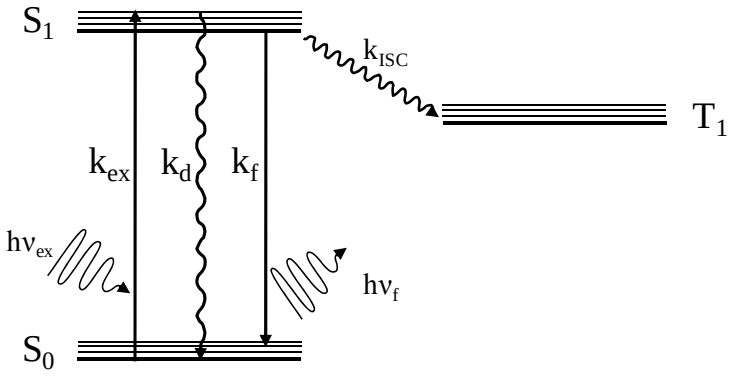

Figure 3.14. Schematic representation of phenomena relating to fluorescence spectroscopy: ex = excitation, d = internal conversion, f = fluorescence, ISC = intersystem crossing.

The decay of fluorescence is determined by the surface arrangement of the fluorescing moieties and possible acceptor molecules. Fluorescence lifetime microscopy (FLM) enables the point-by-

point analysis of a fluorescing sample, where the decay of the fluorescence is measured. An FLM device is based on the illumination of the sample by a laser light, which corresponds to the sample absorbance and real-time fluorescence is detected. When the setting is connected to a microscope, the surface of the studied sample can be monitored two-dimensionally (Figure 3.15). All of the fluorescing layers were studied with FLM in this work. It enabled the study of both the difference in fluorescence lifetime due to polymerization and fluorescence intensity in photopatterned samples.

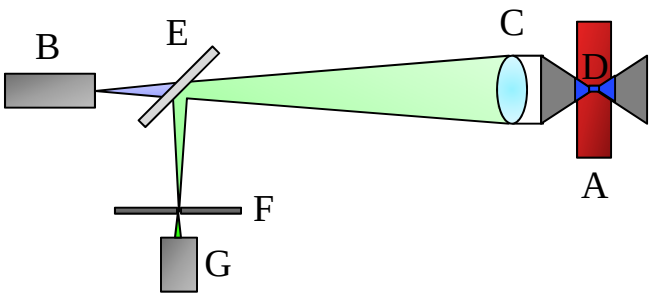

Figure 3.15. Schematic representation of a fluorescence lifetime microscope. The sample (A) is illuminated by a laser (B), which is focused by a lens (C) to a small area (D). The fluorescence is collected by the same lens and the diverted from the exciting light by a dichroic mirror (E) through a pinhole (F) to a detector (G).

3.3.7 AFM

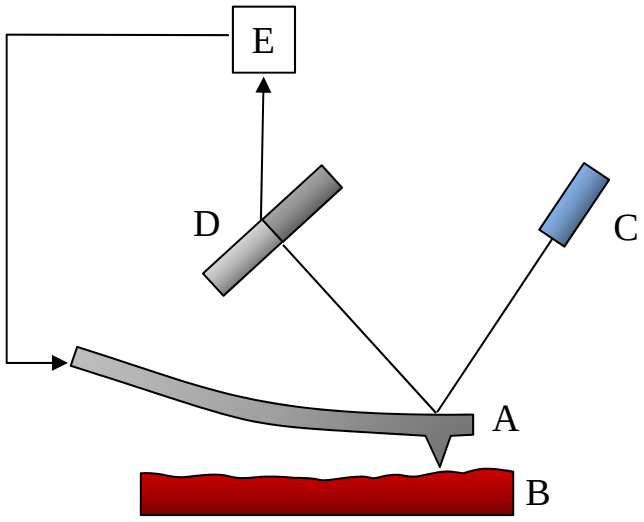

Figure 3.16. Schematic representation of AFM measurement. A tip on a cantilever (A) is placed above the sample surface (B) and oscillated. A laser (C) directs a beam onto the cantilever and a photodiode (D) senses the oscillation from the reflected beam. A detector (E) controls the cantilever so that the tip will not touch the sample surface.

Atomic force microscopy (AFM) was used to study surface fine structure of the samples. The combined forces (such as van der Waals and electrostatic forces) of the surface on a detecting tip are measured to produce an image of nanometer resolution. In tapping mode AFM, which was used in this work, the sample is scanned with cantilever tip, whose oscillation above the surface is monitored by laser and photodiode (Figure 3.16). The surface exerts force upon the tip without touching it, thus yielding data both of surface height and the quality of the surface. The surface structure of several polymer films, specifically their roughness, was measured by AFM.

3.4 Photocurrent Samples

Photocurrent sample preparation requires that the substrates are extremely pure and are not contaminated at any point of the polymerization process, which requires careful control of the multi-step process.

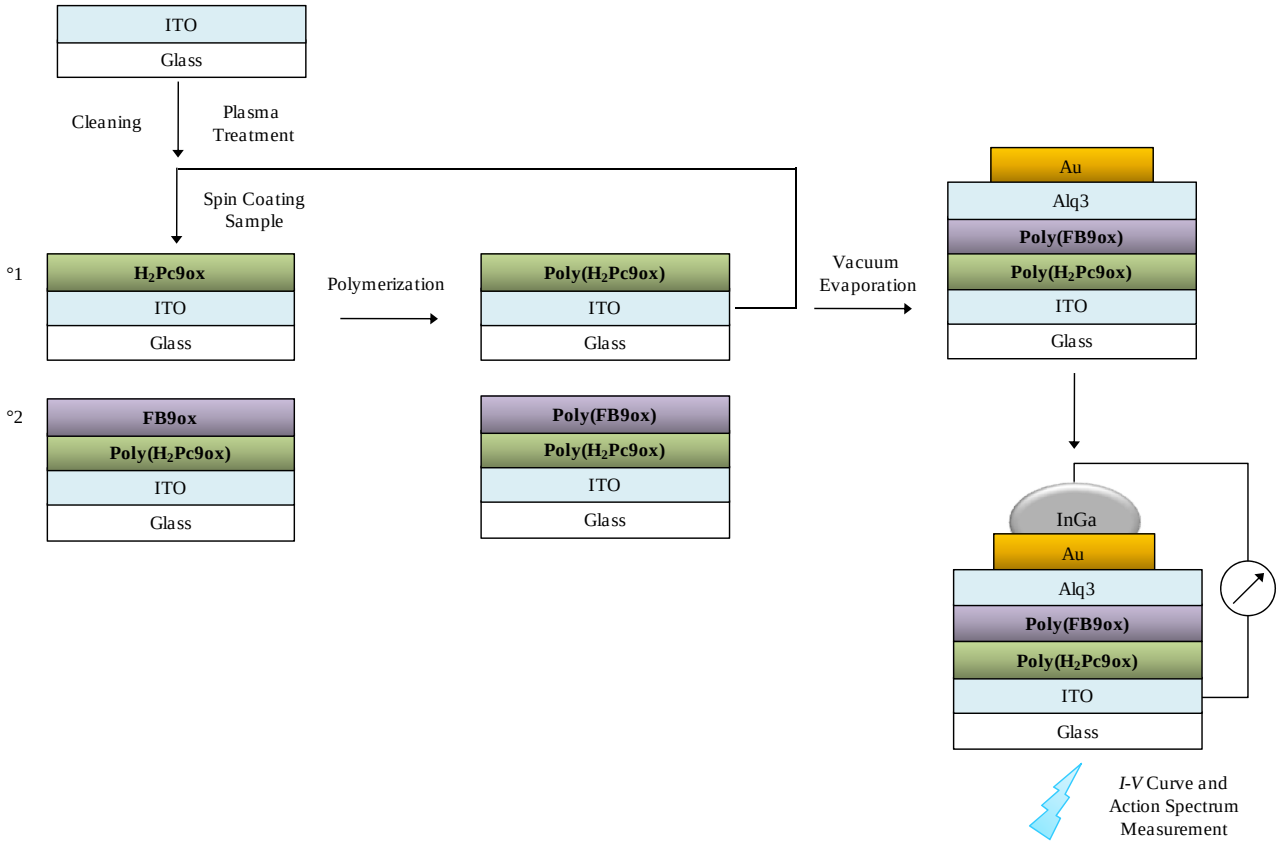

Figure 3.17. Multilayer preparation for photocurrent measurement.

The substrate is cleaned and plasma treated, as depicted in chapter 3.2.2, after which the first film is spin coated immediately and polymerized in a dust free environment, to prevent surface

defects. This can be obtained by sample preparation in open air, but for best results a heated vacuum chamber is used. After the preparation of the first polymer layer the second layer is be spin coated on top, without destroying the bottom layer. The second and possible consecutive layers should be polymerized immediately to prevent dust or grease forming on the interface of the two polymers, rendering the area unsuitable for photocurrent generation. After the preparation of the active layer a thin (~8 nm) hole blocking layer of tris(8-hydroxyquinolinato)aluminum (Alq3) and a gold electrode layer (~50 nm) is evaporated in a vacuum evaporation chamber at high vacuum (below 10^{-5} mbar).[90]

The bilayer samples were prepared as shown in Figure 3.17, where the *p*-type H_2Pc9ox and *n*-type FB9ox monomers were polymerized as separate layers. In the bulk a heterojunction samples H_2Pc9ox and FB9ox were spin coated and polymerized together. In sandwich structures a pure H_2Pc9ox layer was polymerized first, and then a BHJ of H_2Pc9ox and FB9ox and finally a pure FB9ox layer were polymerized before Alq3 and gold evaporation.

3.4.1 Photocurrent Measurement

After the photocurrent samples had been prepared, their current-voltage (*I*-*V*) characteristics were measured. By measuring the current response of the sample cell illuminated under varying voltages, the power conversion efficiency of the cell can be determined. A non-illuminated cell behaves like a diode with little or no current passing through the cell until voltage has increased enough. When the cell is illuminated, the absorbed photons create electrons that may be collected by the electrodes. Short circuit current (I_{SC}) is the current, which flows with zero internal resistance (at $V = 0$, when no bias voltage is applied). Open circuit voltage (U_{OC}) is the voltage when the bias voltage cancels out the photoinduced voltage created by the cell and no current flows through. Fill factor (*FF*) is the maximum power than can be withdrawn from the cell divided by the theoretical power:

$$FF = \frac{P_{MAX}}{I_{SC}\ U_{OC}} = \frac{I_{MAX}\ V_{MAX}}{I_{SC}\ U_{OC}} \tag{3.1}$$

Figure 3.18 shows the schematic diagram of *I*-*V* curves of a photovoltaic cell both in dark and under illumination. The *I*-*V* curve of the illuminated cell is shifted downwards by the amount of photocurrent generated. Maximum power (P_{MAX}) is determined by the point in the curve, where the product of current and voltage ($P = UI$) is the highest. Preferentially this would be close to U_{OC} and I_{SC}, but in practice organic photovoltaics produce their maximum power some ways short of $FF = 1$.

When the *I-V* curve is linear, as was found in many the samples in this work, *FF* is 0.25, where both U_{MAX} and I_{MAX} are half of U_{OC} and I_{SC}.

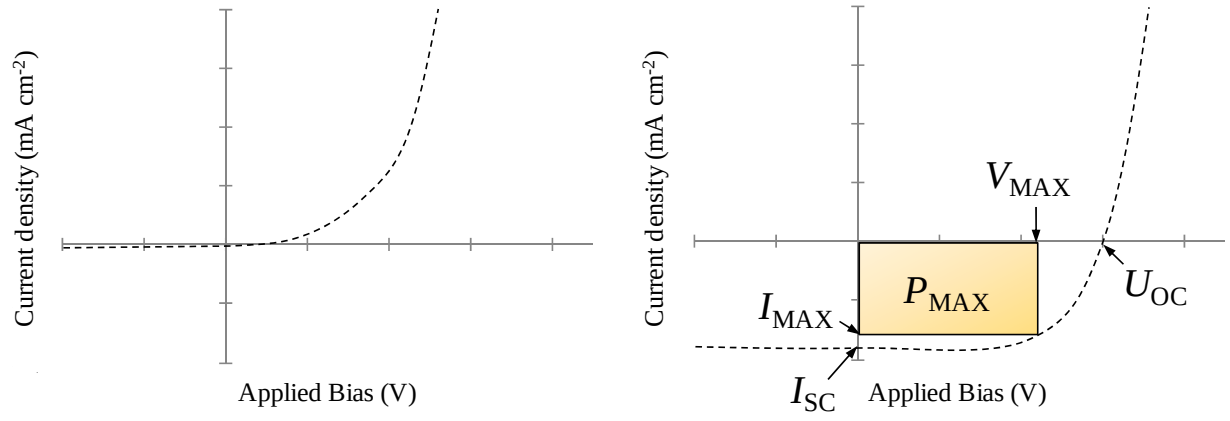

Figure 3.18. Current–voltage (*I–V*) characteristics of an ideal solar cell in dark (left) and under illumination (right).

The power conversion efficiency (PCE) is the ratio of the generated power to the incident optical power (P_0). In the end applications PCE is one of the most important parameters of photovoltaics. In the current work the relative measurement of I_{SC} and U_{OC} between samples played the largest part, as the *in situ* polymerized structures were of proof-of-concept nature and thus produced relatively low efficiencies.

It is essential to know the efficiency of a photocurrent sample at each relevant wavelength. A sample may be very efficient when excited at a specific wavelength, but inefficient overall due to low spectral coverage. When the energy of the absorbed photon and the absorbance of the sample are taken into consideration, the number of electrons created per incident photon, or Incident Photon-to-Current Efficiency (IPCE), can be determined. In action spectrum measurement the samples are illuminated by a monochromatic light source and photocurrent is measured as a function of the wavelength. IPCE is the measure of the internal efficiency, which is especially relevant when studying thin films with small absorptions and/or spectral coverages.

In this work the *I-V* characteristics were measured in a solar simulator Solar Simulator, where the samples were illuminated by a xenon lamp with a filter to match the light source with the solar spectrum.

4 Results and Discussion

This chapter summarizes the essential work leading up to and presented in publications I-IV. Firstly the syntheses of the relevant molecules, as well as the successful syntheses that did not lead to publications, are presented. Secondly the polymerization, both photopolymerization and thermal polymerization, of the fullerene, porphyrin and phthalocyanine derivatives is discussed. Thirdly photocurrent sample preparation and their study are described. Additionally monomer and polymer analyses are shown.

4.1 Synthesis

The initial aim of this study was to find a way toward a photopolymerizable fullerene derivative. The reason for this was partly theoretical, but also practical in the longer run. The design of large, photopolymerizable, chromophores is challenging both from the point of view of synthesis and polymerization, since conventional monomers are significantly smaller than the chromophores of this work, colorless, and resistant to the regular conditions of photopolymerization, especially to UV light.

The newly designed molecules would both have to be synthetically accessible and retain the properties that enable photopolymerization regardless of their high absorptivity in near UV. Soon, however it was realized that if a general method of synthesis of photopolymerizable chromophores was designed, it could lead to further applications in functional thin film preparation. Therefore, the synthetic efforts of the present thesis were directed to develop a convenient and flexible general method of preparation of large aromatic chromophores with polymerizable groups.

4.1.1 Fullerene Derivative

Even more specifically than designing a photopolymerizable fullerene molecule, the very first aim was to incorporate fullerene into a photopolymerizable sol-gel. The idea arose from the growing interest in using photopolymerizable sol-gels in thin film preparation. Photopolymerizable sol-gels provide good mechanical stability and processability required in the coatings industry. It was considered of interest to combine the properties of the sol-gels with those of fullerenes and see whether the resulting polymer would be of use in photovoltaic applications.

The synthetic route to a fullerene derivative, containing a triethoxysilyl group for the sol-gel reaction and a methacrylic group for photopolymerization, and its sol-gel reaction is shown in Scheme 4.1. The synthesis was successful until it was time to attach the methacrylic moiety. ^{1}H NMR of the fullerene precursor (5) (2-hydroxyethyl 1-[3-(triethoxysilyl)propyl]fulleropyrrolidine) is shown in Figure 4.1.

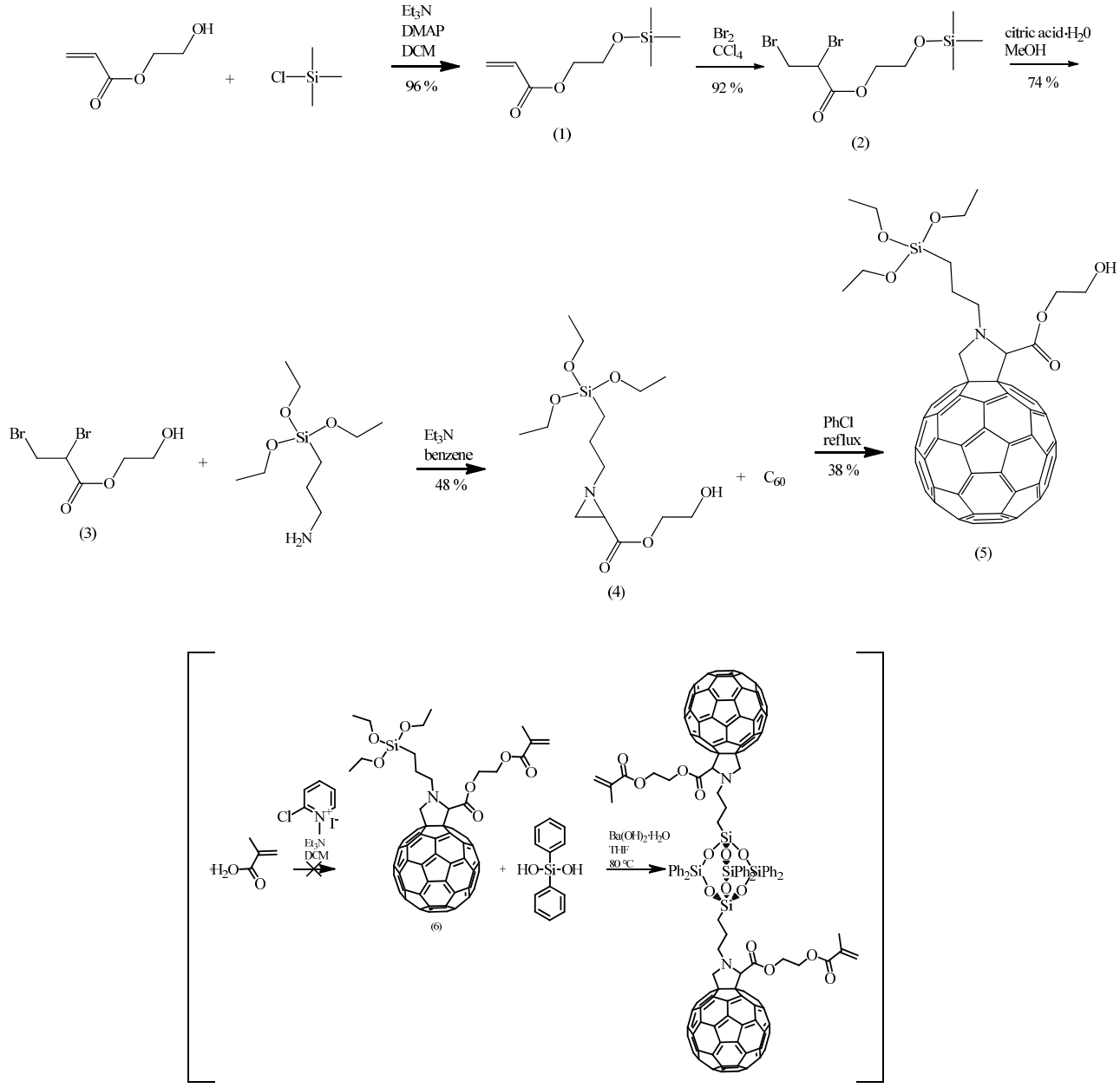

Scheme 4.1. Synthesis of methacrylic tris(ethoxy)silylfulleropyrrolidine sol-gel. The unsuccessful part in square brackets.

Attachment of methacrylic acid was attempted first on the compound (5) with 2-chloro-1-methyl-pyridinium iodide (Mukaiyama reagent), and as it was not successful methacrylation was

attempted several times with the aziridine precursor (4), with (i) methacryloyl chloride, Et_3N, DMAP, DCM, (ii) methacrylic acid, DMAP, DCC, DCM, Mukaiyama reagent (iii) methacrylic acid, Et_3N, , DCM, and (iv) methacrylic acid, Et_3N, benzotriazole-1-yl-oxy-tris-(dimethylamino)-phosphonium hexafluorophosphate (BOP), DCM. None of the reactions were successful despite modifications to the reaction conditions, such as reaction temperature and reagent concentration.

It was concluded that the sol-gel approach would have to wait. Later it was found that working with fullerene photopolymerization, even without the additional complications introduced by sol-gel chemistry, was challenging enough and all later work was done without sol-gels.

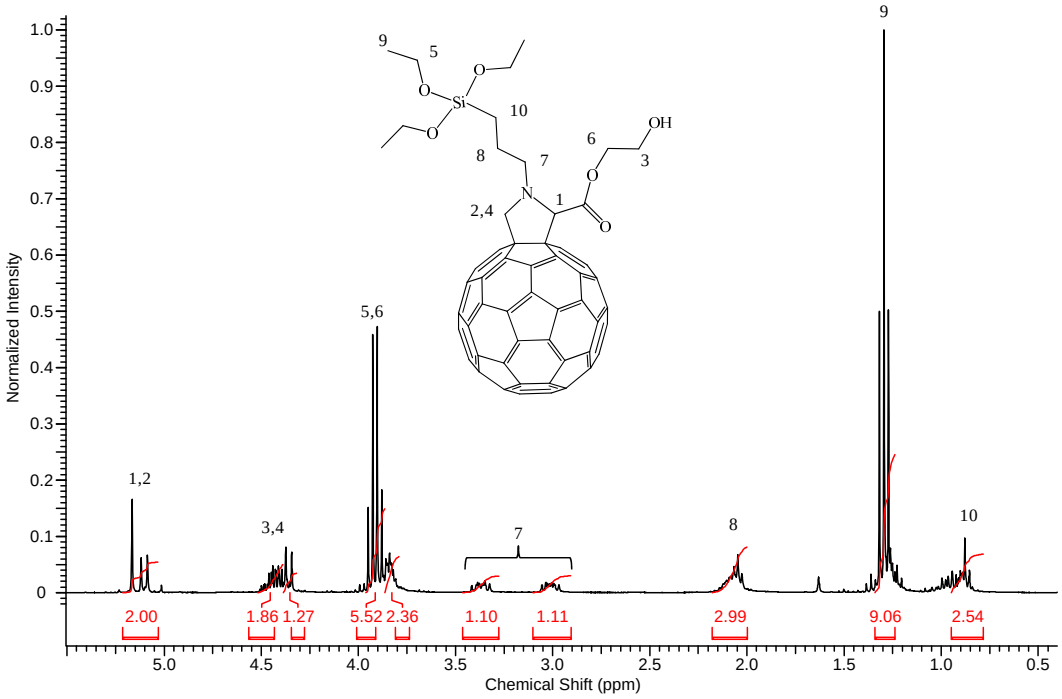

Figure 4.1. ^{1}H NMR of 2-hydroxyethyl 1-[3-(triethoxysilyl)propyl]fulleropyrrolidine.

A simpler version of the fullerene monomer, without an alkoxysilyl group, was designed (Scheme 4.2). The synthesis itself was done in two steps (three if counting the preparation of methacryloyl chloride, which is also commercially available). First 3-(2-hydroxyethoxy)-benzaldehyde was stirred with methacryloyl chloride in dichloromethane (DCM) in the presence of pyridine overnight. Second the product, 2-(3-formylphenoxy)ethyl methacrylate (7) was heated at reflux with N-methylglycine and fullerene in toluene to afford the target, 3-methyl(4-phenoxyethoxy methacrylate)fulleropyrrolidine (8, MPEMF, ^{1}H NMR shown in Figure 4.2.).

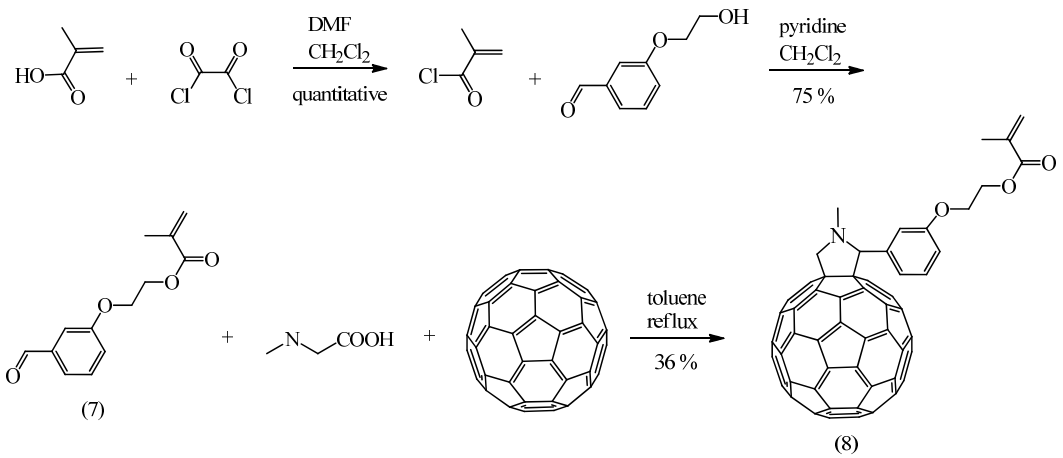

Scheme 4.2. MPEMF synthesis.

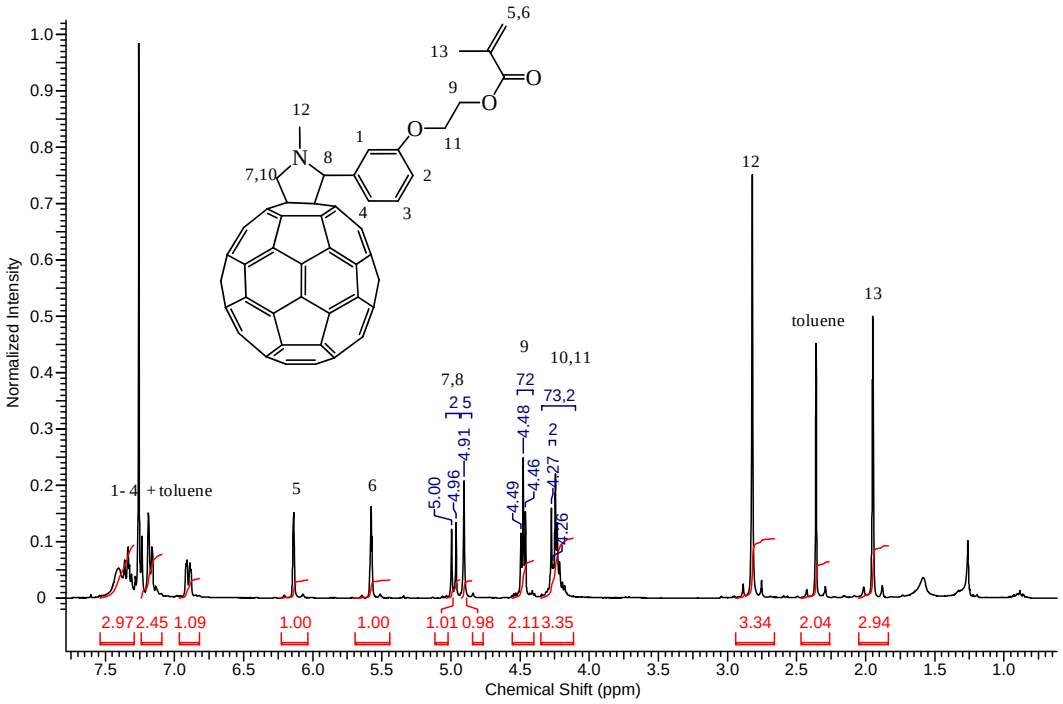

Figure 4.2. ^{1}H NMR of MPEMF.

As the quite extensive photopolymerization experiments conducted with MPEMF did not result in photopolymerization, the design of the monomer was revisited. The MPEMF monomer was crystalline at room temperature, which meant that a film made thereof could only polymerize if the methacrylic moieties were packed closely together to account for the loss of monomer mobility (liquid molecules are in motion, whereas crystalline molecules can vibrate at most). As no way was seen to enable the polymerizable groups to pack together when dealing with a molecule with a bulky fullerene moiety, the only way to achieve a polymerizable fullerene monomer was to make it liquid.

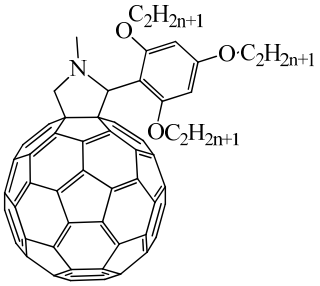

n = 8, 12, 16 or 20

Figure 4.3. (a) Structure of the liquid Michinobu C_{60} derivative.[52]

In 2006 Michinobu *et al*. published the synthesis of a liquid fullerene monomer (Figure 4.3).[52] The molecule consisted of a phenylfulleropyrrolidine with three alkyloxy groups attached to the phenyl moiety at 2,4,6-positions. The derivative with three dodecoxy moieties linked to phenylfulleropyrrolidine was the smallest liquid molecule. The synthesis allowed for easy modification of the alkylic groups, enabling the synthesis of a liquid fullerene molecule capped with polymerizable moieties

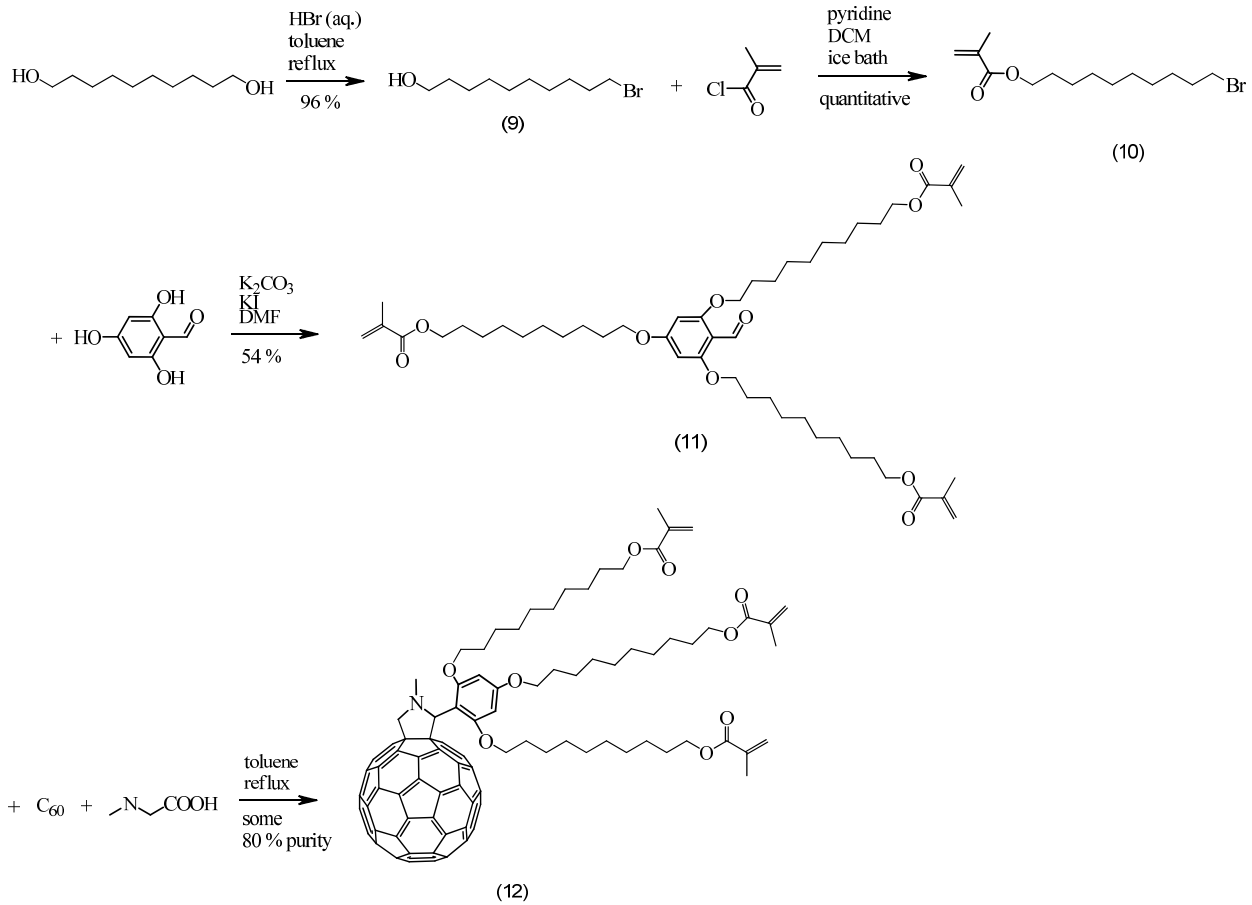

Scheme 4.3. MT10MF synthesis by the first pathway.

The new monomer was designed with the alkoxy groups replaced by alkoxy methacrylates, which would introduce only one additional step (Scheme 4.3). The synthesis was simple and produced a liquid fullerene monomer in good quantity. There was, however, a problem of the purification of the final product, 3-methyl(1,3,5-triyltrisdecane10,1-diyl)tris(2-methacrylate)fulleropyrrolidine (12, MT10MF). The chromatographic procedure used could not separate the benzaldehyde precursor (11) from the product in one run. After repetitive isolations the column retained most of the target product, leaving a small sample of 80 % purity by ^{1}H NMR. Therefore a new synthetic pathway was attempted (Scheme 4.4), where Prato reaction with fullerene was conducted before methacrylation to avoid self polymerization and loss of product during column purification. The new synthetic route was a success and produced MT10MF as a black tarry liquid (^{1}H NMR shown in Figure 4.4.). However the problem of self-polymerization persisted. The compound MT10MF was unstable and could not be stored for any prolonged time

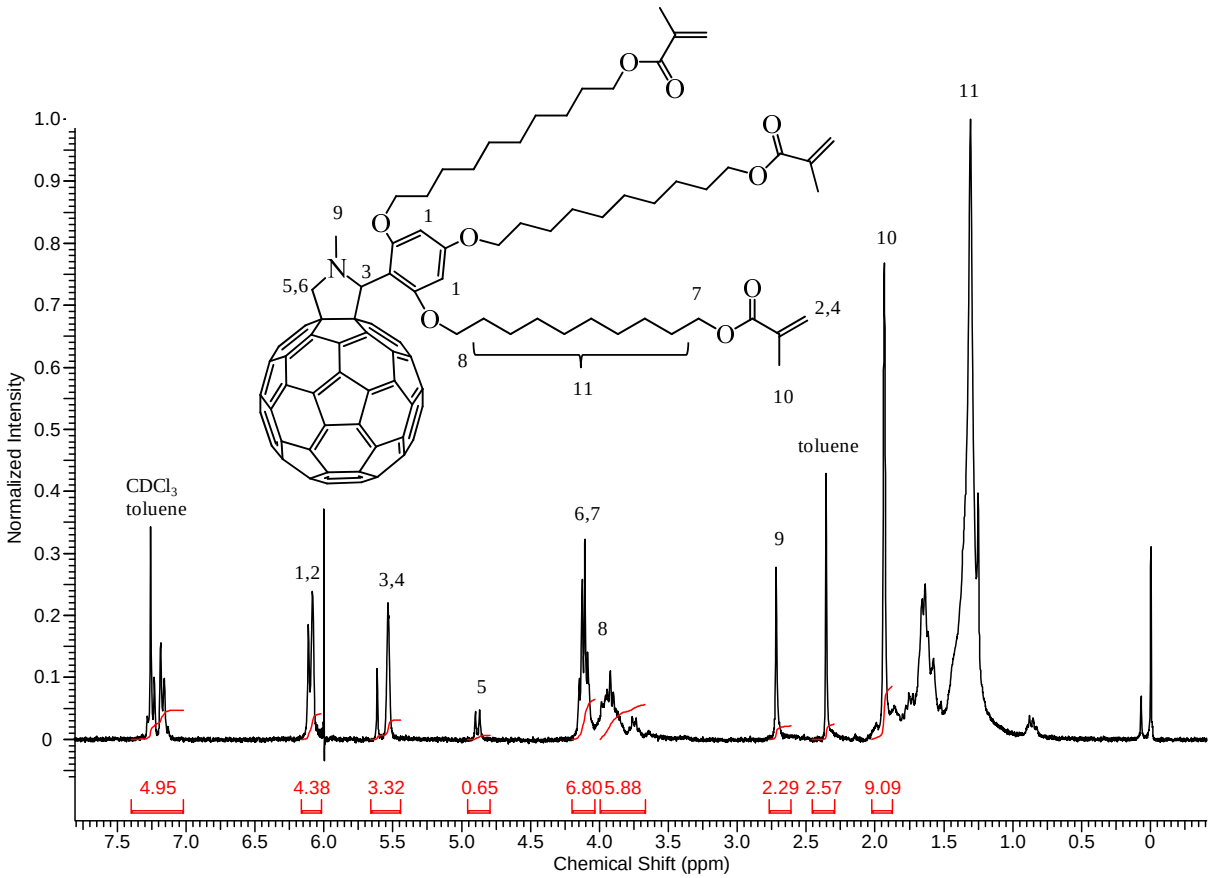

Figure 4.4. ^{1}H NMR of MT10MF.

This posed a surprising problem: the reactivity of the monomer made the polymerization analysis very difficult, as it would polymerize spontaneously, but polymerization was still inhibited

by oxygen in thin films. However, as the synthetic route was easily adapted to other polymerizable groups, new functional moieties were tested.

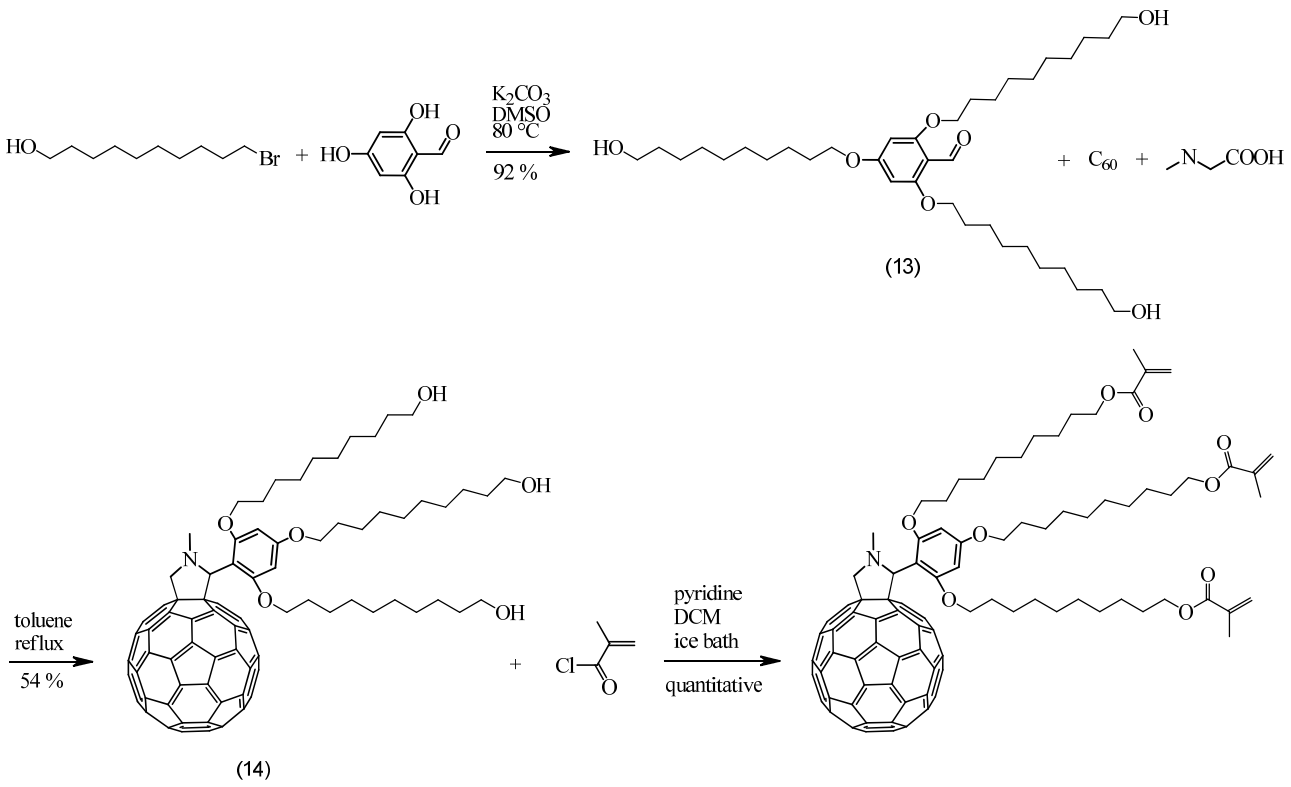

Scheme 4.4. MT10MF synthesis by the second pathway.

Cationic polymerization requires a strong acid to initiate and thus is not prone to self-initiate, neither to oxygen inhibition. Literature review revealed two serious candidates for polymerizable moieties: oxirane (traditionally called epoxy) and oxetane rings. Synthesis of the liquid oxetane-functionalized fullerene derivative is shown in Scheme 4.5. Addition of the oxetane group was conducted in a mixture of hexane and 50 % aqueous NaOH, with tetrabutylammonium bromide as a phase transfer catalyst, with a 40 % yield of compound 15, which is relatively good considering possible bis-addition. The attachment of 15 to trihydroxybenzaldehyde proceeded well (84 % yield), but the final Prato reaction produced the compound 17 with a modest 28 % yield.

The synthesis of the oxirane derivative (FB9ox) is published in paper I and shown in Scheme 4.6. The oxirane moiety was formed by epoxidation of 11-bromoundecene with *meta*-chloroperbenzoic acid (MCPBA) in DCM on ice bath with a quantitative yield. The two final steps were conducted with 96 % (product 18) and 81 % (product 19) yields, respectively. FB9ox was decided to be tested more closely, as it could be synthesized with a high yield. FB9ox was studied

in papers I and IV. The oxetane monomer, despite being available, was left for future studies, as the analysis of FB9ox and its photopolymerization took considerable time.

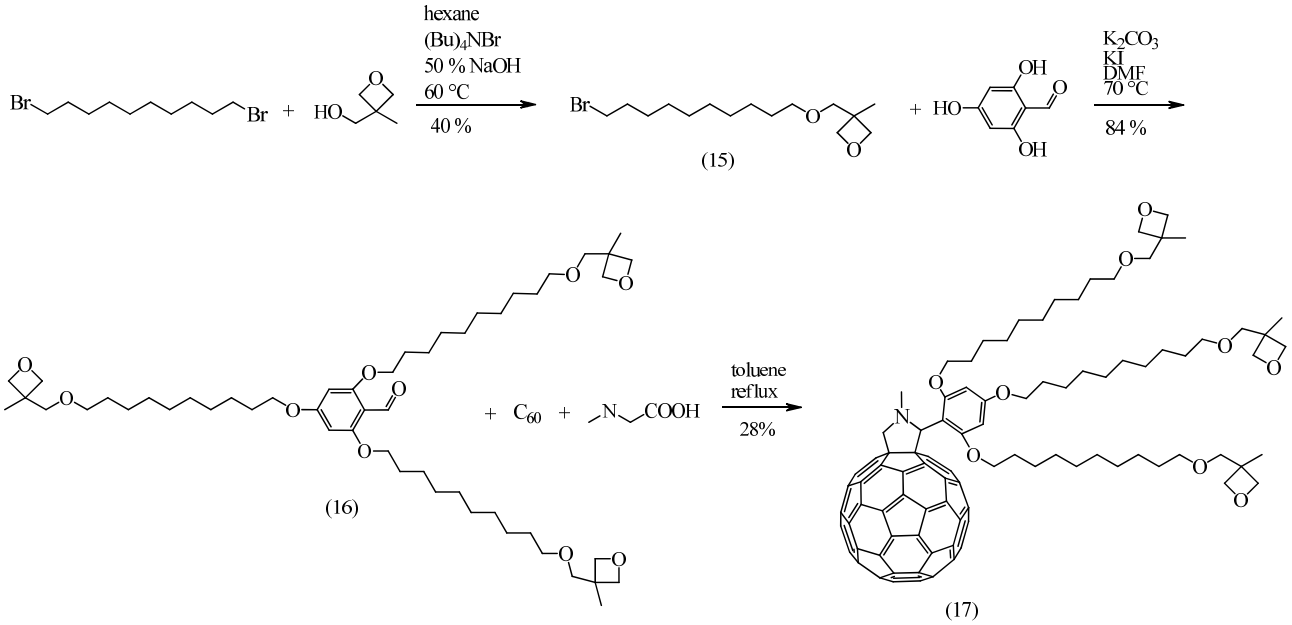

Scheme 4.5. Liquid tris(alkyloxetane)fullerene synthesis.

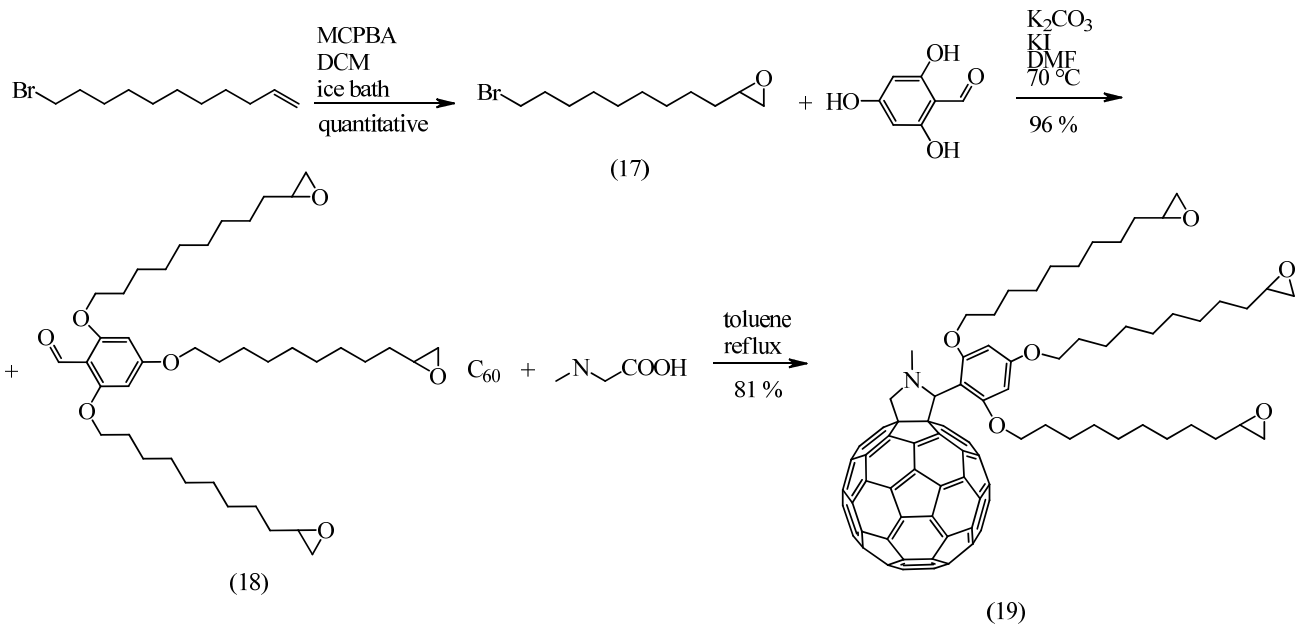

Scheme 4.6. Liquid tris(alkyloxirane)fullerene (FB9ox) synthesis.

The purification of all of the fullerene derivatives required very careful control of the chromatographic systems, as the fullerene derivatives and the benzaldehyde precursors had very similar retention factors. The ultimate purity of the products was monitored by ^{1}H NMR spectra, by

making sure that the integrals of the peaks relating to the product match. Of especial importance were the pyrrolidine protons, which were the main indicator of the existence of the fullerene moiety, which itself is not visible in ^{1}H NMR.

The fullerene derivatives (5), (8), (12) and (19) all have properties that are of interest, as they can be used in polymerization reactions, and will be used in future studies.

4.1.2 Phthalocyanine Derivative

The work conducted on the liquid fullerene derivative showed that it was possible to synthesize photopolymerizable chromophores. The applicability of alkyloxirane capping on other chromophores was tested on the synthesis of a photopolymerizable phthalocyanine monomer.

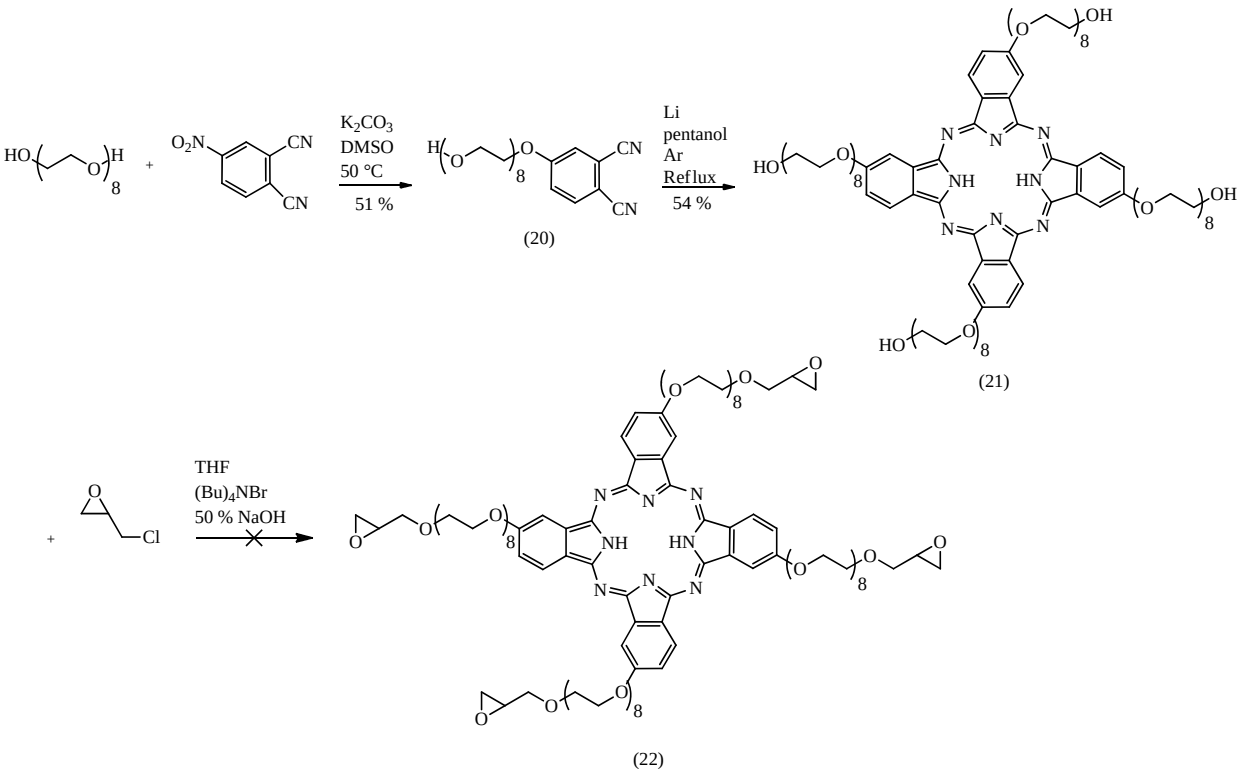

Scheme 4.7. First synthetic pathway for 2,9,16,24-tetrakis{[1-(oxiran-2-yl)-2,5,8,11,14,17,20,23-octaoxapentacosan-25-yl]oxy}-29*H*,31*H*-phthalocyanine.

Literature review showed a large amount of liquid crystalline phthalocyanine derivatives, but far fewer liquid phthalocyanine derivatives.[54-59] All of the published liquid phthalocyanines were tetra or octa substituted polyethylene glycol (PEG) derivatives of phthalocyanine. Thus a phthalocyanine derivative with four octaethylene glycol tails capped with oxirane units was designed (Scheme 4.7).

At first the synthesis was attempted with PEG400, a polyethylene glycol mixture of with an average molecular weight of 400 g/mol, translating with ca. 9.5 ethylene glycol units per molecule.[53,55,58] Soon it was found that pure octaethylene glycol would have to be used for proper purification of the target compound. Tetrakis(octaethylene glycol)phthalocyanine (21) was therefore synthesized, but its further reaction with epichlorohydrin was not possible, despite several modifications of the reaction conditions.[91-93]

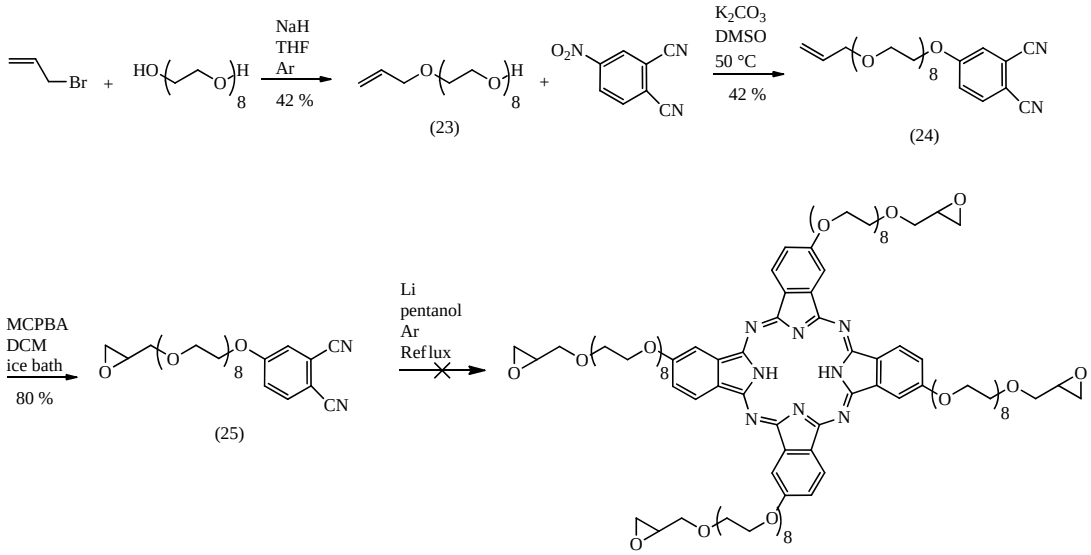

Scheme 4.8. Second synthetic pathway for 2,9,16,24-tetrakis{[1-(oxiran-2-yl)-2,5,8,11,14,17,20,23-octaoxapentacosan-25-yl]oxy}-29*H*,31*H*-phthalocyanine.

The epichlorohydrin attachment was also attempted on the phthalonitrile precursor (20) and on octaethylene glycol, but as neither reaction was successful, a wholly new synthetic pathway was developed for the same end product (22), shown in Scheme 4.8. 3-Bromopropene reacted with octaethylene glycol with a decent yield of 42 % and the product (23) was further reacted with 4-nitrophthalonitrile producing compound (24) with 42 % yield. Epoxidation of (24) was a bit slower than for previous reactions, but an 80 % yield was still achieved. Unfortunately, tetramerization of epoxyphthalonitrile (25) was not successful. The formation of phthalocyanine macrocycle was accompanied by polymerization of epoxy groups, thus no individual monomeric phthalocyanine could be isolated from the reaction mixture.

Propene-terminated phthalonitrile (24) tetramerized into phthalocyanine (26) with good yield. However, further treatment with MCPBA resulted in fast and complete destruction of the macrocycle (Scheme 4.9).

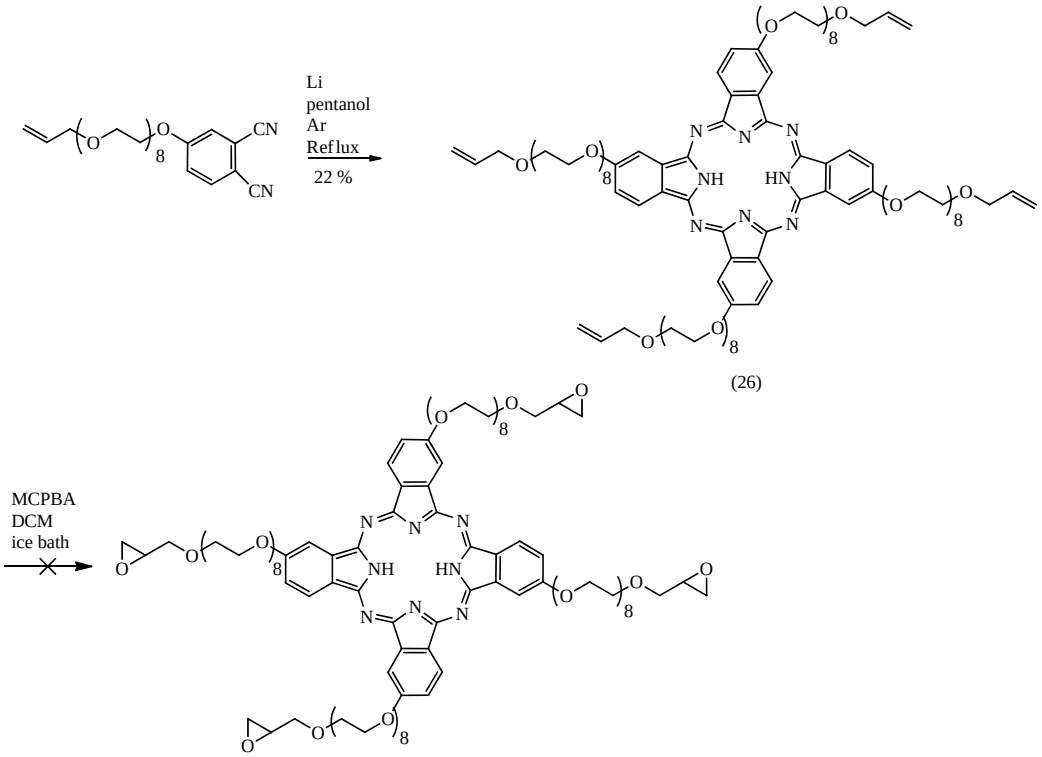

Scheme 4.9. Third synthetic pathway for 2,9,16,24-tetrakis{[1-(oxiran-2-yl)-2,5,8,11,14,17,20,23-octaoxapentacosan-25-yl]oxy}-29*H*,31*H*-phthalocyanine.

After the first attachment of the epichlorohydrin failed, a parallel synthesis of an alkyloxirane derivative of phthalocyanine was designed (Scheme 4.10). The synthesis was successful, with relatively good yields. The major problem however was that the target phthalocyanine was crystalline and as such not suitable for photopolymerization.

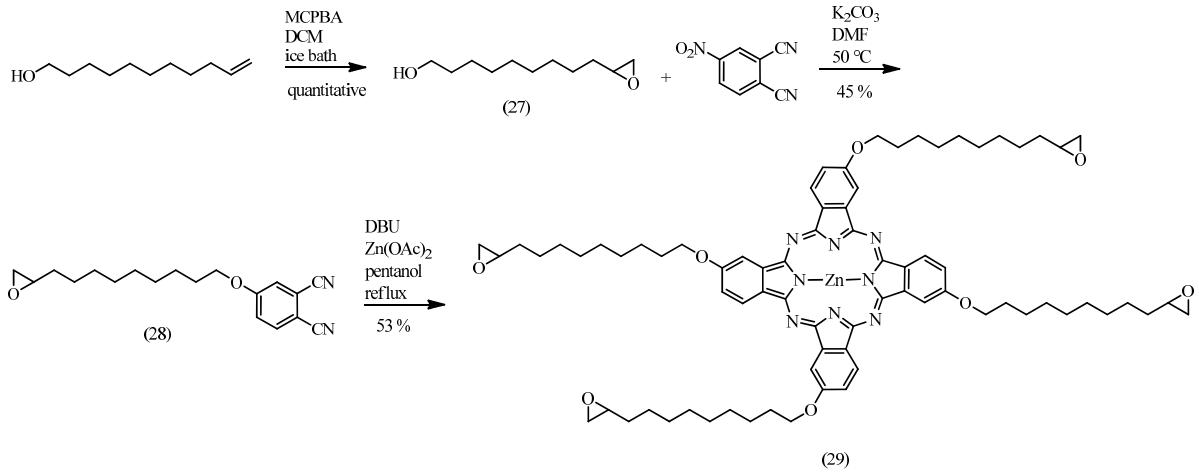

Scheme 4.10. Synthesis of [2,9,16,23-tetrakis{[9-(oxiran-2-yl)nonyl]oxy}-29*H*,31*H*-phthalocyaninato(2-)-k^2N^{29},N^{31}]zinc.

The phthalocyanine formation generally requires a lithium alkoxide solution, which opens the oxirane rings. Indeed, synthesis without lithium was possible in the case of tetra(alkyloxirane) phthalocyanine, but DBU activation is not always applicable. On the other hand the *meta*-chloroperbenzoic acid used in epoxidation of the double bond destroys the macrocycle. Evidently the synthesis of the polymerizable phthalocyanine would have to be split into two halves: the one with the phthalocyanine macrocycle formation and the one with the formation of the polymerizable group (epoxidation in this case). After the two limiting steps, the two parts should be connected with a mild reaction. Esterification was considered the best option, as very good reagents enabling near quantitative reactions with chromophores or large molecules exists.[94-97]

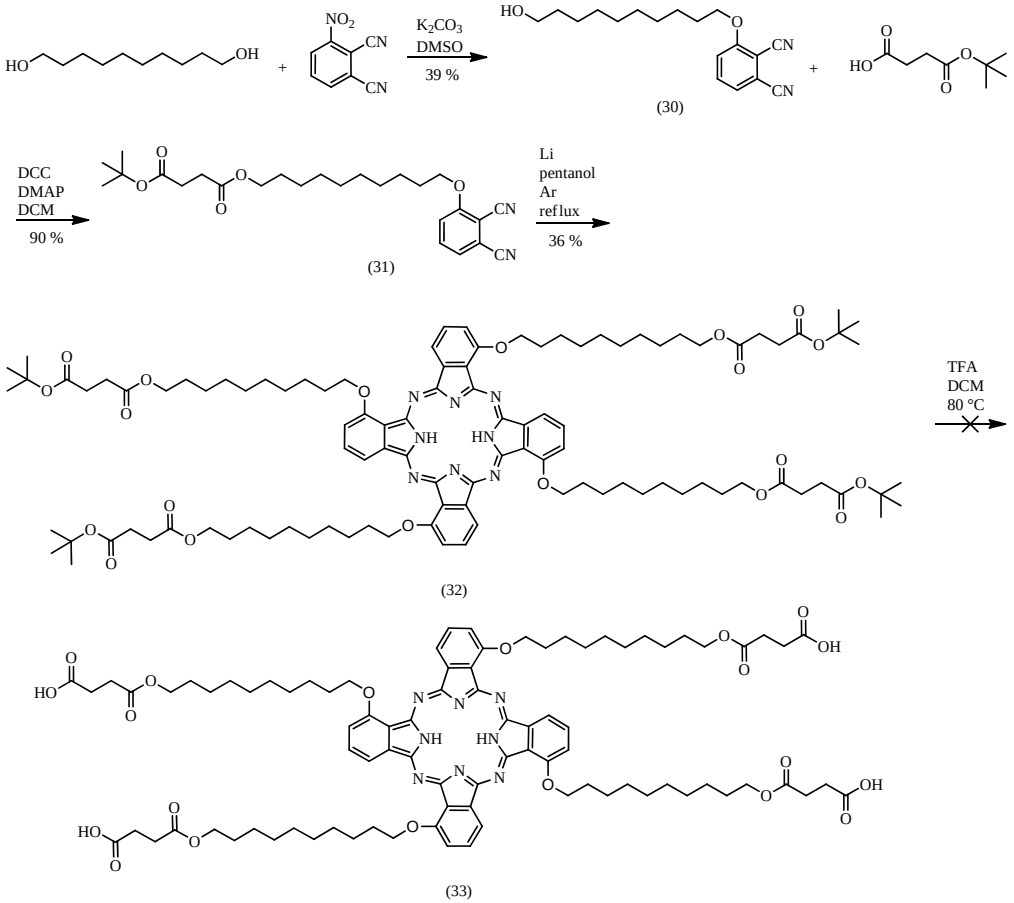

Scheme 4.11. Synthesis of 4,4',4",4"'-[29*H*,31*H*-phthalocyanine-1,8,15,22-tetrayltetrakis(oxydecane-10,1-diyloxy)]tetrakis(4-oxobutanoic acid).

Acylation of tetra(octaethylene glycol)phthalocyanine (21), with mono-*tert*-butyl succinic acid was attempted first to yield a molecule that could be reacted with 9-hydroxynonyloxirane (27) after deprotection. Even though the esterification itself was possible, the target molecule was so hard to separate from the mono- bis- and tris-adducts by column, including the fact that a further

deprotection and esterification with the 9-hydroxynonyloxirane were still required, it was decided that a whole new synthetic route would be more reasonable.

A synthesis of an alkyloxyphthalocyanine that would be connected with 9-hydroxynonyloxirane by a succinic bridge was devised (Scheme 4.11). The synthesis was possible up until the deprotected succinic phthalocyanine (33), but due to difficulties with purification, the synthetic pathway was modified so that the succinic moiety would be attached first to 9-hydroxynonyloxirane and only after that to tetra(10-hydroxydecoxy)Pc (Scheme 4.12). As trifluoroacetic acid used for deprotection also opens the oxirane ring, the deprotection had to be conducted before epoxidation. The *tert*-butyl succinic moiety would be attached first to 10-undecenol, deprotected and only after that epoxidized. Unfortunately the reactivity of the long succinic alkyloxirane (37) was rather poor and only a monoadduct could be obtained.

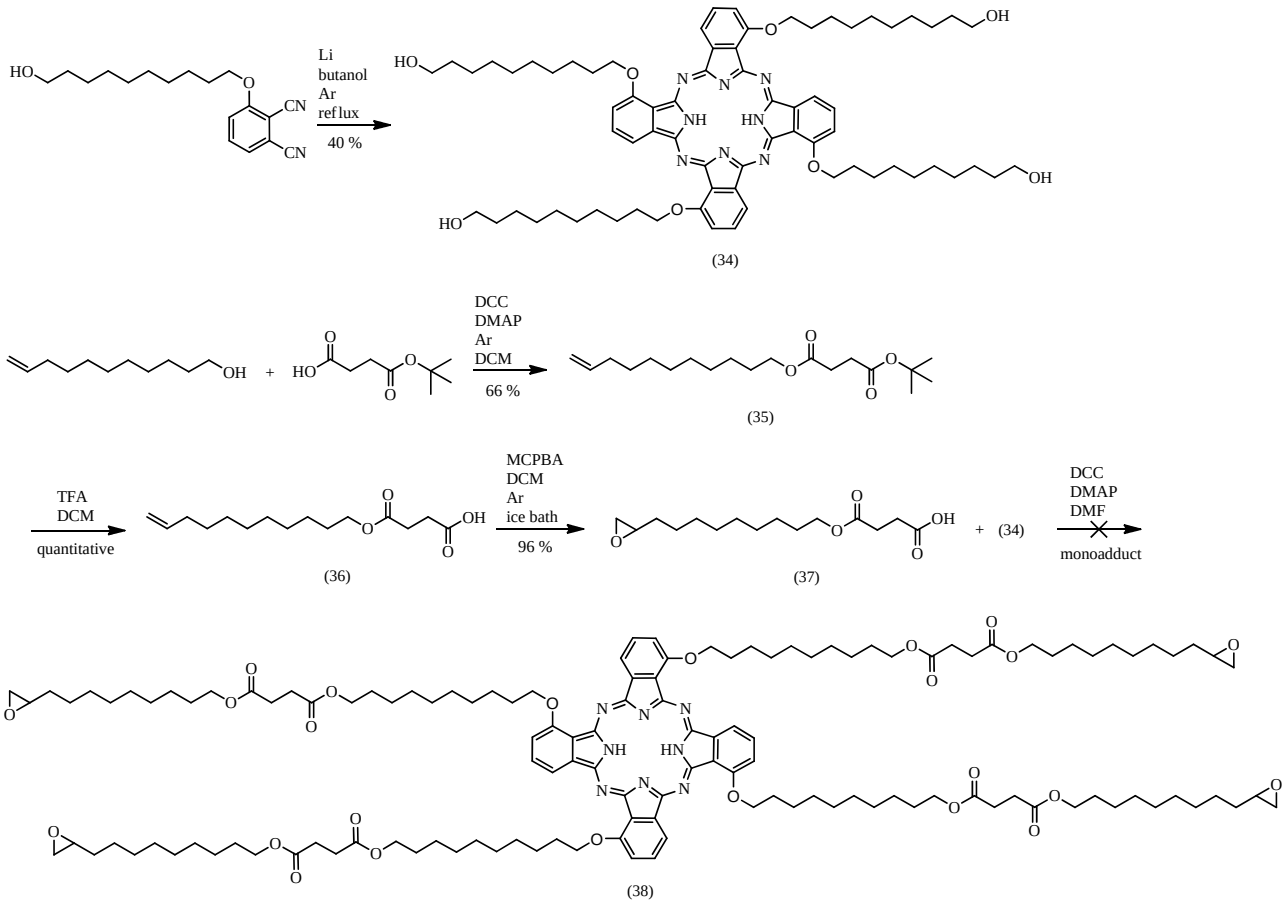

Scheme 4.12. Synthesis of 4,4',4",4"'-tetrakis[9-(oxiran-2-yl)nonyl] 1,1',1",1"'-[29*H*,31*H*-phthalocyanine-1,8,15,22-tetrayltetrakis(oxydecane-10,1-diyl)] tetrasuccinate.

As the final esterification step of Scheme 4.12 was rather inefficient, the bulky succinic alkyloxirane (37) was replaced with a smaller alkyloxiranoic acid. 9-Oxiranyl-nonanoic acid (ONA,

39 in Scheme 4.13) is the longest alkyloxiranoic acid that can easily be synthesized, so it was chosen. ONA synthesis from undecenoic acid has already been published, using peracetic acid.[98] The epoxidation reaction had a conversion of 80 % and the yield after purification was 17 % (15 g of 70 g of crude product inserted into column).

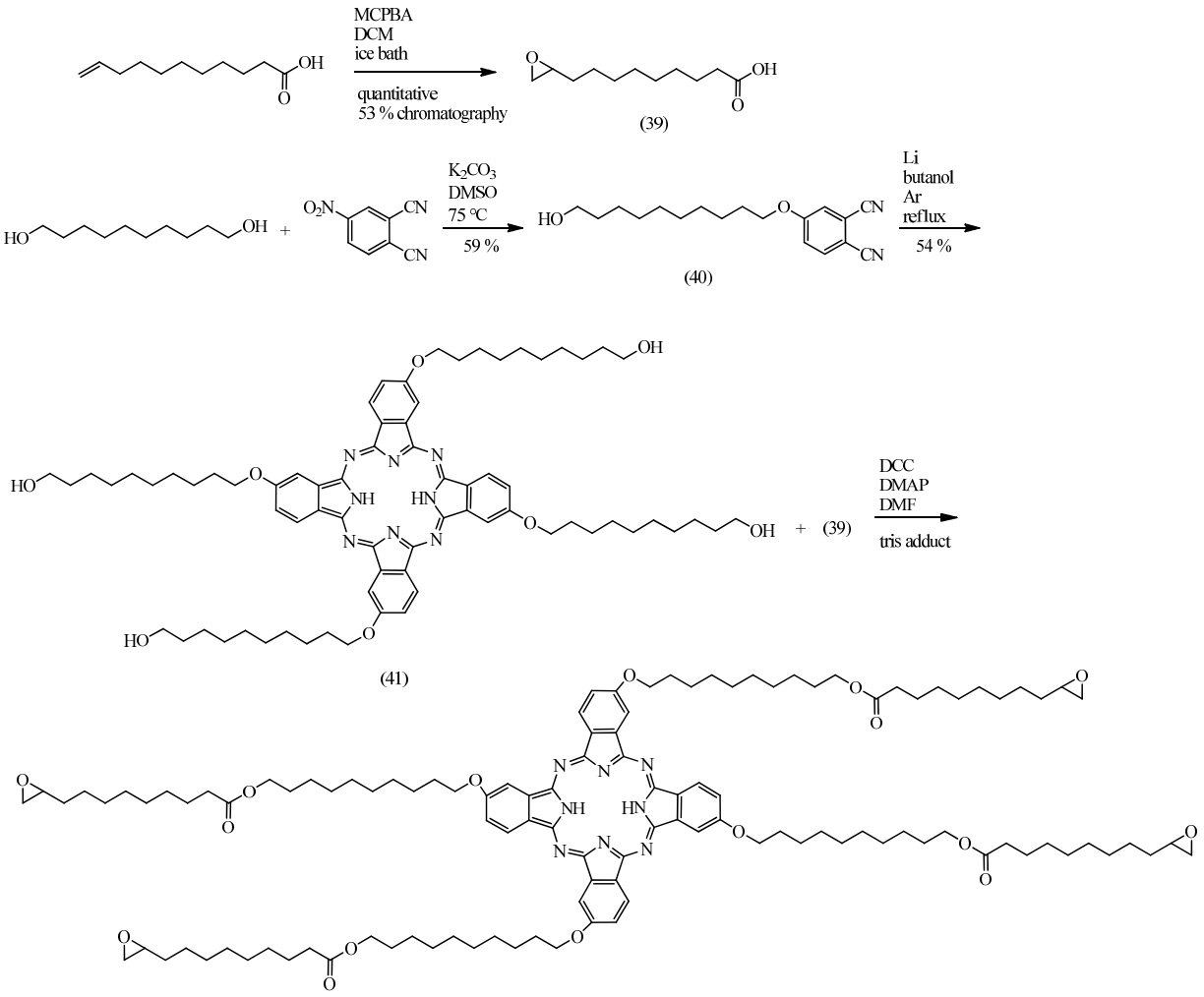

Scheme 4.13. Synthesis of 29*H*,31*H*-phthalocyanine-2,9,16,23-tetrayltetrakis(oxydecane-10,1-diyl) tetrakis[9-(oxiran-2-yl)nonanoate]

When undecenoic acid was epoxidized with metachloroperbenzoic acid the conversion of the reaction was quantitative (the crude product had no double bond peaks left in ^{1}H NMR). The column chromatography of the product was challenging, though. As the purification consisted of separating two acids, the product and metachlorobenzoic acid, and both come in broad bands in the column and have very similar retention times, the chromatography had to be very precise. An added difficulty is that the detection of metachlorobenzoic acid in the target mixture was only possible by ^{1}H NMR. However with flash chromatography the product could be purified with 53 % yield using

a very narrow gradient of MeOH in DCM. Now tetrakis[β(10-hydroxydecyl)oxy]phthalocyanine (41) could be acylated with ONA, however the reaction still produced only trisadduct at best.

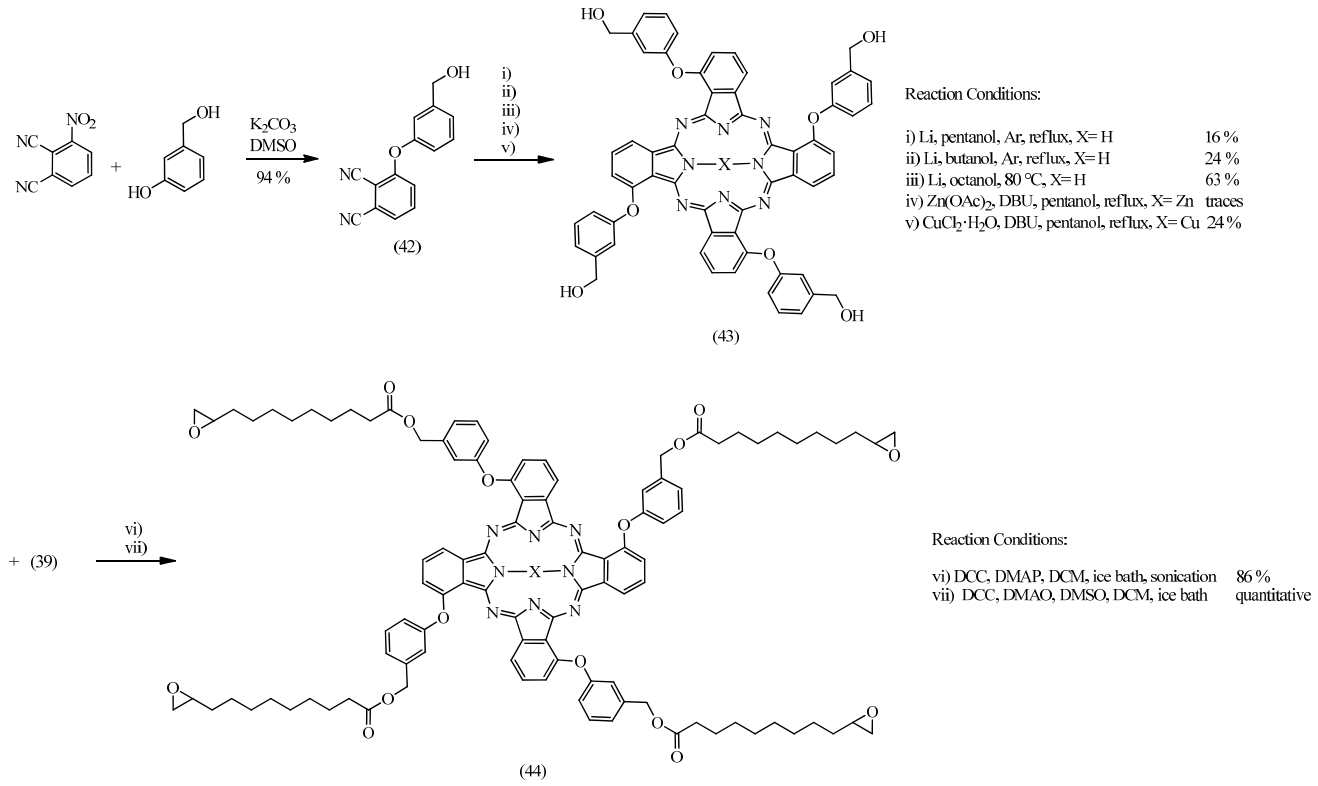

Scheme 4.14. Synthesis of 29*H*,31*H*-phthalocyanine-1,8,15,22-tetrayltetrakis(oxy-3,1-phenylenemethylene) tetrakis[9-(oxiran-2-yl)nonanoate] (H_2Pc9ox).

As the phthalocyanine product (41) was very bulky and hard to purify, a new phthalocyanine core (43) specifically designed for esterification[99] was tested. ONA was used with compound (43) with good results (Scheme 4.14). The synthesis begins with S_NAr reaction of 3-methoxyphenol and 3-nitrophthalonitrile to yield 3-(3-hydroxymethylphenoxy)phthalonitrile (42) in near quantitative yield. Refluxing of (42) in lithium pentoxide/pentanol or lithium butoxide/butanol solution both gave phthalocyanine (43) in modest yields (16 % and 24 %, respectively) and as isomeric mixtures. Heating of (42) at 80 °C in lithium octoxide/octanol gave (43) in 63 % yield in high isomeric purity. Reaction with DBU and $Zn(OAc)_2$ in pentanol at reflux gave only traces of the zinc complex, but reaction with DBU and $CuCl_2$ in pentanol gave the copper complex in 24 % yield. Reaction with ONA suffers from poor solubility of tetrahydroxyphthalocyanine precursor in DCM, which is a mandatory solvent for this esterification. Thus, reactions in DMF or THF resulted in much lower yields despite much better solubility of the starting material. Two routes were found that produced

the esterified product in good yield, either to keep the solution on ultrasonic bath, for several hours, which was rather cumbersome, or to add a drop of DMSO to aid the solubility of (43). Tetrakis[α(2-methoxyphenyl)(9-oxirane)nonanoate]phthalocyanine (H_2Pc9ox) and its copper complex was studied in paper IV.

4.1.3 Porphyrin Derivative

From the synthetic point of view, the design of the porphyrin monomer was the easiest task. As the phthalocyanine monomer had been synthesized, the same modular approach was applied to porphyrin.

Porphyrins are less used in organic photovoltaic cells striving for good efficiency (apart from its recent growth in interest as a sensitizer in dye sensitized solar cells).[100,101] However as due to its very high extinction coefficient and good electron-donating ability, porphyrins have been extensively studied as model compounds for organic photovoltaics[102,103] and sensors.[104,105] An easily accessible porphyrin derivative (45) with four hydroxyl groups, was used for acylation with ONA (Scheme 4.15).[78]

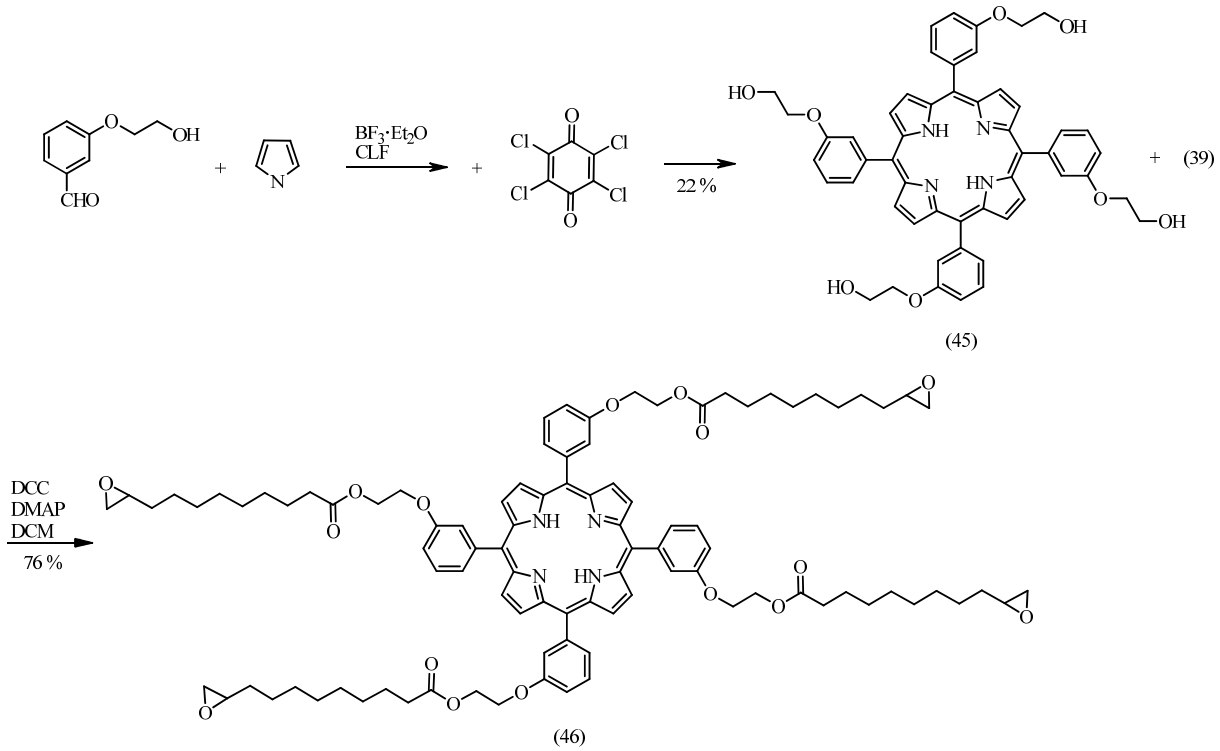

Scheme 4.15. Synthesis of tetrakis-[3(2-Hydroxyethoxy-2-(9-Oxirane)Nonanoate)Phenyl]Porphyrin (TAEP).

Hydroxyethoxybenzaldehyde was reacted with pyrrole in the presence of boron trifluoride etherate to yield porphyrinogen, which was oxidized with para-chloranil into tetrakis(hydroxyethoxyphenyl)porphyrin (45). The next step was nearly identical to phthalocyanine acylation, producing tetrakis-[3(2-hydroxyethoxy-2-(9-oxirane)nonanoate)phenyl]porphyrin (TAEP) in good yield (76 %).

Despite the ease of synthesis, the porphyrin monomer had some unique properties, which are described in papers II and III. The most remarkable one is that the porphyrin monomer can co-initiate its own photopolymerization.

4.2 Monomer Analysis

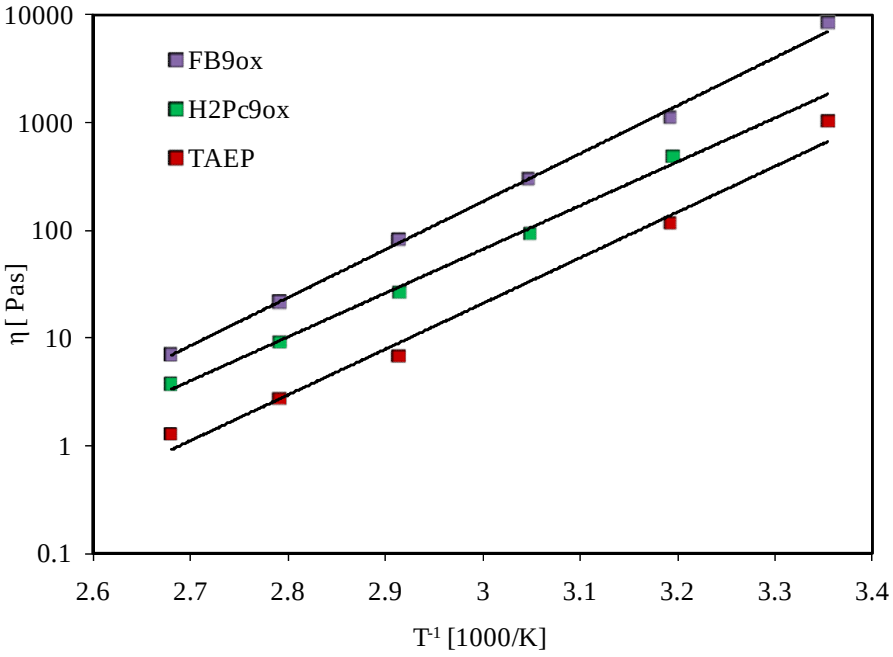

Figure 4.5. Arrhenius plot of the fullerene, porphyrin and phthalocyanine monomer viscosities.

The monomers had to be analyzed to determine the conditions required for polymerization. UV-Vis and IR spectra were measured as a reference for the polymerization analysis. DSC graphs of the monomers revealed their glass transition temperatures, which correlate to their minimum operational temperature. The highest T_g value of 5 °C was for the fullerene monomer (19), while the porphyrin (46) and phthalocyanine (44) monomers had much lower T_g values of -23 °C and -35 °C, respectively. This, however, was not yet enough to determine an appropriate temperature for polymerization, as the viscosity of the monomers was still unknown. Rheological measurements

(Figure 4.5) showed that all of the monomers behaved as Newtonian liquids and had very high viscosities, even at elevated temperatures. Thus at 100 °C all of the viscosities fall between 7 and 1 Pa·s, which is still just above the limit at which polymerizations are usually conducted. On the other hand, the temperature of 100 °C is also very close to the level, where the initiators used for photopolymerization cleave thermally.

4.3 Thin Film Polymerization

The initial polymerization results indicated that all of the thin film polymerization experiments would have to be conducted on rigid and even substrates, such as glass or quartz. Hexafluoroantimonate salts of diaryliodonium have been shown to produce strong enough photoacid for the photopolymerization of relatively large monomers used in OLED fabrication.[7-9] The chosen initiator was p-(octyloxyphenyl)phenyliodonium hexafluoroantimonate (OMAN071). Of the visible light co-initiators curcumin was chosen due to its proven efficacy and availability.[11,81] Most of the polymerizations were conducted near or above 100 °C, where the viscosity of the monomers is in the range of that of regular monomers.[79,83]

4.3.1 Porphyrin Photopolymerization

A specific limitation with thin film polymerization has been its analysis: the thinner the polymerized films get, the harder they are to analyze. Up to now most publications presenting polymerized film of sub-micrometer scale have studied polymerization by AFM or optical microscopy.[7,106,107] Neither of these methods indicate changes in the chemical structure of the films (opening of the monomer moieties). If the polymerization reaction is difficult and the yields are low, such images show nothing of the chemical nature of the film. Thus it would be beneficial to analyze thin film polymerization by other means.

The results of the thin film polymerization of porphyrin (44) will be discussed first, because the porphyrin monomer enables a much more detailed study of photopolymerization and greatly assists in analyzing other polymerizations.

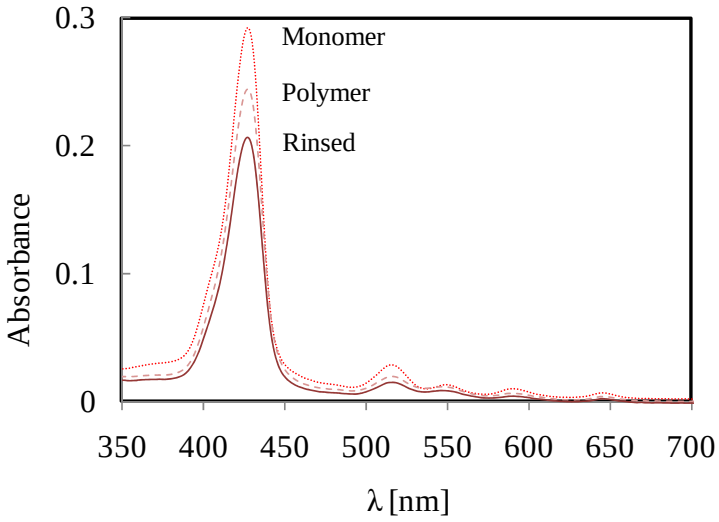

Figure 4.6. UV-Vis spectra of a ca. 10 nm TAEP film: before and after polymerization and after rinsing the monomer residue from the polymer.

At first the porphyrin thin film polymerization samples were prepared by spin-coating a solution of TAEP and initiator OMAN071 in chloroform onto a glass plate, cleaned with sulfochromic acid. Because of its high extinction coefficient, the ca. 10 nm film had a strong and sharp absorption peak at 430 nm (Figure 4.6). As the polymerization of TAEP results in a cross-linked polymer, the film is not soluble in the chloroform after polymerization. Therefore, for all the samples the UV-Vis spectra were collected three times: before and after polymerization, to determine whether polymerization affected the sample absorbance, and after rinsing the polymerized film in chloroform, to dissolve and remove all unreacted monomer (Figure 3.10).

During the polymerization experiments the following parameters were varied: substrate temperature; speed of heating; illumination time and wavelength (UV and visible); atmosphere (ambient, N_2 and Ar); concentration of the co-initiator (curcumin).

The nature of substrate and the method of surface treatment play an important role. Thus the parameters that produced only minor polymerization on glass yielded a quantitative polymerization on quartz.

When the substrate was changed to ITO covered glass, the results were initially just as poor as with the glass substrates. However after improving the cleaning procedure and activating the surface by nitrogen plasma treatment, the polymerization results were almost as good as with quartz. Additionally when the same surface treatment was applied to the quartz substrate, the polymerization was even faster. However the same treatment did not seem to have any effect on the glass substrates. The full nature of the quality of the surface and the effect of surface treatment should be studied more thoroughly with AFM, SEM and other methods of surface analysis, but for

this work only an initial analysis was conducted by AFM. It does seem that proper polymerization requires full wetting of the surface, for which an absolute prerequisite is good smoothness of the substrate. The surface treatment for hydrophilicity improves wetting even further.

The polymerization could be conducted at 90 °C, where no major thermal polymerization occurs. It was found that UV illumination could initiate photopolymerization, but even a rather short exposure partly bleaches the monomer. If the film was illuminated with visible light, polymerization was slower, but still possible. A rather surprising finding was that no co-initiator was needed for visible light photopolymerization, *i.e.* TAEP would co-initiate its own photopolymerization.

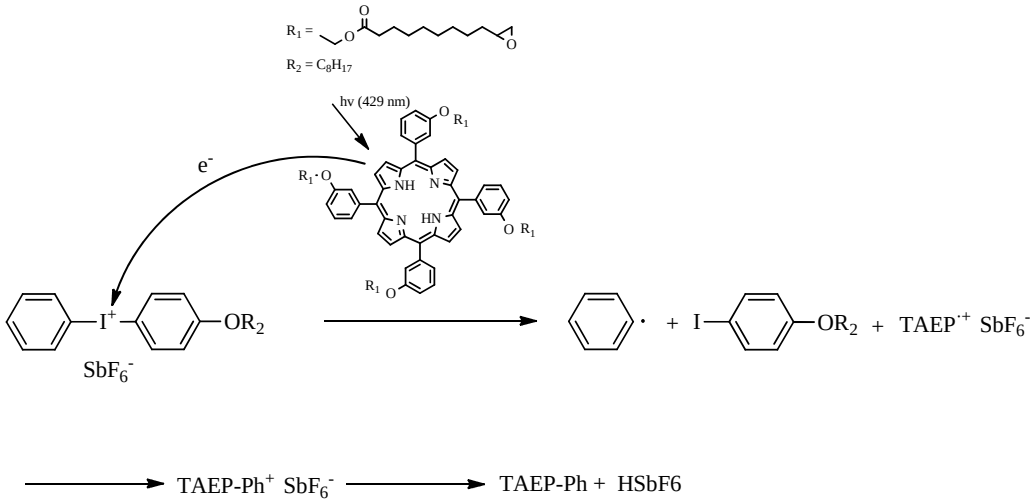

Scheme 4.16. Possible mechanism for visible light photoinitiation of TAEP. The phenyl can be added to anywhere in the conjugated macrocycle.

Scheme 4.16 shows the proposed mechanism of TAEP assisted photoinitiation. As the photochemical study of the exact mechanism was beyond the scope of this work, the scheme is based on the proven ability of TAEP to act as an initiator.[32] The exact order of the reactions may change during further analysis. At first TAEP absorbs photons at the absorption maximum and forms an excited state.[11,28-31] Electron transfer occurs from the excited TAEP to the diaryliodonium cation and a TAEP radical cation is formed. The diaryliodonium initiator cleaves and form an iodoaryl molecule and an aryl radical that combines with the TAEP radical cation. Hexafluoroantimonate anion abstracts a proton from the TAEP-phenyl cation, forming the superacid, $HSbF_6$, that can initiate polymerization.

When the same polymerization reaction is conducted in the dark, practically no polymerization is visible, which shows that the mechanism truly is photopolymerization. When the medium

pressure Hg/Xe light source (with UV cutoff filter) is replaced by blue LED (centered at 450 nm, reaching well into the 430 nm band of TAEP), photopolymerization still occurs, which confirms that the reaction is visible light sensitization, and not caused by residual UV light due to a non-optimal cutoff filter. The polymerization still has not yet been conducted with monochromatic light, but for quantitative photochemistry it would be required.

It was found that some polymerization would occur when temperature was raised to 125 °C or above, but at this point the initiation was due to thermal cleavage of the photoinitiator as well.

The initial measurement of TAEP polymerization kinetics was conducted with the UV-Vis method, specifically designed for the purposes of this work. A batch of identical samples was heated with or without light illumination, the samples were taken off the hot plate one by one in certain time intervals, and polymerization yields were determined. The method provided rather accurate data of thin film polymerization, since the studied monomers had a sufficiently high absorbance to be detectable by UV-Vis spectroscopy and the reaction was assumed to stop after the sample was cooled to ambient temperature. The method, however, provides rather low time resolution and requires many identical samples just for one time-resolved graph, which makes it expensive and time-consuming.

Another opportunity is to study TAEP with specifically tailored polarization modulation infrared reflection adsorption spectroscopy (PM-IRRAS). The method allows the IR absorption spectrum of a thin film to be measured in real time in ambient conditions. The device was specifically modified so that the TAEP samples could be kept at constant temperature for the duration of the experiment, either dark when required or illuminated by a blue LED light for photopolymerization.

A series of samples at different polymerization temperatures were measured to enable kinetic analysis. It could be seen that the IR spectrum of TAEP measured by ATR-IR was reproduced by PM-IRRAS, but the resolution at lower wavenumbers was clearly worse than that of ATR-IR (Figure 4.7). Additionally the epoxy vibration peak around 850 cm^{-1}, usually monitored in oxirane polymerization, fell out of the PM-IRRAS sensitivity range. The ether region of 1000 - 1200 cm^{-1} can be monitored instead, as the oxirane ring opening causes the formation of a polyether backbone. TAEP spectrum already contains peaks in this region from the eight C-O groups of the oxyethoxy linker in the core, which causes a doubling of signal intensity at full polymerization, at best. Due to the non-uniform chemical environment the C-O vibrations of the polymer are distributed along a wide range of wavelengths, which requires the C-O intensity to be measured from an integral of the entire affected region.

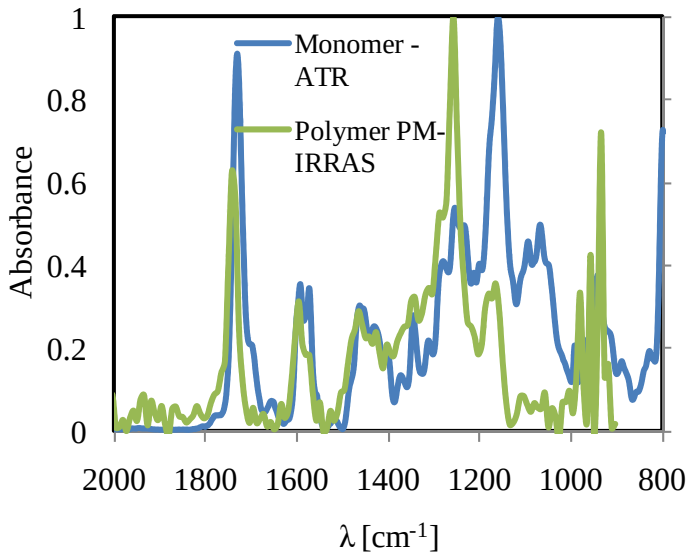

Figure 4.7. IR spectra of TAEP (blue) and its polymer (green), measured by ATR-IR and PM-IRRAS. The PM-IRRAS spectrum does not produce reliable data below 950 cm $^{-1}$.

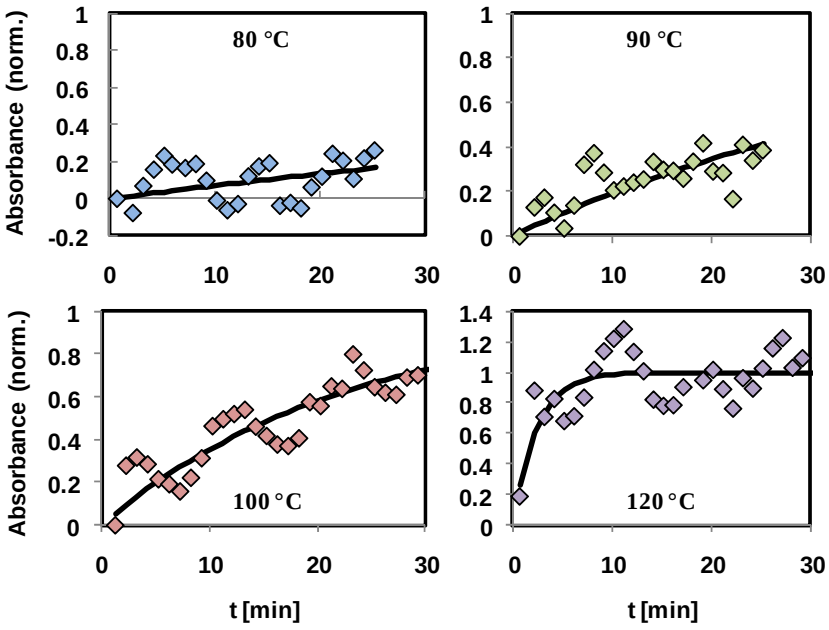

Figure 4.8. Photopolymerization of TAEP from 80 °C to 120 °C.

The 10 nm thickness of the TAEP film was a challenge for the detection limit of the PM-IRRAS device. A compromise between resolution of the kinetics graph and the resolution of individual spectra had to be made, with spectra being measured every 60 seconds. The data thus obtained had a considerable amount of noise, which could be reduced by averaging the adjacent spectra and normalizing the spectra by an unchanging region. The integrated area of the ether region

was plotted against time. Even after normalization, some undulation in the spectrum remained, which was probably due to fluctuations in temperature. Nevertheless, the PM-IRRAS method clearly can be used to study phenomena that were beyond experimental reach before.

With the UV-Vis method it had already been seen that 90 °C was the first temperature at which TAEP photopolymerization was easily detectable and at 125 °C polymerization occurred in a matter of minutes (and was at least partly thermal polymerization). The PM-IRRAS data clearly confirmed this (Figure 4.8). The polymerization occurring at 80 °C was so small that the changes could hardly be detected from the signal noise. At 90 °C and 100 °C the signal was still noisy, but the polymerization was pronounced enough. At 120 °C the polymerization was too fast for the steep slope to be resolved.

If all of the initiators form photoacids nearly instantaneously, the reduction rate of monomer concentration can be assumed to be linearly proportional to monomer concentration, with the speed of reduction, *k*, being dependent on the photoacid, viscosity and temperature (eq. 4.1). When eq. 1 is integrated (eqs. 4.2-4.4), a correlation between monomer concentration and time can be derived (eq. 4.4). As the sum of the polymerized and unpolymerized monomer is always 100 %, a correlation between conversion, α, and monomer concentration (eq. 4.5) can be inserted into eq. 4.4, yielding the correlation between conversion and time (eq. 4.6). By rewriting eq. 4.6 it can be seen that polymerization follows exponential growth (eq. 4.7).

$$\frac{d[M]}{dt} = -k[M] \tag{4.1}$$

$$\int_{[M]_0}^{[M]} \frac{d[M]}{[M]} = \int_{t_0}^{t} -kdt \tag{4.2}$$

$$ln[M] - ln[M]_0 = -kt \tag{4.3}$$

$$\ln\left(\frac{[M]}{[M]_0}\right) = -kt \tag{4.4}$$

$$\frac{[M]}{[M]_0} = 1 - \alpha \tag{4.5}$$

$$\ln(1 - \alpha) = -kt \tag{4.6}$$

$$\alpha = 1 - e^{-kt} \tag{4.7}$$

The rate constant, *k*, is dependent on polymerization temperature through the Arrhenius equation (eq. 4.8). The equation can be split so that it can be seen that the natural logarithm of *k* is

linearly related to the inverse of temperature, with the slope of the equation being the activation energy, E_a, divided by the gas constant, R (eq. 4.9).

$$k = Ae^{-E_a/RT} \quad (4.8)$$

$$ln\,(k) = \ln(A) + E_a/R\frac{1}{T} \quad (4.9)$$

If eq. 4.7 is fitted to TAEP photopolymerization data at various temperatures, their k values can be obtained and when ln(k) values are fitted against T^{-1}, the value of E_a can be calculated (Figure 4.9). The obtained E_a value is 115 kJ/mol, which is in perfect agreement with typical oxirane polymerization values.[108]

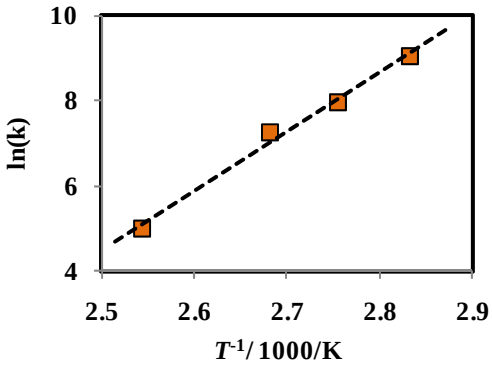

Figure 4.9. The k values of TAEP photopolymerization obtained from exponential fits plotted against T in an Arrhenius plot.

4.3.2 Photopolymerization of Fullerene and Phthalocyanine

The initial fullerene photopolymerization results were published in paper I. Even though the proper initiation system was used, the results were partly misguided, especially regarding the required temperatures, in light of later findings, partly published in paper IV.

As the effect of substrate was not yet known and the UV-Vis and PM-IRRAS method had not yet been developed, the analysis of photopolymerization was mainly done by scraping the polymerized sample for ATR-IR analysis. The diminishing of the oxirane peak at 913 cm^{-1} could be seen, which was an indication of at least partial polymerization. The polymerized film displayed the hardness of a regular epoxy polymer, and the UV-Vis spectrum showed that the layer was not

affected. All of this was strong evidence for successful polymerization, but was lacking in distinguishing between thermal and photo-processes.

By paper IV the methods of photopolymerization analysis were so developed that the photopolymerization of FB9ox could be revisited. This time the samples were prepared on plasma treated quartz substrates and polymerization was monitored from UV-Vis spectra of batches of samples, where only one parameter was varied from batch to batch. Figure 4.10 shows that FB9ox polymerization is more efficient using UV light than visible light. A surprising finding is that FB9ox photopolymerization is possible at much lower temperatures than with TAEP, even though the viscosity of FB9ox is higher than that of TAEP.

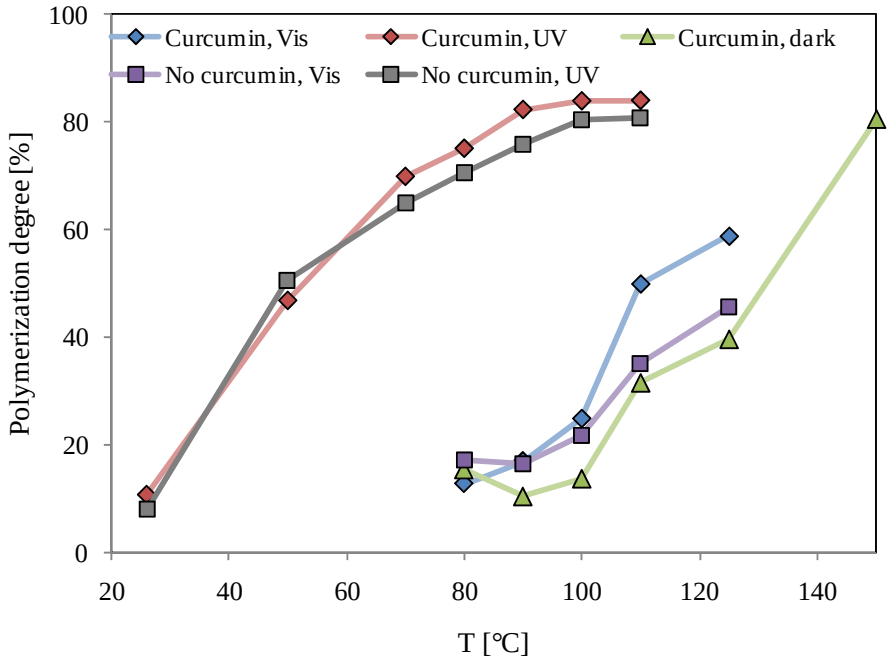

Figure 4.10. Thermal, visible light and UV polymerization of FB9ox on ITO at varying temperatures for 30 minutes. Curcumin denotes the use of co-initiator curcumin, Vis denotes the use of 400 nm cutoff filter and UV denotes full Hg/Xe lamp illumination.

An explanation for this fact could be found when all initiators were removed from the fullerene monomer, but the UV-Vis measurements still showed significant photopolymerization (Figure 4.11 A). As the energy of the ultraviolet photon is not high enough to open the oxirane ring the only possible explanation is that FB9ox molecules are fused together at the fullerene moieties. Such fusion has been recorded in literature, but always under high pressure. This would make FB9ox the first recorded fullerene polymerized at ambient pressure. Additionally photopolymerization of

FB9ox is possible even at room temperature, if initiator is used (Figure 4.8 B). In this case the polymerization is at least partly regular UV polymerization.

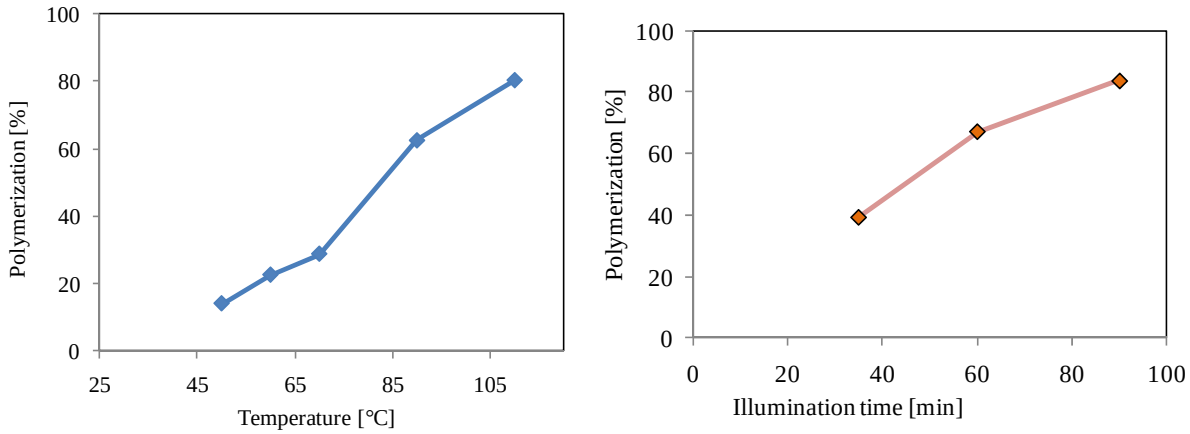

Figure 4.11. UV photopolymerization of FB9ox, without initiators, at varying temperatures for 10 min (a) an and at room temperature (26 °C), with OMAN071 (b).

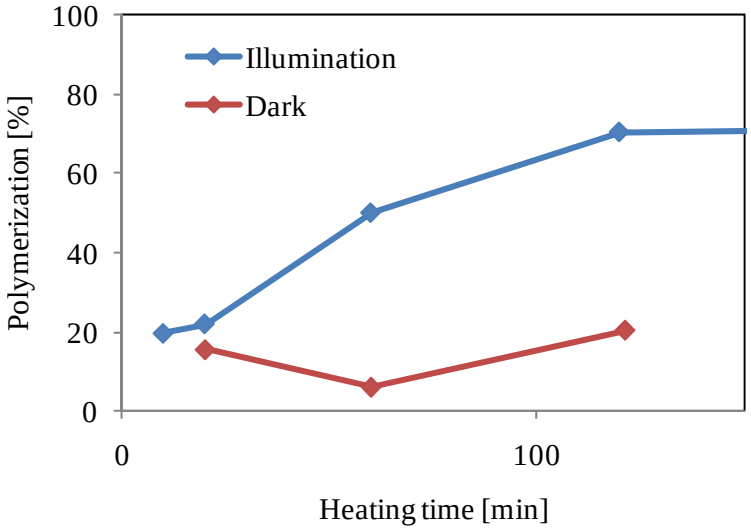

Figure 4.12. Visible light polymerization of **H_2PCP9ox** at 90 °C, with OMAN071 and curcumin.

Photopolymerization of phthalocyanine monomer **H_2PCP9ox** was the most challenging task. UV polymerization was out of the question, as UV illumination would bleach the monomer. Visible light polymerization was not as straightforward as with porphyrin monomer TAEP, either, as phthalocyanine does not co-initiate its photopolymerization. The only option was to use curcumin co-initiator at just the limit of thermal polymerization, at 90 °C (Figure 4.12). As the photopolymerization is a two-component process, involving the co-initiator curcumin[10,11] and the diaryliodonium initiator OMAN071, the speed of the reaction is limited. In comparison to TAEP

photopolymerization, where all of the diaryliodonium initiators were close to porphyrin, in the case of **H_2PCP9ox** photopolymerization initiation was via the curcumin co-initiator and thus less efficient, as the 3 mol-% curcumin concentration was much smaller than the 97 mol-% concentration of TAEP that co-initiated itself.

4.3.3 Thermal Polymerization

Although all of the three monomers studied in this work are photopolymerizable, their use in photovoltaic applications requires quantitative conversion, as the unpolymerized regions cause short circuiting, when metal top electrodes are deposited. Quantitative conversion is not practically possible with photopolymerization. However, at the temperatures above 100 °C the process is not purely photopolymerization anymore. When the monomer films with photoinitiators are heated above approximately 110 - 120 °C, the initiator cleaves thermally and starts the polymerization. Figure 4.13 shows the behavior of **H_2PCP9ox** when heated at various temperatures for 10 minutes. The experimental data can be described by combining Equations 4.7 and 4.9

$$\alpha = 1 - e^{-(Ae^{-Ea/RT})t} \tag{4.10}$$

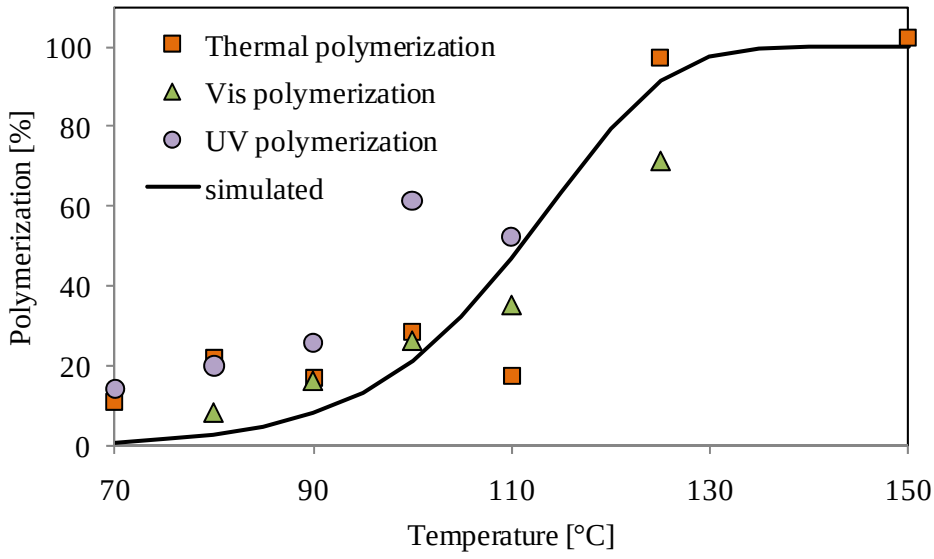

Figure 4.13. Thermal polymerization of **H_2PCP9ox** at varying temperatures for 10 min, with OMAN071 and curcumin.

When the activation energy of oxirane polymerization is inserted onto eq. 4.10 the simulated data can be fitted somewhat to the experimental data of thermal polymerization. As eq. 4.10

assumes that all of the initiators have reacted instantaneously, it produces a higher value of polymerization at temperature of 110 °C than experimental data produces. If the sample is illuminated with visible light, however, the polymerization fits the equation better. UV polymerization fits even better, but the bleaching associated with the polymerization renders UV polymerization unusable in practice.

4.3.4 Multilayer Polymerization

For the fabrication of multilayer solar cells with the monomers synthesized in this work, it is required that the polymerized layer on the bottom is as smooth as the substrate surface. Even if the first layer polymerizes 'perfectly', *i.e.* with a 100 % polymerization yield, the second layer may not polymerize at all. This is usually due to the first layer being polymerized as droplets, which is mostly due to impurities introduced into the film either during spin-coating or from the environment afterwards. The best way to avoid this is to prepare bulk solutions in the cleanest surroundings possible and conduct polymerizations immediately after sample preparation in most dust-free environment.

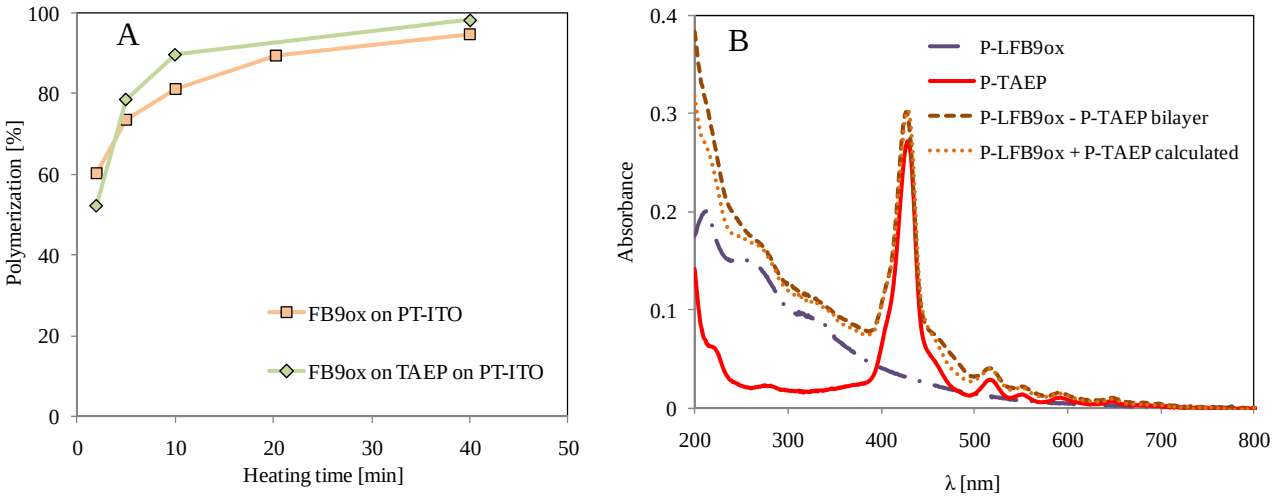

Figure 4.14. (A) UV polymerization of FB9ox at 90 °C on plasma treated (PT) ITO and on TAEP. (B) UV-Vis spectra of P-FB9ox, P-TAEP, P-FB9ox – P-TAEP bilayer and calculated P-FB9ox + P-TAEP.

There are other limitations for multilayer processing. Figure 4.14 A shows the UV polymerization of FB9ox at 90 °C on a neat PT-ITO and on TAEP layer. The fullerene polymerization curves are practically identical, but the porphyrin layer was partly bleached with UV

light during the process (only the FB9ox absorbance is monitored in Figure 4.14 A). So even though the fullerene polymerization is successful, the conditions of the photopolymerization affect the bottom layer negatively. Figure 4.11 B shows that the absorption spectrum of the P-FB9ox – P-TAEP bilayer matches well with the sum of P-FB9ox and P-TAEP spectra.

When TAEP visible light photopolymerization is attempted on FB9ox at 90°C, the polymerization does not initiate. When the temperature is raised to the thermal polymerization level, the polymerization proceeds normally again. As a possible explanation, electron transfer from TAEP to FB9ox is much more favorable than electron transfer from TAEP to the diphenyliodonium initiator. The electron transfer from porphyrin to fullerene has been shown to occur in from >100 fs to 800 fs,[102,109] which is much faster than the 50-350 ps reported for electron transfer of sensitizer-diphenyliodonium pair.[10,110]

Thermal polymerization does not seem to be as affected by the bottom layer, just as long as it is smooth. For this reason the majority of the photocurrent samples in this work were prepared thermally.

4.3.5 TAEP Photopatterning

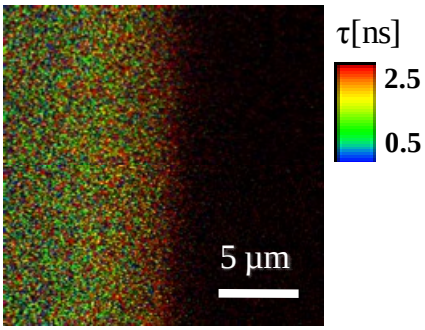

Figure 4.15. Fluorescence lifetime microscope image of photopatterned TAEP**.**

As the TAEP monomer fluoresces and can be efficiently photopolymerized, its photopatterning can be studied by fluorescence lifetime microscopy (FLM). When a film of TAEP with OMAN071 was partially masked and illuminated by visible light at 90 °C, the film could be polymerized only on the illuminated side. After the monomer had been rinsed, the film was analyzed by FLM (Figure 4.15). The image showed that the illuminated region was fully polymerized and displayed the same fluorescence properties as a fully photopolymerized film. The masked region was practically non-fluorescing, with very weak signal almost indistinguishable from noise. The edge between the

fluorescing and non- fluorescing region was ca. 2 µm, which indicates that TAEP can be used for micrometer scale photopatterning.

4.3.6 Photobleaching

The UV-Vis measurement indicated a reduced absorbance of the porphyrin and phthalocyanine chromophores under UV illumination, but quantitative measurements were difficult due to the small number of data points. With PM-IRRAS it was possible to study photobleaching of TAEP by the increase of the C=O vibration peaks around 1700 - 1800 cm^{-1}. The Kräutler group has studied the oxidation of chlorophyll, which is nearly identical to porphyrin in its core,[34,111,112] and based on their results the bleaching product of TAEP, shown in Figure 4.16, seems the most probable.

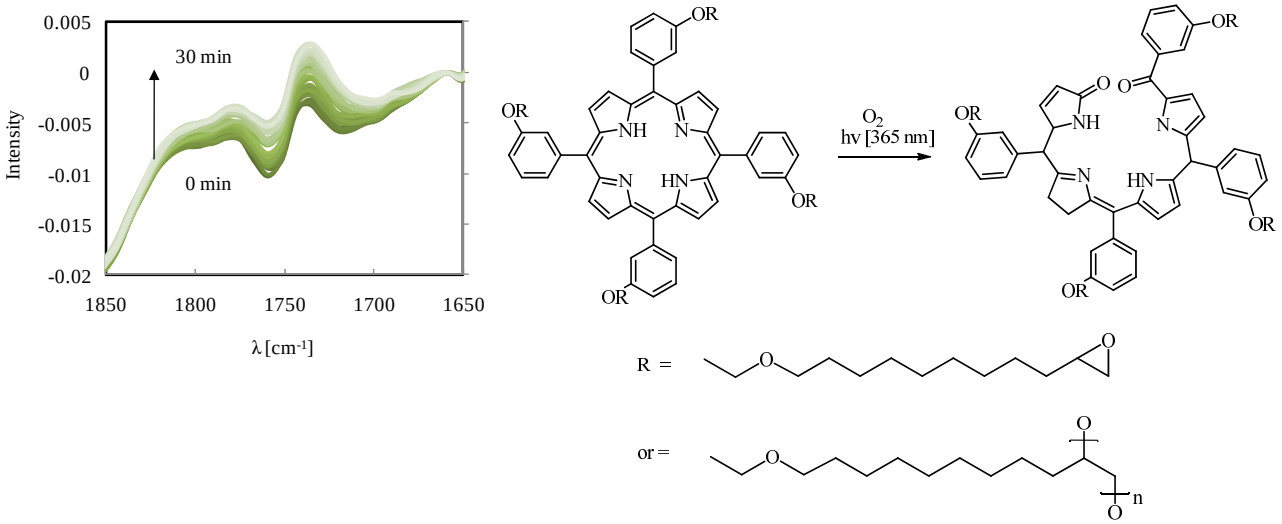

Figure 4.16. PM-IRRAS spectrum of TAEP photobleaching and its proposed bleaching mechanism.

4.4 Polymer Analysis

The thickness of the polymers was measured by optical profilometer (Figure 4.17). Several samples of P-TAEP, P-FB9ox and P-H_2PCP9ox of specific absorbance were measured and the thicknesses of the all of the future samples were determined by comparing their absorbance to the profilometer reference. The correlation between absorbance and sample thickness is linear. The sample preparation was reproducible to within less than 5 % thickness.

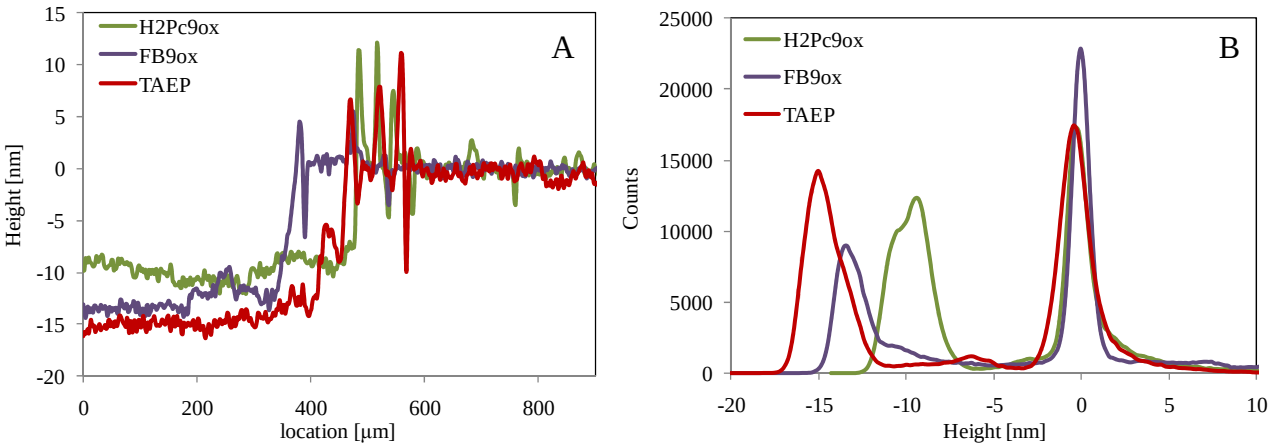

Figure 4.17. Profilometry graphs (A) and histograms (B) of H_2Pc9ox, FB9ox and TAEP. The two peaks in the histogram correspond with the level of the neat substrate (at left) and the monomer surface (zero, at right). The thickness of the film is the distance from one peak to the other.

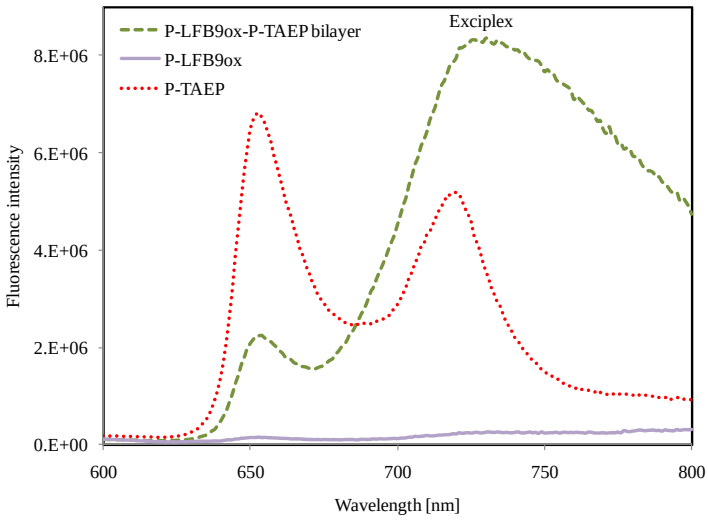

Figure 4.18. P-TAEP (red dotted line line), **P**-FB9ox (purple solid line) and **P**-FB9ox - **P**-TAEP bilayer (green dashed line) fluorescence spectra.

TAEP was the easiest to study, as it emits strongly when excited at 430 nm. The fluorescence spectrum of P-TAEP (Figure 4.18) with two maxima at 650 and 720 nm was typical for free base porphyrins.[113] The P-FB9ox fluorescence at 430 nm excitation is weak, but if a layer of TAEP is polymerized on P-FB9ox, a stronger emission around 730 nm is formed. This can be attributed to the orbitals of fullerene and porphyrin combining into a common excited state, called an exciplex.[113]

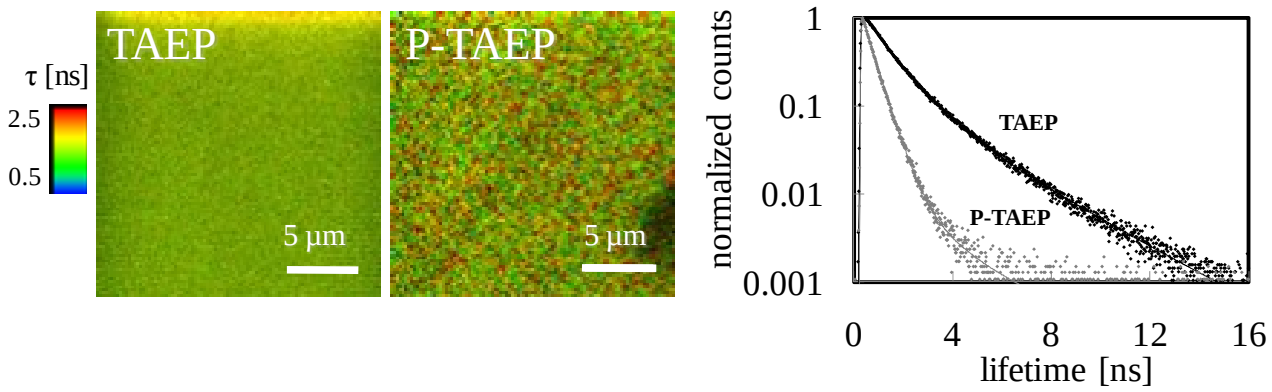

Figure 4.19. Fluorescence lifetime microscope image of TAEP monomer, polymer and patterned polymer and fluorescence lifetime spectrum of the first two.

With fluorescence lifetime imaging it is seen that when the TAEP film is polymerized, its fluorescence lifetime is reduced from 1.04 ± 0.03 ns to 0.464 ± 0.012 ns (Figure 4.19). This can be attributed to self-quenching due to the proximity of other porphyrin moieties.[114]

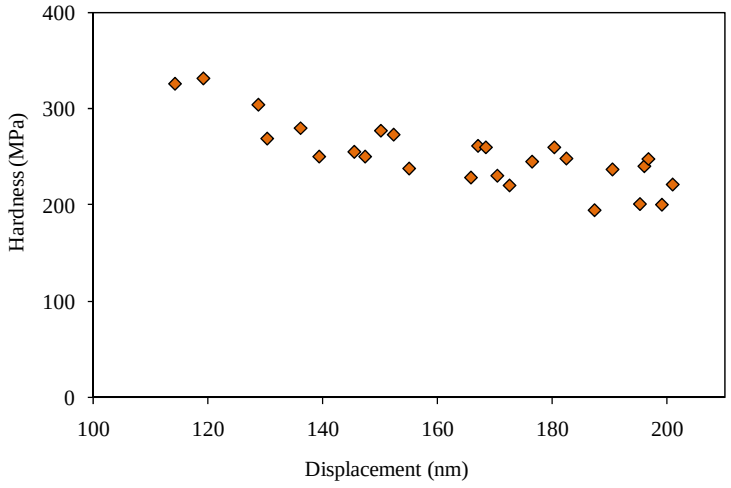

Figure 4.20. Hardness measurement of an FB9ox polymer.

Polymer hardness was measured for the fullerene polymer (P-FB9ox). A slightly thicker (200 nm) film was prepared, as the nanoindentation device was at the limit of its capacity at the thickness. Any thinner film would also measure the hardness of the substrate. The measurement showed that the fullerene polymer displayed very similar hardness of an epoxy polymer, 200 – 300 MPa (Figure 4.20).[115]

The surface fine structure of the polymer was studied with AFM. The surface properties were significantly different depending on the polymerization method and the type of substrate. The smoothest surfaces were obtained, when TAEP was photopolymerized on ITO (Figure 4.21 A).

Thermal polymerization on quartz produced rather smooth surfaces as well. However the thermal polymerization on ITO, which was the method used for photocurrent samples created the roughest surface, with clearly visible spots. This was a major issue to be dealt with in the photocurrent sample preparation, as discussed in chapter 4.5.

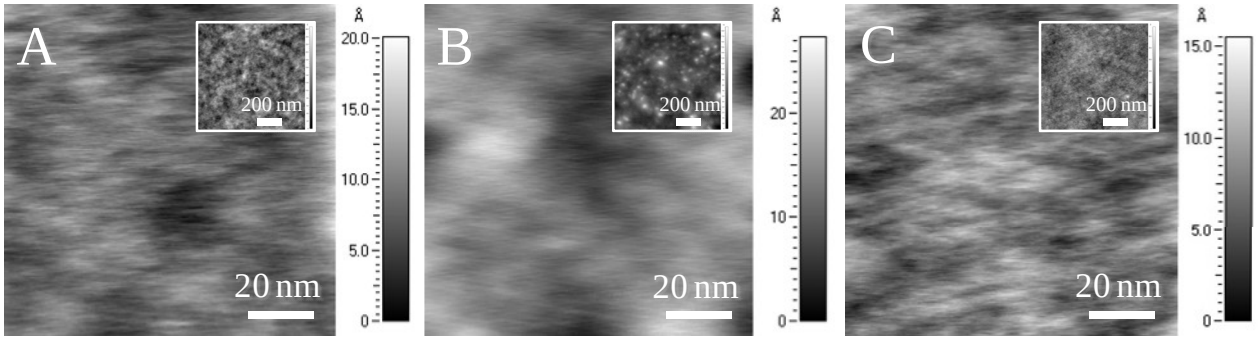

Figure 4.21. Tapping mode AFM images of TAEP: photopolymerized at 90 °C on ITO (A), thermally polymerized at 175 °C on ITO (B) and thermally polymerized at 175 °C on fused quartz (C).

4.5 Photocurrent Experiments

The goal was to test whether photopolymerizable chromophore monomers can be used to prepare photovoltaic samples. Photoinduced charge and electron transfer from porphyrin and phthalocyanine to fullerene derivatives has been addressed by multiple publications by our group, as well as others.[102,103,116-118] However no other group has thus far (August 2010) prepared *in situ* polymerizable monomer samples for photovoltaic active layers. Some papers have been published in the past few years introducing cross-linkable moieties to polymers to fix the active layer for multilayer preparation.[119]

Due to the novel approach for photovoltaic cell preparation there remained many questions to be answered. It is well known that the crystallinity of *p*-type layer affects its hole mobility and reduced crystallinity causes diminished photovoltaic efficiency.[23,120] However *in situ* polymerization requires the monomers to be liquid, which is opposite to the requirement of crystallinity. Despite phthalocyanine and porphyrin being sometimes displaying liquid crystalline behavior, it wasn't observed in the synthesized monomers, at least in DSC. The requirement of fullerene crystallinity is not as high as the fullerene balls are spherical and electron transfer between fullerene moieties is possible just as long as they are in close enough proximity.[121]

Another issue is the general morphology of the active layer. The best recorded efficiencies have been attained by active layers of highly optimized structure.[44] The first requirement is that all of the

generated excitons are close enough to the interface of the *p*-type and *n*-type materials for the charge separation to occur.[122] The second requirement is that all of the generated charges should have an unobstructed path to their respective electrodes.[122] If additionally the solar spectrum coverage is good, the photovoltaic efficiency can be good as well. *In situ* polymerization enables the formation of a fully electron donor bottom layer, a mixed donor and acceptor middle layer and a fully electron acceptor top layer (Figure 4.22). This should enable the transfer of only holes to the bottom electrode and electrons to the top electrode, but still retain a large surface area between the donor and the acceptor. However there is very possibility in assisting phase separation of the *n*-type and *p*-type region.

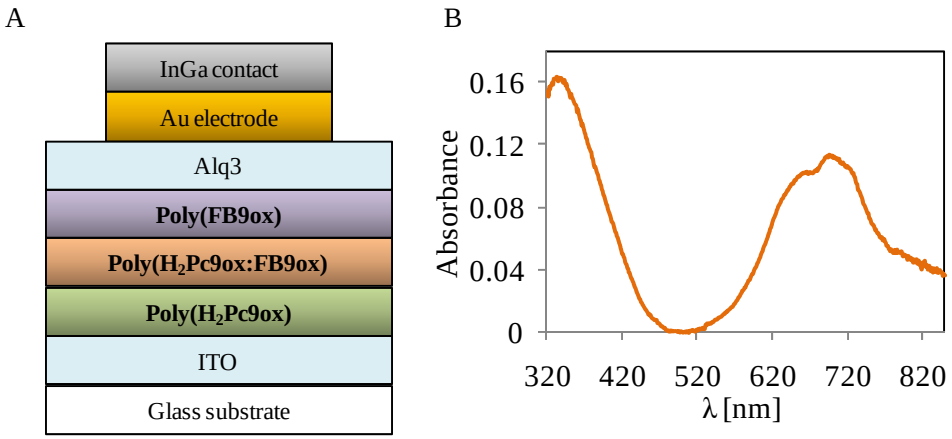

Figure 4.22. Schematic structure of the phthalocyanine-fullerene sandwich solar cell sample (A) and the corresponding absorption spectrum (B).

Additionally there are several parameters of active layer polymerization that can influence device performance, such as polymerization temperature, initiator concentration and film thickness. Even though TAEP - FB9ox photovoltaic samples were prepared, only H_2Pc9ox - FB9ox samples were published in paper IV. The article involved mostly the general method of preparing *in situ* polymerizable photovoltaic samples and the parameters affecting its performance. As H_2Pc9ox - FB9ox has a larger spectral coverage (see Figure 4.23 b) and produced higher initial efficiencies, the study was focused on it.

4.5.1 Influence of Polymerization Temperature

It was soon found that any not fully polymerized sample would cause short circuiting due to defects and/or holes in the layers. This is why most photocurrent samples were prepared at temperatures

where polymerization is thermal by nature. The diphenyliodonium initiator is also efficient in thermal polymerization, as the species determining polymerization speed is the photoacid, $HSbF_6$, which is formed by thermal cleaving just as well as with photoreaction.

Table 4.1. Open circuit voltage (U_{OC}), short circuit current (I_{SC}) and fill factor (FF) of bilayer cells with 13 nm of FB9ox on top of 10 nm of H_2Pc9ox, polymerized at different temperatures.

H_2Pc9ox pol. *T* (°C)	FB9ox pol. *T* (°C)	I_{SC} (μA/cm²)	U_{OC}(V)	*FF* (%)
150	175	-0.64	-0.08	25
200	175	0.32	0.05	26
175	150	4.00	0.16	26
175	175	3.57	0.14	26
175	200	3.06	0.24	25

Annealing is an important part of regular organic photovoltaic cell preparation. Annealing causes the active layer to settle onto its lowest energy level, which corresponds with crystallization of the active molecules and phase separation due to their propensity to crystallize with identical molecules.[123] However the effect of increased temperature in the case of thermally polymerizing layers was unclear. The effect of polymerization temperature was tested for both FB9ox and H_2Pc9ox layers. It was found that even at 150 °C there were some holes left, which caused short circuiting. Full polymerization was achieved at 175°C and samples would not short circuit. Increasing the polymerization temperature to 200 °C seemed to have little effect so most polymerizations were conducted at 175 °C, which is the temperature limit of the heated vacuum chamber used for photocurrent samples preparation (Table 4.1).

4.5.2 Influence of Initiator Concentration

In situ polymerization of a photovoltaic cell causes the initiator to remain in the active layer. Even though the literature references on photopolymerized OLEDs indicate that the initiator does not have deleterious effects, [35] the influence of initiator concentration was tested in the present study. It was found that the concentration of 1 mol-% of initiator to oxirane groups was not enough to result

in full polymerization of neither H_2Pc9ox nor FB9ox, causing seriously reduced performance (Table 4.2). If the initiator concentration was increased beyond 3 mol-% the voltage was significantly reduced. Therefore we used 3% of OMAN071 in further photocurrent measurements.

Table 4.2. Solar cell performance parameters open circuit voltage (U_{OC}) and short circuit current (I_{SC}) for initiator concentration experiments for a bilayer cell with 13 nm of FB9ox on top of 10 nm of H_2Pc9ox.

Initiator conc. (mol-%)	I_{SC} (μA/cm²)	U_{OC} (V)
1	1.23	0.09
2	3.99	0.16
3	3.57	0.14
4.5	4.23	0.05
6	3.64	0.01

4.5.3 Influence of Sample Thickness

Table 4.3. Open circuit voltage (U_{OC}) and short circuit current (I_{SC}) for polymer thickness experiments.

H_2Pc9ox thickness (nm)	FB9ox thickness (nm)	I_{SC} (μA/cm²)	U_{OC} (V)
5	7	short circuit	
10	13	1.21	0.12
20	26	1.01	0.14
40	52	0.13	0.10

Sample thickness is one of the crucial factors affecting performance of solar cells. On one hand, the photovoltaic cell should absorb nearly all of the light shone upon it, and therefore should be thick enough. Additionally, the top layer should withstand further deposition of a metal electrode. On the other hand, the serial resistance increases in a thick sample. Thus, when the sample was 5 nm and 7 nm per H_2Pc9ox and FB9ox layer, respectively, all the electrodes were short circuited (Table 4.3). For the film thicknesses 10 nm and 20 nm per layer the current and voltage were nearly the same,

and at 40 nm per layer current was especially reduced. The results correlate well with the exciton diffusion length of a fullerene-phthalocyanine photovoltaic cell.[124]

4.5.4 Hybrid Bilayer-Bulk Heterojunction

Pure bulk heterojunction samples of H_2Pc9ox and FB9ox did not produce any photocurrent, probably due to the high miscibility of the two monomers. However if a bulk heterojunction layer was sandwiched between single layers of H_2Pc9ox and FB9ox, the performance of the sample improved over a simple bilayer considerably. Especially significant was the influence of the FB9ox upper layer combined with a bulk heterojunction. The electron conductivity of FB9ox seems rather good, whereas the hole conductivity of H_2Pc9ox seems to limit the current (Table 4.4)

Table 4.4. Open circuit voltage (U_{OC}) and short circuit current (I_{SC}) for bilayer / bulk heterojunction sandwich experiments.

H_2Pc9ox thickness (nm)	BHJ thickness (nm)	FB9ox thickness (nm)	I_{SC} (μA/cm²)	U_{OC} (V)
5	24	7	short circuit	
5	12	7	0.40	0.15
10	12	13	1.29	0.25
10	24	13	2.30	0.26
10	12	-	1.24	0.12
-	12	13	4.24	0.24

Besides the parameters of polymerization, of at least equal importance is the purity and structure (as well as isomeric ratio in the case of phthalocyanines) of the monomers. The results shown in Table 4.4 were obtained with H_2Pc9ox of high isomeric purity, where the phthalocyanine formation was conducted at 80 °C in octanol. However another batch of H_2Pc9ox, where phthalocyanine formation was conducted by refluxing in pentanol, producing a mixture of the four possible isomers, yielded an eightfold increase in PCE, compared with a batch of higher isomeric purity (Table 4.5). The most probable explanation for this difference in efficiency is the change in hole mobility of the respective polymers. However this remains as a topic of future work.

Table 4.5. Open circuit voltage (U_{OC}) and short circuit current (I_{SC}) for bilayer / bulk heterojunction sandwich experiments.

H_2Pc9ox thickness (nm)	BHJ thickness (nm)	H_2Pc9ox : FB9ox ratio	FB9ox thickness (nm)	I_{SC} (μA/cm²)	U_{OC} (V)
5	12	4:1	7	8.75	0.35
5	12	4:1	4	8.65	0.40
5	12	2:1	7	10.20	0.19
5	12	4:1	7	13.42	0.37
5	12	6:1	7	19.23	0.09

4.5.5 Photopolymerized Samples

Table 4.6. Open circuit voltage (U_{OC}), short circuit current (I_{SC}) and fill factor (*FF*) for photopolymerization experiments: UV denotes polymerization by UV light, Vis polymerization by visible light.

Photopolymerized layer	I_{SC} (μA/cm²)	U_{OC} (V)	*FF* (%)
H_2Pc9ox (Vis)	2.5	0.11	26
FB9ox (UV)	short circuit		
FB9ox (Vis)	1.8	0.01	25

Despite that the main focus of this work has been to synthesize and photopolymerize liquid chromophores, the focus of paper IV was on thermally polymerized photovoltaic samples, purely because of the better performance of samples thus prepared. However as has been shown, the used monomers can all be photopolymerized. Due to the limitations of multiple layer photopolymerization, the photopolymerized photovoltaic samples were prepared with photopolymerization of one component, and thermal polymerization of the other, to ensure that the effect of both monomers can be analyzed separately (Table 4.6).

When H_2Pc9ox was photopolymerized at 100 °C, with a yield of 88 %, and FB9ox thermally polymerized, I_{SC} was a decent 2.5 μA/cm², but U_{OC} was a weak 0.11 V. Despite of the 97 % UV

polymerization of FB9ox (with H_2Pc9ox thermally polymerized), the samples did short circuit, presumably because the polymerization is not purely cationic in this case, but there UV light also causes the fullerene moieties to fuse, which apparently reduces the electron conductivity and/or evenness of the P-FB9ox layer.[46] On the other hand when FB9ox was polymerized by visible light at 100 °C, polymerization yield was just 50 %, which probably left the FB9ox layer thickness so low at places that U_{OC} became negligible.

According to the initial results of photopolymerized photovoltaic samples, it should be possible to produce photopolymerizable photovoltaic samples of better efficiency, but with modifications to the monomers. Probably the easiest way would be to replace the polymerizable group with oxetane, which has yielded good results with OLEDs.

4.5.6 Analysis of the Optimized Structure

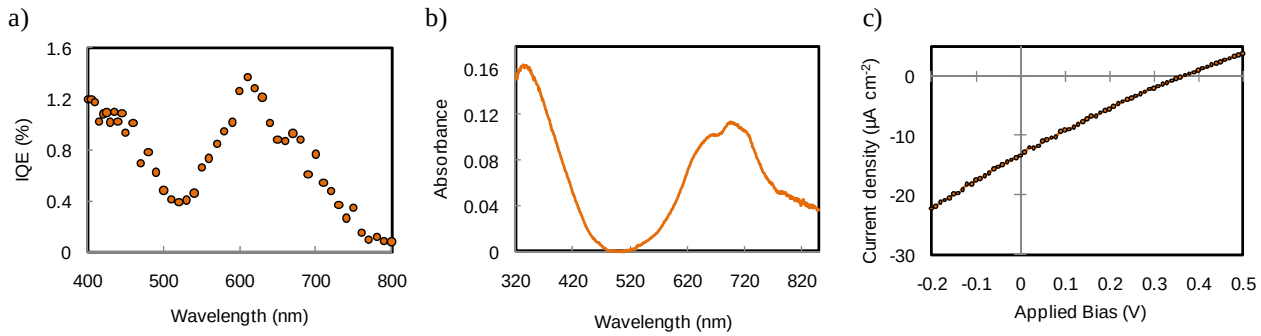

Figure 4.23. (a) Internal quantum efficiency (IQE) spectrum of H_2Pc9ox - FB9ox bilayer/bulk heterojunction sandwich structure and the corresponding absorption spectrum (b) and *I-V* curve (c).

The sandwich structure of FB9ox | FB9ox : H_2Pc9ox | H_2Pc9ox (Figure 4.22) produced the highest efficiency of the studied samples. The action spectrum of the cell follows its absorption spectrum quite closely (Figure 4.23 a & b). The internal quantum efficiency of 1.4 % at 610 nm is significantly lower than the recorded efficiencies of up to 85 %.[125-128] This can be explained by the low hole mobility of the H_2Pc9ox polymer and the high miscibility of the FB9ox:H_2Pc9ox mixture, causing charge recombination due to the lack of continuous *n* and *p*-type regions. Nevertheless, improvement over bilayers and BHJ is visible, and evidently, more monomers of different structures need to be tested. Indeed, the concept of polymerization allows combining homomolecular and BHJ layers, which is very difficult to achieve by other methods, but the main

challenge of improving *in situ* polymerizable, and specifically photopolymerizable, photovoltaics will be to find the proper monomers.

5 Conclusions

The design of photopolymerizable chromophores must account for the viability of their synthesis, their polymerizability and their performance in their end applications. The photopolymerizability of bulky chromophores requires liquid monomers. The synthesis of the liquid fullerene monomer could be done in three steps with good yields and the synthesis can be easily modified to replace the polymerizable oxirane moiety with oxetane or methacrylic moiety. The appropriate phthalocyanine monomer was synthesized in four steps. By separating the steps of the phthalocyanine macrocycle formation and the epoxidation of the double bond, it was possible to test several types of phthalocyanine-polymerizable moiety couples, as their combination by simple acylation can easily be accomplished. The porphyrin monomer was synthesized in three steps, with the addition of the polymerizable group being an application of the modular approach designed for the phthalocyanine synthesis.

All of the three monomers can be photopolymerized. Due to their high viscosity, the polymerization has to be conducted very close to the thermal polymerization limit. The fullerene monomer can also be photopolymerized even at room temperature, as the fullerene moieties can fuse due to UV illumination.

The porphyrin monomer is a molecule with unique properties, which can act as a co-initiator of its own photopolymerization. The molecule can be used to study thin film photopolymerization in ways previously not attempted, as it is clearly visible by UV-Vis spectroscopy even in monomolecular films, and requires no additional co-initiator.

A method for analyzing thin film photopolymerization by UV-Vis spectroscopy was employed. In nanometer scale films, the percentage of polymerization can be linked with the proportion of the film which is insoluble. Thus the photopolymerization of thin films can be monitored by preparing a batch of samples, whose polymerization is stopped at convenient intervals to obtain polymerization yields.

PM-IRRAS (polarization modulation infrared reflection adsorption spectroscopy) was used for the first time to analyze thin film photopolymerization kinetics. The method enables real-time analysis of nanometer scale films. The porphyrin monomer could be analyzed by the method, yielding the activation energy of oxirane polymerization from the data, verifying the validity of the method.

Polymerized layers of phthalocyanine (or porphyrin) monomer and fullerene monomer produce photocurrent. The *in situ* polymerization method enables the fabrication of hybrid bilayer-bulk

heterojunction structures with higher efficiencies than either bilayer or bulk heterojunction alone can produce.

References

1. Ewing, B.; Goldfinger, S.; Wackernagel, M.; Stechbart, M.; Rizk, S. M.; Reed, A.; Kitzes, J. *The Ecological Footprint Atlas 2008;* Global Footprint Network: Oakland, 2008.

2. Sun, S.-S.; Sariciftci, N. S. The Story of Solar Cells. In *Organic Photovoltaics;* Taylor & Francis: Boca Raton, 2005; pp 3-15.

3. Liang, Y.; Xu, Z.; Xia, J.; Tsai, S.-T.; Wu, Y.; Li, G.; Ray, C.; Yu, L. For the Bright Future - Bulk Heterojunction Polymer Solar Cells with Power Conversion Efficiency of 7.4%. *Adv. Mater.* **2010,** *22,* E135 - E138.

4. Konarka Technologies, Inc., 2010. http://www.konarka.com/media/pdf/konarka_40series_04092010.pdf (accessed August 24, 2010).

5. Konarka Technologies, Inc., 2010. http://www.konarka.com/media/pdf/konarka_bagpanel_04092010.pdf (accessed August 24, 2010).

6. Antonias, H. *Overview of OLED Display Technology;* OSRAM.

7. Bacher, E.; Jungermann, S.; Rojahn, M.; Wiederhirn, V.; Nuyken, O. Photopatterning of Crosslinkable Hole-Conducting Materials for Application in Organic Light-Emitting Devices. *Macromol. Rapid Commun.* **2004,** *25,* 1191–1196.

8. Bacher, E.; Bayerl, M.; Rudati, P.; Reckefuss, N.; Müller, C. D.; Meerholz, K.; Nuyken, O. Synthesis and Characterization of Photo-Cross-Linkable Hole-Conducting Polymers. *Macromolecules* **2005,** *38,* 1640-1647.

9. Müller, C. D.; Falcou, A.; Wiederhirn, V.; Rudati, P.; Frohne, H.; Nuyken, O.; Becker, H.; Meerholz, K. Multi-colour organic light-emitting displays by solution processing. *Nature* **2003,** *421,* 829-833.

10. Crivello, J. V.; Bulut, U. Curcumin: A Naturally Occurring Long-Wavelength Photosensitizer

for Diaryliodonium Salts. *J. Polym. Sci., Part A: Polym. Chem.* **2005,** *43,* 5217–5231.

11. Crivello, J. V.; Bulut, U. Indian Turmeric and its Use in Cationic Photopolymerizations. *Macromol. Symp.* **2006,** *240,* 1–11.

12. Karasu, F.; Arsu, N.; Jockusch, S.; Turro, N. J. Mechanistic Studies of Photoinitiated Free Radical Polymerization Using a Bifunctional Thioxanthone Acetic Acid Derivative as Photoinitiator. *Macromolecules* **2009,** *42,* 7318–7323.

13. Yilmaz, G.; Aydogan, B.; Temel, G.; Arsu, N.; Moszner, N.; Yagci, Y. Thioxanthone−Fluorenes as Visible Light Photoinitiators for Free Radical Polymerization. *Macromolecules* **2010,** *43,* 4520–4526.

14. Decker, C. Kinetic Study and New Applications of UV Radiation Curing. *Macromol. Rapid Commun.* **2002,** *23,* 1067–1093.

15. Arrais, C. A.; Giannini, M.; Rueggeberg, F. A. Effect of sodium sulfinate salts on the polymerization characteristics of dual-cured resin cement systems exposed to attenuated light-activation. *J. Dent.* **2009,** *37,* 219-227.

16. Retsch, M.; Walther, A.; Loos, K.; Müller, A. H. E. Synthesis of Dense Poly(acrylic acid) Brushes and Their Interaction with Amine-Functional Silsesquioxane Nanoparticles. *Langmuir* **2008,** *24,* 9421-9429.

17. Blaudez, D.; Bonnier, M.; Desbat, B.; Rondelez, F. Two-Dimensional Polymerization in Langmuir Films: A PM-IRRAS Study of Octadecyltrimethoxysilane Monolayers. *Langmuir* **2002,** *18,* 9158-9163.

18. Zacharias, P.; Gather, M. C.; Köhnen, A.; Rehmann, N.; Meerholz, K. *Angew. Chem. Int. Ed.* **2009,** *48,* 1-5.

19. Gather, M.; Köhnen, A.; Falcou, A.; Becker, H.; Meerholz, K. Solution-Processed Full-Color Polymer Organic Light-Emitting Diode Displays Fabricated by Direct Photolithography. *Adv. Funct. Mater.* **2007,** *17,* 191-200.

20. Crivello, V. J.; Fouassier, J. P.; Rabek, J. F. *In Radiation Curing in Polymer Science and*

Technology; Elsevier Applied Science: London, 1993; Vol. II.

21. Georgakoudi, I.; Foster, T. H. Singlet Oxygen- Versus Nonsinglet Oxygen-Mediated Mechanisms of Sensitizer Photobleaching and Their Effects on Photodynamic Dosimetry. *Photochem. Photobiol.* **1998,** *67,* 612-625.

22. Soja, G. R.; Watson, D. F. TiO2-Catalyzed Photodegradation of Porphyrins: Mechanistic Studies and Application in Monolayer Photolithography. *Langmuir* **2009,** *25,* 5398–5403.

23. Chen, M.-H.; Hou, J.; Hong, Z.; Yang, G.; Sista, S.; Chen, L.-M.; Yang, Y. Efficient Polymer Solar Cells with Thin Active Layers Based on Alternating Polyfluorene Copolymer/Fullerene Bulk Heterojunctions. *Adv. Mater.* **2009,** *21,* 1–5.

24. Sipani, V.; Scranton, A. B. Dark-Cure Studies of Cationic Photopolymerizations of Epoxides: Characterization of the Active Center Lifetime and Kinetic Rate Constants. *J. Polym. Sci., Part A: Polym. Chem.* **2003,** *41,* 2064–2072.

25. Akatsuka, M.; Aida, T.; Inoue, S. High-speed "Immortal" Polymerization of Epoxides Initiated with Aluminum Porphyrin. Acceleration of Propagation and Chain-Transfer Reactions by a Lewis Acid. *Macromolecules* **1994,** *27,* 2820-2825.

26. Aida, . T.; Inoue, S. *Makromol. Chem., Rapid Commun.* **1980,** *1,* 677.

27. Ohkuma, S.; Yamashita, T. Two-Photon Sensitized Polymerization of Vinyl Ethers via Electron Transfer of ZnTTBP. *J. Photopolym. Sci. Technol.* **2002,** *15,* 23-28.

28. Aydogan, B.; Gunbas, G. E.; Durmus, A.; Toppare, L.; Yagci, Y. Highly Conjugated Thiophene Derivatives as New Visible Light Sensitive Photoinitiators for Cationic Polymerization. *Macromolecules* **2010,** *43,* 101–106.

29. Crivello, J. V.; Jiang, F. Development of Pyrene Photosensitizers for Cationic Photopolymerizations. *Chem. Mater.* **2002,** *14,* 4858-4866.

30. Gomez, M. L.; Avila, V.; Montejano, H. A.; Previtali, C. M. A mechanistic and laser flash photolysis investigation of acrylamide polymerization photoinitiated by the three component system safranine-T/triethanolamine/diphenyliodonium chloride. *Polymer* **2003,** *44,* 2875–

2881.

31. Kim, D.; Scranton, A. The Role of Diphenyl Iodonium Salt (DPI) in Three-Component Photoinitiator Systems Containing Methylene Blue (MB) and an Electron Donor. *J. Polym. Sci., Part A: Polym. Chem.* **2004,** *42,* 5863–5871.

32. Podsiadły, R. 12H-Quinoxalino[2,3-b][1,4]benzothiazine derivatives as novel visible photosensitizers in cationic photopolymerization. *J. Photoch. Photobio. A* **2009,** *208,* 147–153.

33. Bacher, A.; Erdelen, C. H.; Paulus, W.; Ringsdorf, H.; Schmidt, H.-W.; Schuhmacher, P. Photo-Cross-Linked Triphenylenes as Novel Insoluble Hole Transport Materials in Organic LEDs. *Macromolecules* **1999,** *32,* 4551-4557.

34. Kräutler, B.; Jaun, B.; Matile, P.; Bortlik, K. *Angew. Chem. Int. Ed. Eng.* **1991,** *30,* 1315.

35. Müller, C. D.; Falcou, A.; Wiederhirn, V.; Rudati, P.; Frohne, H.; Nuyken, O.; Becker, H.; Meerholz, K. *Nature* **2003,** *421,* 829-833.

36. de Barros, R.; de Azevedo, W.; de Aguiar, F. Photo-induced polymerization of polyaniline. *Mater. Charact.* **2003,** *50,* 131– 134.

37. Domercq, B.; Hreha, R. D.; Zhang, Y.-D.; Haldi, A.; Barlow, S.; Marder, S. R.; Kippelen, B. Organic Light-Emitting Diodes with Multiple Photocrosslinkable Hole-Transport Layers. *J. Polym. Sci., Part B: Polym. Phys.* **2003,** *41,* 2726–2732.

38. Kimoto, A.; Cho, J.-S.; Ito, K.; Aoki, D.; Miyake, T.; Yamamoto, K. Novel Hole-Transport Material for Efficient Polymer Light-Emitting Diodes by Photoreaction. *Macromol. Rapid Commun.* **2005,** *26,* 597–601.

39. Zacharias, P.; Gather, M. C.; Köhnen, A.; Rehmann, N.; Meerholz, K. Photoprogrammable Organic Light-Emitting Diodes. *Angew. Chem. Int. Ed.* **2009,** *48,* 1 – 5.

40. Gather, M.; Köhnen, A.; Falcou, A.; Becker, H.; Meerholz, K. *Adv. Funct. Mater.* **2007,** *17,* 191-200.

41. Kroto, H. W.; Heath, J. R.; O'Brien, S. C.; Curland, R. F.; Smalley, R. E. *Nature* **1985,** *318,* 162.

42. Giacalone, F.; Martín, N. Fullerene Polymers: Synthesis and Properties. *Chem. Rev.* **2006,** *106,* 5136-5190.

43. Kuciauskas, D.; Lin, S.; Seely, G. R.; Moore, A. L.; Moore, T. A.; Gust, D.; Drovetskaya, T.; Reed, C. A.; Boyd, P. D. W. Energy and Photoinduced Electron Transfer in Porphyrin-Fullerene Dyads. *J. Phys. Chem.* **1996,** *100,* 15926-15932.

44. Xue, J.; Uchida, S.; Rand, B. P.; Forrest, S. R. Asymmetric tandem organic photovoltaic cells with hybrid planar-mixed molecular heterojunctions. *Appl. Phys. Lett.* **2004,** *85,* 5757-5759.

45. Kratschmer, W.; Lamb, L. D.; Fostiropoulos, K.; Huffman, D. R. *Nature* **1990,** *347,* 354.

46. Cataldo, F. On C60 fullerene photopolymerization. *Polym. Int.* **1999,** *48,* 143-149.

47. Cataldo, F.; Heymann, D. A study of polymeric products formed by C60 and C70 fullerene ozonation. *Polym. Degrad. Stab.* **2000,** *70,* 237-243.

48. Scamporrino, E.; Vitalini, D.; Mineo, P. *Macromolecules* **1999,** *32,* 4247.

49. Sun, Y.-P.; Liu, B.; Lawson, G. E. *Photochem. Photobiol.* **1997,** *66,* 301.

50. Sariciftci, N. S.; Heeger, A. J. In *Handbook of Organic Conductive Molecules and Polymers;* Nalwa, H. S., Ed.; Wiley: New York, 1997; p 413.

51. Sonmez, G.; Shen, C. K. F.; Rubin, Y.; Wudl, F. *Adv. Mater.* **2005,** *17,* 897.

52. Michinobu, T.; Nakanishi, T.; Hill, J. P.; Funahashi, M.; Ariga, K. Room Temperature Liquid Fullerenes: An Uncommon Morphology of C60 Derivatives. *J. Am. Chem. Soc.* **2006,** *128* , 10384–10385.

53. Sastre, A.; Bassoul, P.; Fretigny, C.; Simon, J.; Roger, J.-P.; Thami, T. A mesomorphic amphiphilic phthalocyanine derivative used for the functionalization of the grid surface of a field effect transistor. *New J. Chem.* **1998,** 569-578.

54. Maya, E. M.; Shirk, J. S.; Snow, A. W.; Roberts, G. L. Peripherally-substituted polydimethylsiloxane phthalocyanines: a novel class of liquid materials. *Chem. Commun.* **2001,** 615–616.

55. Toupance, T.; Bassoul, P.; Mineau, L.; Simon, J. Poly(oxyethylene)-Substituted Copper and Lutetium Phthalocyanines. *J. Phys. Chem.* **1996,** *100,* 11704-11710.

56. Ban, K.; Nishizawa, K.; Ohta, K.; Shirai, H. Discotic liquid crystals of transition metal complexes 27: supramolecular structure of liquid crystalline octakisalkylthiophthalocyanines. *J. Mater. Chem.* **2000,** *10,* 1083-1090.

57. Basova, T. V.; Gürek, A. G.; Atilla, D.; Hassan, A. K.; Ahsen, V. Synthesis and characterization of new mesomorphic octakis(alkylthio)-substituted lead phthalocyanines and their films. *Polyhedron* **2007,** *26* , 5045–5052.

58. Gürek, A.; Durmus, M.; Ahsen, V. Synthesis and mesomorphic properties of tetra- and octa-substituted phthalocyanines. *New J. Chem.* **2004,** *28,* 693–699.

59. Kimura, M.; Wada, K.; Ohta, K.; Hanabusa, K.; Shirai, H.; Nagao, N. Organic-Inorganic Composites Comprised of Ordered Stacks of Amphiphilic Molecular Disks. *J. Am. Chem. Soc.* **2001,** *123,* 2438-2439.

60. Chaure, N. B.; Basova, T.; Zahedi, M.; Ray, A. K.; Sharma, A. K.; Durmuş, M.; Ahsen, V. Solution processed tetrasubstituted zinc phthalocyanine as an active layer in organic field effect transistors. *J. Appl. Phys.* **2010,** *107,* 114503.

61. Gearba, R. I.; Bondar, A. I.; Goderis, B.; Bras, W.; Ivanov, D. A. Tailoring the Thermotropic Behavior of Tetra-Substituted Phthalocyanines via the Lateral Chains Architecture. *Chem. Mater.* **2005,** *17,* 2825-2832.

62. Nowak-Król, A.; Gryko, D.; Gryko, D. T. Meso-Substituted Liquid Porphyrins. *Chem. Asian J.* **2010,** *5,* 641.

63. Kastler, M.; Pisula, W.; Davies, R. J.; Gorelik, T.; Kolb, U.; Müllen, K. Nanostructuring with a Crosslinkable Discotic Material. *Small* **2007,** *3,* 1438–1444.

64. O'Brien, A. K.; Bowman, C. N. Modeling the Effect of Oxygen on Photopolymerization Kinetics. *Macromol. Theory Simul.* **2006,** *15,* 176–182.

65. Falk, B.; Vallinas, S. M.; Crivello, J. V. Monitoring Photopolymerization Reactions with

Optical Pyrometry. *J. Polym. Sci., Part A: Polym. Chem.* **2003,** *41,* 579–596.

66. BelBruno, J. J.; Richter, A.; Campbell, S. E.; Gibson, U. J. Detection of functional states of molecularly imprinted thin films with multi-cycling nanoindentation. *Polymer* **2007,** *48,* 1679-1687.

67. Nowicki, M.; Richter, A.; Wolf, B.; Kaczmarek, H. Nanoscale mechanical properties of polymers irradiated by UV. *Polymer* **2003,** *44,* 6599–6606.

68. Shaheen, S. E.; Ginley, D. S.; Jabbour, G. E. Organic-Based Photovoltaics: Toward Low-Cost Power Generation. *MRS Bull.* **2005,** *30,* 10-19.

69. Gregg, B. A. Excitonic Solar Cells. *J. Phys. Chem. B* **2003,** *107,* 4688-4698.

70. Kim, Y.; Nelson, J.; Zhang, T.; Cook, S.; Durrant, J. R.; Kim, H.; Park, J.; Shin, M.; Nam, S.; Heeney, M.; McCulloch, I.; Ha, C.-S.; Bradley, D. D. C. Distorted Asymmetric Cubic Nanostructure of Soluble Fullerene Crystals in Efficient Polymer:Fullerene Solar Cells. *ACS Nano* **2009,** *9,* 2557–2562.

71. Zhao, D. W.; Tan, S. T.; Kec, L.; Liu, P.; Kyaw, A.; Sun, X.; Lo, G.; Kwong, D. Optimizationofaninvertedorganicsolarcell. *Sol. Energy Mater. Sol. Cells* **2010,** *94,* 985–991.

72. Kim, J. Y.; Kim, S. H.; Lee, H.-H.; Lee, K.; Ma, W.; Gong, X.; Heeger, A. J. New Architecture for High-Efficiency Polymer Photovoltaic Cells Using Solution-Based Titanium Oxide as an Optical Spacer. *Adv. Mater.* **2006,** *18,* 572–576.

73. Brabec, C. J.; Hauch, J. A.; Schilinsky, P.; Waldauf, C. Production Aspects. *MRS Bull.* **2005,** *30*.

74. Ameri, T.; Dennler, G.; Lungenschmied, C.; Brabec, C. J. Organic tandem solar cells: A review. *Energy Environ. Sci.* **2009,** *2,* 347–363.

75. Kim, J. Y.; Lee, K.; Coates, N. E.; Moses, D.; Nguyen, T.-Q.; Dante, M.; Heeger, A. J. Efficient Tandem Polymer Solar Cells Fabricated by All-Solution Processing. *Science* **2007,** *317,* 222-225.

76. Janssen, A. G. F.; Riedl, T.; Hamwi, S.; Johannes, H.-H.; Kowalsky, W. Highly efficient

organic tandem solar cells using an improved connecting architecture. *Appl. Phys. Lett. 91,* 073519.

77. Servaites, J. D.; Yeganeh, S.; Mark, T. J.; Ratner, M. A. Efficiency Enhancement in Organic Photovoltaic Cells: Consequences of Optimizing Series Resistance. *Adv. Funct. Mater.* **2010,** *20,* 97–104.

78. Efimov, A.; Vainiotalo, P.; Tkachenko, N. V.; Lemmetyinen, H. Efficient synthesis of highly soluble doubly-bridged porphyrin-fullerene dyad. *J. Porphyrins Phthalocyanines* **2003,** *7,* 593-599.

79. Moorjani, S. K.; Rangarajan, B.; Scranton, A. B. The Effect of Viscosity on the Rate of Photosensitization of Diaryliodonium Salts by Anthracene. In *Photopolymerization;* ACS Symposium Series, 1997; Vol. 673, p 95–106.

80. Crivello, J. V. The Discovery and Development of Onium Salt Cationic Photoinitiators. *J. Polym. Sci., Part A: Polym. Chem.* **1999,** *37,* 4241–4254.

81. Crivello, J. V.; Bulut, U. Curcumin: A Naturally Occurring Long-Wavelength Photosensitizer for Diaryliodonium Salts. *J. Polym. Sci., Part A: Polym. Chem.* **2005,** *43,* 5217–5231.

82. Schowalter, W. R. *Mechanics of Non-Newtonian Fluids Pergamon;,* 1978.

83. Sasaki, H. Curing properties of cycloaliphatic epoxy derivatives. *Progress in Organic Coatings* **2007,** *58,* 227–230.

84. Buffeteau, T.; Desbat, B.; Turlet, J. M. Polarization Modulation FT-IR Spectroscopy of Surfaces and Ultra-thin Films: Experimental Procedure and Quantitative Analysis. *Appl. Spectrosc.* **1991,** *45,* 380-389.

85. Allara, D. L.; Swalen, J. D. An Infrared Reflection Spectroscopy Study of Oriented Cadmium Arachidate Monolayer Films on Evaporated Silver. *J. Phys. Chem.* **1982,** *86,* 2700-2704.

86. Viitala, T. *Characterising nanoscale films with Polarisation-Modulation Infrared Reflection Spectrometry;* KSV Instruments Ltd.: Helsinki, 2007.

87. Richerson, D. W. *Modern Ceramic Engineering,* 2nd ed.; Marcel Dekker Inc., 1992.

88. McNaught, A. D.; Wilkinson, A. *IUPAC. Compendium of Chemical Terminology*, 2nd ed.; Blackwell Scientific Publications: Oxford, 1997.

89. Crivello, J. V.; Falk, B.; Zonca, J. M. R. Study of Cationic Ring-Opening Photopolymerizations Using Optical Pyrometry. *J. Appl. Polym. Sci.* **2004,** *92,* 3303–3319.

90. Vivo, P.; Jukola, J.; Ojala, M.; Chukharev, V.; Lemmetyinen, H. Influence of Alq3/Au cathode on stability and efficiency of a layered organic solar cell in air. *Sol. Energy Mater. Sol. Cells* **2008,** *92,* 1416– 1420.

91. Miller, M. A.; Malkar, N. B.; Severynse-Stevens, D.; Yarbrough, K. G.; Bednarcik, M. J.; Dugdell, R. E.; Puskas, M. E.; Krishnan, R.; James, K. D. Amphiphilic Conjugates of Human Brain Natriuretic Peptide Designed for Oral Delivery: In Vitro Activity Screening. *Bioconjugate Chem.* **2006,** *17,* 273.

92. Matthews, S. E.; Pouton, C. W.; Threadgill, M. D. Formation of hybrid polymethylene–poly(oxyethylene) macrocycles. *Tetrahedron Lett.* **2001,** *42,* 1355–1357.

93. Jiang, S.; Liu, Z.-H.; Sheng, G.; Zeng, B.-B.; Cheng, X.-G.; Wu, Y.-L.; Yao, Z.-J. Mimicry of Annonaceous Acetogenins: Enantioselective Synthesis of a (4R)-Hydroxy Analogue Having Potent Antitumor Activity. *J. Org. Chem.* **2002,** *67,* 3404-3408.

94. Neises, B.; Steglich, W. Simple Method for the Esterification of Carboxylic Acids. *Angew. Chem. Int. Ed.* **1978,** *17,* 522–524.

95. Luo, J.; Liu, S.; Haller, M.; Liu, L.; Ma, H.; Jen, A. K.-Y. Design, Synthesis, and Properties of HighlyEfficient Side-Chain Dendronized Nonlinear Optical Polymers for Electro-Optics. *Adv. Mater.* **2002,** *14,* 1763-1768.

96. Háda, M.; Nagy, V.; Gulyás-Fekete, G.; Deli, J.; Agócs, A. Towards Carotenoid Dendrimers: Carotenoid Diesters and Triesters with Aromatic Cores. *Helv. Chim. Acta* **2010,** *93,* 1149-1155.

97. Tannert, R.; Milroy, L.-G.; Ellinger, B.; Hu, T.-S.; Arndt, H.-D.; Waldmann, H. Synthesis and Structure-Activity Correlation of Natural-Product Inspired Cyclodepsipeptides Stabilizing F-Actin. *J. Am. Chem. Soc.* **2010,** *132,* 3063–3077.

98. White, J. E.; Earls, J. D.; Sherman, J. W.; López, L. C.; Dettloff, M. L. Step-growth polymerization of 10,11-epoxyundecanoic acid. Synthesis and properties of a new hydroxy-functionalized thermoplastic polyester. *Polymer* **2007,** *48*, 3990-3998.

99. Isosomppi, M.; Tkachenko, N. V.; Efimov, A.; Vahasalo, H.; Jukola, J.; Vainiotalo, P.; Lemmetyinen, H. Photoinduced electron transfer of double-bridged phthalocyanine–fullerene dyads. *Chem. Phys. Lett.* **2006,** *430* , 36–40.

100. Campbell, W. M.; Burrell, A. K.; Officer, D. L.; Jolley, K. W. Porphyrins as light harvesters in the dye-sensitised TiO2 solar cell. *Coord. Chem. Rev.* **2004,** *248* , 1363–1379.

101. Cid, J.-J.; Yum, J.-H.; Jang, S.-R.; Nazeeruddin, M. K.; Martinez-Ferrero, E.; Palomares, E.; Ko, J.; Grätzel, M.; Torres, T. Molecular Cosensitization for Efficient Panchromatic Dye-Sensitized Solar Cells. *Angew. Chem.* **2007,** *119*, 8510 –8514.

102. Lehtivuori, H.; Lemmetyinen, H.; Tkachenko, N. V. Exciplex-Exciplex Energy Transfer and Annihilation in Solid Films of Porphyrin-Fullerene Dyads. *J. Am. Chem. Soc.* **2006,** *128*, 16036-16037.

103. Schuster, D. I.; Li, K.; Guldi, D. M.; Palkar, A.; Echegoyen, L.; Stanisky, C.; Cross, R. J.; Niemi, M.; Tkachenko, N. V.; Lemmetyinen, H. Azobenzene-Linked Porphyrin-Fullerene Dyads. *J. Am. Chem. Soc.* **2007,** *129* , 15973–15982.

104. Young, A. C.; Dragavon, J.; Strovas, . T.; Molter, T.; Zheng, L.; Burgess, L.; Jen, A. K.-Y.; Lidstrom, M. E.; Meldrum, D. R. Two-Photon Lithography of Platinum-Porphyrin Oxygen Sensors. *IEEE Sensors J.* **2007,** *7*, 931-936.

105. Guo, M.; Chen, J.; Zhang, Y.; Chen, K.; Pan, C.; Yao, S. Enhanced adhesion/spreading and proliferation of mammalian cells on electropolymerized porphyrin film for biosensing applications. *Biosens. Bioelectron.* **2008,** *23*, 865–871.

106. Charas, A.; Alves, H.; Martinho, J. M.; Alcacer, L.; Fenwick, O.; Cacialli, F.; Morgado, J. Photoacid cross-linkable polyfluorenes for optoelectronics applications. *Synth. Met.* **2008,** *158*, 643–653.

107. Charas, A.; Ferreira, Q.; Farinhas, J.; Matos, M.; Alcacer, L.; Morgado, J. Insoluble Patterns of Cross-Linkable Conjugated Polymers from Blend Demixing in Spin Cast Films.

Macromolecules **2009,** *42,* 7903–7912.

108. Bednarek, M.; Kubisa, P.; Penczek, S. *Macromolecules* **1999,** *32,* 5257.

109. Lehtivuori, H.; Kumpulainen, T.; Efimov, A.; Lemmetyinen, H.; Kira, A.; Imahori, H.; Tkachenko, N. V. Photoinduced Electron Transfer in Langmuir-Blodgett Monolayers of Double-Linked Phthalocyanine-Fullerene Dyads. *J. Phys. Chem. C* **2008,** *112,* 9896-9902.

110. Khopde, S. M.; Priyadarsini, K. I.; Palit, D. K.; Mukherjee, T. Effect of Solvent on the Excited-state Photophysical Properties of Curcumin. *Photochem. Photobiol.* **2000,** *72,* 625-631.

111. Oberhuber, M.; Berghold, J.; Kräutler, B. Chlorophyll Breakdown by a Biomimetic Route. *Angew. Chem. Int. Ed.* **2008,** *47,* 3057–3061.

112. Müller, T.; Ulrich, M.; Ongania, K.-H.; Kräutler, B. Colorless Tetrapyrrolic Chlorophyll Catabolites Found in Ripening Colorless Tetrapyrrolic Chlorophyll Catabolites Found in Ripening. *Angew. Chem. Int. Ed.* **2007,** *46,* 8699-8702.

113. Kesti, T. J.; Tkachenko, N. V.; Vehmanen, V.; Yamada, H.; Imahori, H.; Fukuzumi, S.; Lemmetyinen, H. Exciplex Intermediates in Photoinduced Electron Transfer of Porphyrin-Fullerene Dyads. *J. Am. Chem. Soc.* **2002,** *124,* 8067-8077.

114. Maiti, N. C.; Mazumdar, S.; Periasamy, N. J- and H-Aggregates of Porphyrin-Surfactant Complexes: Time-Resolved Fluorescence and Other Spectroscopic Studies. *J. Phys. Chem. B* **1998,** *102,* 1528-1538.

115. Lam, D. C. C.; Chong, A. C. M. Effect of cross-link density on strain gradient plasticity in epoxy *Mater. Sci. Eng. A* **2000,** *281,* 156–161.

116. Lehtivuori, H.; Kumpulainen, T.; Hietala, M.; Efimov, A.; Lemmetyinen, H.; Kira, A.; Imahori, H.; Tkachenko, N. V. Photodynamics of Charge Separation and Recombination in Solid Alternating Films of Phthalocyanine or Phthalocyanine-Fullerene Dyad and Perylene Dicarboximide. *J. Phys. Chem. C* **2009,** *113,* 1984–1992.

117. Kaunisto, K.; Chukharev, V.; Tkachenko, N. V.; Efimov, A.; Lemmetyinen, H. Energy and Electron Transfer in Multilayer Films Containing Porphyrin-Fullerene Dyad. *J. Phys. Chem. C*

2009, *113,* 3819–3825.

118. Fazio, M. A.; Durandin, A.; Tkachenko, N. V.; Niemi, M.; Lemmetyinen, H.; Schuster, D. I. Synthesis, Conformational Interconversion, and Photophysics of Tethered Porphyrin–Fullerene Dyads with Parachute Topology. *Chem. Eur. J.* **2009,** *15,* 7698-7705.

119. Miyanishi, S.; Tajima, K.; Hashimoto, K. Morphological Stabilization of Polymer Photovoltaic Cells by Using Cross-Linkable Poly(3-(5-hexenyl)thiophene). *Macromolecules* **2009,** *42,* 1610-1618.

120. Joshi, S.; Grigorian, S.; Piets, U.; Pingel, P.; Zen, A.; Neher, D.; Scherf, U. Thickness Dependence of the Crystalline Structure and Hole Mobility in Thin Films of Low Molecular Weight Poly(3-hexylthiophene). *Macromolecules* **2008,** *41,* 6800-6808.

121. MacKenzie, R. C. I.; Frost, J. M.; Nelson, J. A numerical study of mobility in thin films of fullerene derivatives. *J. Chem. Phys.* **2010,** *132,* 064904.

122. Peumans, P.; Uchida, S.; Forrest, S. R. Efficient bulk heterojunction photovoltaic cells using small-molecular-weight organic thin films. *Nature* **2003,** *425,* 158-162.

123. Nilsson, S.; Bernasik, A.; Budkow, A.; Moons, E. Morphology and Phase Segregation of Spin-Casted Films of Polyfluorene/PCBM Blends. *Macromolecules* **2007,** *40,* 8291-8301.

124. Xue, J.; Rand, B. P.; Uchida, S. Mixed donor-acceptor molecular heterojunctions for photovoltaic applications. II. Device performance. *J. Appl. Phys.* **2005,** *98,* 124903.

125. Kim, I.; Haverinen, H. M.; Wang, Z.; Madakuni, S.; Kim, Y.; Li, J.; Jabbour, G. E. Efficient Organic Solar Cells Based on Planar Metallophthalocyanines. *Chem. Mater.* **2009,** *21,* 4256–4260.

126. Drechsel, J.; Männig, B.; Gebeyehu, D.; Pfeiffer, M.; Leo, K.; Hoppe, H. MIP-type organic solar cells incorporating phthalocyanine/fullerene mixed layers and doped wide-gap transport layers. *Org. Electron.* **2004,** *5,* 175-186.

127. Yang, F.; Forrest, S. R. Photocurrent Generation in Nanostructured Organic Solar Cells. *ACS Nano* **2008,** *2,* 1022-1032.

128. Shaheen, S. E.; Brabec, C. J.; Sariciftci, S. N.; Padinger, F.; Fromherz, T.; Hummelen, J. C. 2.5% efficient organic plastic solar cells. *Appl. Phys. Lett.* **2001,** *78,* 841-843.